

APPROXIMATE MODELS FOR  
STOCHASTIC LOAD COMBINATION

by

CHARLES BENJAMIN WAUGH

B.S.E., The University of Michigan  
(1975)

Submitted in partial fulfillment  
of the requirements for the degree of  
Master of Science in Civil Engineering

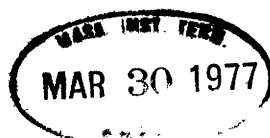
at the  
Massachusetts Institute of Technology  
January 1977

Signature of Author . . . . .  
Department of Civil Engineering, January 21, 1977

Certified by . . . . .  
Thesis Supervisor

Accepted by . . . . .  
Chairman, Departmental Committee on Graduate Students  
of the Department of Civil Engineering

Archives



ABSTRACT

APPROXIMATE MODELS FOR  
STOCHASTIC LOAD COMBINATION

by

CHARLES BENJAMIN WAUGH

Submitted to the Department of Civil Engineering on January 21, 1977, in partial fulfillment of the requirements for the degree of Master of Science in Civil Engineering.

This work deals with load combinations both from theoretical and practical viewpoints.

Starting first with theoretical considerations, load combinations are treated as mean outcrossing rate problems. A modified square wave (jump discontinuous) process is considered, and the expression for the outcrossing rate from a two dimensional region derived. This result is compared to results relating to multidimensional Gaussian processes.

Next, a series of case studies is carried out. These studies deal with reinforced concrete columns subjected to both time varying, random lateral and gravity loads. It is demonstrated that for cases of practical interest, interaction diagrams may be replaced with linear boundaries for purposes of reliability analyses.

It is also shown that by considering such linear boundaries, an outcrossing rate problem is reduced to an upcrossing rate problem, which is simpler from both conceptual and computational viewpoints. Further simplifications relating to upcrossing rate problems are also presented.

Engineering practice is considered in terms of building design codes. Present codes are discussed, and then theoretical objectives of modern probabilistic codes are outlined. Finally, some recent draft proposals are considered. Using the methodology developed earlier, these are checked for risk consistency. While no improvements on these formats are offered, it is concluded that such codified approaches appear to meet presently stated objectives.

Thesis Supervisor:

C. Allin Cornell

Title:

Professor of Civil Engineering

### ACKNOWLEDGEMENTS

Sincere thanks to the faculty at M.I.T., especially to Professor C. Allin Cornell, without whose help and direction this work would not have been possible.

Thanks also to the National Science Foundation, who sponsored the author as a N.S.F. Fellow, and also for their sponsorship of this work under Grant No. RANN-GI-44060.

TABLE OF CONTENTS

	Page
Title Page	1
Abstract	2
Acknowledgements	3
Table of Contents	4
List of Figures	6
List of Tables	8
Chapter 1 Introduction	
1.1 Motivation	9
1.2 Formal Definitions	10
1.3 Review of Other Work	10
1.4 Issues of Modeling	23
1.5 Purpose and Scope of Research	35
Chapter 2 Load Combinations as Mean Outcrossing Rate Problems	
2.1 Outcrossing Rate Results for Modified Square Wave Processes	37
2.2 Outcrossing Rate Results for Gaussian Processes	42
2.3 Case Studies: Reinforced Concrete Columns	47
2.3.1 Parameter Selection	48
2.3.2 Computational Procedures	52
2.3.3 Study 1	53
2.3.4 Study 2	61

2.3.5	Study 3	67
2.3.6	Conclusions drawn from Case Studies	74
2.4	Linearizations in Load Effect Space	80
Chapter 3 Scalar Load Combinations Problems		
3.1	Upcrossing Rates for Scalar Sums of Processes	89
3.2	A Markovian Approach	92
3.3	Further Simplifications	96
3.3.1	Results for High Failure Thresholds	97
3.3.2	Transience	98
3.4	Computational Procedures	98
Chapter 4 Engineering Practice for Load Combinations		
4.1	Past and Present Practice	100
4.2	Theoretical Objectives in Codified Design	106
4.3	Recent European Developments	109
4.3.1	C.E.B. Drafts	110
4.3.2	N.K.B. Draft	113
4.3.3	E.C.E. Draft	117
4.3.4	Reliability Consistency of the European Formats	121
Chapter 5 Conclusions and Recommendations		127
References		130
Appendix: Computer Programs		133

FIGURES

	Page	
1.1	The Borges--Castenheta model.	12
1.2	Structural interaction in the work of Borges and Castenheta.	13
1.3	Effect of adding a probability mass at the origin of a distribution function.	16
1.4	Hypothetical realizations of modified square wave processes.	17
1.5	Three equivalent load combination formulations.	19
1.6	Event representation of a thunderstorm.	26
1.7	Event representation of a severe thunderstorm.	26
1.8	Effect of excessive variability in the secondary process.	29
1.9	The effect of filtering.	30
1.10	Interpretation of influence coefficients.	33
2.1	Hypothetical realization of a two dimensional square wave process.	38
2.2	Important points on the failure boundary.	38
2.3	Integrations involved in the two dimensional modified square wave process.	40
2.4	Outcrossing of a two-dimensional Gaussian process.	45
2.5	Details of the segment $B_1$ .	45
2.6	Reinforced concrete column parameters.	50
2.7	Interaction diagram in load effect space, study 1.	55
2.8	Interaction diagram in load space, study 1.	55
2.9	Reduced space diagram, cases 1A and 1B.	56
2.10	Reduced space diagram, case 1C.	56
2.11	Continuous and jump process results, study 1.	57
2.12	Linearizations of the jump process, study 1.	58

2.13	Interaction diagram in load effect space, study 2.	62
2.14	Reduced space diagram, study 2.	63
2.15	Continuous and jump process results, study 2.	64
2.16	Linearizations of the jump process, study 2.	65
2.17	Interaction diagram in load effect space, study 3.	69
2.18	Reduced space diagram, study 3, cases A - D.	69
2.19	Reduced space diagram, case 3E.	70
2.20	Reduced space diagram and amended linearization, case 3E.	70
2.21	Continuous and jump process results, study 3.	71
2.22	Linearizations of the jump process, study 3.	72
2.23	Approximations of circular boundaries by a line.	77
2.24	Approximation of an elliptical boundary by a line.	78
2.25	Transformation of the failure region into an open domain.	79
2.26	Veneziano's searching scheme.	82
2.27	Linearizations in load effect space.	83
2.28	Linearization example in load effect space.	87
3.1	Relationship between square wave processes and Markov states 0, 1, 2, and 1*2.	95
4.1	Case A, normal distributions.	123
4.2	Case A, gamma distributions.	123
4.3	Case B, normal distributions.	124
4.4	Case B, gamma distributions.	124
4.5	Case C, normal distributions.	125
4.6	Case C, gamma distributions.	125

TABLES

	Page
1.1 Intervals assumed by Borges and Castenheta.	13
2.1 Parameter Values and Results for Study 1.	60
2.2 Parameter Values and Results for Study 2.	66
2.3 Parameter Values and Results for Study 3.	73
4.1 (After the C.E.B.) Recommended $\gamma_s$ values.	111
4.2 (After the N.K.B.) Recommended $\gamma_s$ values.	116
4.3 Numbers of intervals used in the E.C.E. scheme.	120



## INTRODUCTION

1.1 Motivation

Civil engineering structures are subjected to an environment comprised of a host of different loads. Natural phenomena, such as wind, snow, or temperature, and the actions of men, such as building occupancy loads must all be considered. In the face of this, the engineer is charged with the responsibility of designing structures that are both safe and economical. Since these two aims are contrary, a balance must be struck. Traditionally, this balance depended only upon the judgement of the engineer and those he serves: architects, owners, and building authorities.

Recently, probabilistic methods have been advanced in a quest to aid the design process. Engineers now generally accept the notion that both loads and a structure's resistance to them are random in nature. Furthermore, rational methods to choose load and resistance safety factors have been proposed. These typically assume knowledge of only the means and variances of the random variables pertaining to any problem, and so are known as second-moment methods. Important contributions have been made by Cornell [13], Ditlevsen [15], Hasofer and Lind [25], Paloheimo and Hannus [30], and Veneziano [39].

However, while these second-moment methods are capable of considering multiple loads and resistances, in and of themselves they do not account for a very significant aspect. All fail to explicitly treat the stochastic (temporal) variability of loads. That is, loads are considered to be random, but the important element of time is left out.

This shortcoming has not been ignored by engineers involved with research into structural safety. On the contrary, it is widely recognized. Basic mathematical research is still underway, and furthermore, so are investigations of how to apply such results to practical needs. Both constitute aspects of stochastic load combination.

### 1.2 Formal Definitions

Stochastic load combination problems are those for which the safety or serviceability of structures depends upon multiple loads that vary randomly in time.

In this work, stochastic load combination is to be distinguished from either probabilistic or statistical load combination. Problems that consider loads modeled simply as random variables (i.e., that do not explicitly consider variation in time) we call probabilistic. Statistical load combination deals with the application of data, either real or simulated, to the task. Clearly then, probabilistic load combination is less general a field of study than stochastic load combination. On the other hand, the study of statistical load combination involves an entirely different emphasis and set of mathematical tools.

### 1.3 Review of Other Work

There is a paucity of modern work dealing with stochastic load combination. Therefore, this section will be able to examine the work in moderate detail.

Borges and Castenheta treat load combinations extensively [7]. They

model each load as a random sequence of values that are constant during elementary intervals of fixed length. This is illustrated in figure 1.1. Values of load intensity are assumed to be mutually independent, both within a given load process or between processes. Table 1.1 indicates the duration of the elementary intervals for different types of loads considered, as well as the total number of repetitions so obtained for a 50 year period.

Given the above assumptions, the probability of a n-dimensional load vector  $\vec{S}$  falling within the domain  $ds_1, ds_2, \dots, ds_n$  at least once during the structural lifetime was found.

However, the result is difficult to apply, and so a simplified result is also presented. It assumes the first load to be a dead load (i.e.,  $k_1 = 1$  in the illustration, figure 1.1) and that there is only a small probability that two other loads will occur in combination with it:

$$f(\vec{S})ds_1ds_2ds_3 \cong k_2 f_1(s_1) f_2(s_2) f_{k_3/k_2}(s_3) ds_1 ds_2 ds_3 \quad (1.1)$$

where the  $f_i(\cdot)$  and  $F_i(\cdot)$  are p.d.f.'s and c.d.f.'s relating to individual load intensities within elementary intervals. The k's are the number of repetitions, with  $k_3 > k_2 > k_1$ , and:

$$f_{k_3/k_2}(s_3) = d[F_3(s_3)^{k_3/k_2}]$$

This is the expression actually used for the rest of the Borges-Castenheta book.

Careful inspection reveals that the equation 1.1 is not a proper density function, however. To be such, it must account for the probability

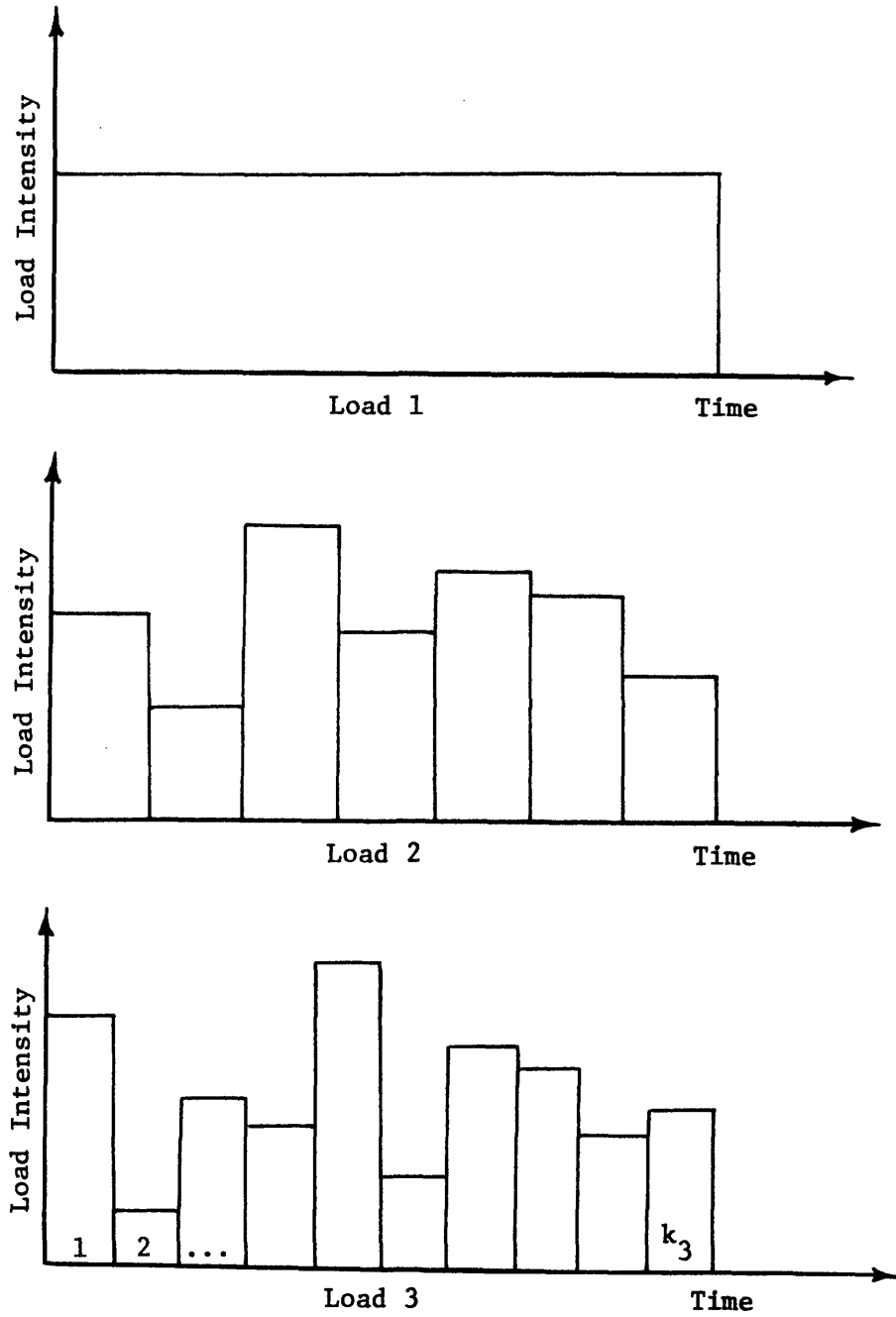


Figure 1.1: The Borges--Castenheta model.

Table 1.1 (After Borges and Castenheta)  
Intervals assumed by Borges and Castenheta

Load Type	Duration of each elementary interval	Number of independent repetitions in 50 years
Permanent	50 years	1
Live load on buildings	10 years*	5
	2 years	25
Wind	1 hour	$50 \times 10^3$
Earthquakes	30 seconds	$50 \times 10^6$

\*Duration depends on the occupancy type.

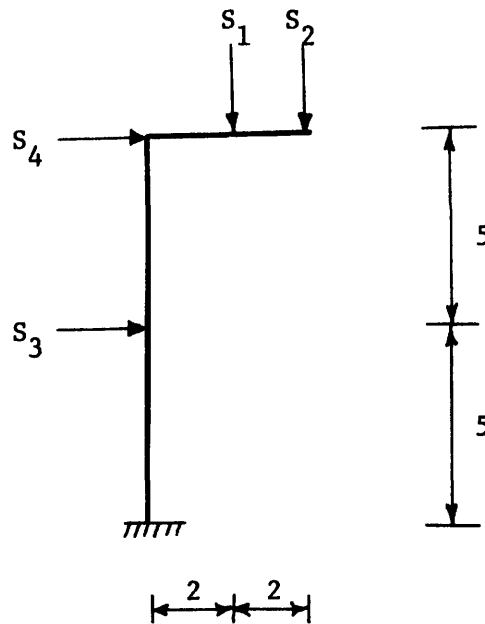


Figure 1.2 (After Borges and Castenheta)  
Structural Interaction in the work of Borges and Castenheta.

that the vector  $\vec{s}$  will fall into the region around  $(s_1, s_2, s_3)$  exactly one time during the lifetime considered, and never in any other region. That is, a distribution function must account for the probability of any single (exclusive) outcome. However, it actually accounts for the probability that the event occurs one or more times among many outcomes. Borges asserts that the two probabilities should approach each other if they are sufficiently small. Therefore, equation 1.1 is offered as such an approximation. The assertion is reasonable, but evidence has not yet been offered in its support or to bound its range of validity.

The transformation from loads to load effects is also considered. Although non-linear structural behavior is discussed in general terms, most of the study assumes a linear transformation from loads to effects. Figure 1.2 is an example of such a transformation, which can be expressed concisely in matrix form:

$$\vec{q} = [c]\vec{s}$$

where loads are denoted by  $\vec{s}$ , their effects by  $\vec{q}$ .

While it is shown in general terms how to use an expression such as equation 1.1 to compute failure probabilities, computations are not carried out. Instead, four examples combining loads on the structure were worked out to the point of plotting lines of equal probability density resulting from equation 1.1. Study of these examples may help to motivate an intuitive understanding of the nature of load combination problems. They do not, however, lead directly and unambiguously to simple methods for the selection of design loads or load factors.

Bosshard [9] generalized the elementary interval model of Borges and Castenheta, and then studied the problem of combining two such processes,

in the sense of summing scalar values. These two points will be discussed in turn below.

The generalized model proposed by Bosshard consists of a Poisson square wave process with a mixed distribution on load intensities. The latter feature calls for the inclusion of a new parameter,  $p$ , which is the probability that after any given Poisson renewal of the process, a zero value of intensity is assumed. The effect of the inclusion of this new parameter is illustrated in figure 1.3. Successive renewals are again assumed to be independent. Poisson square wave models had been used previously, such as in Peir's study [32], and with mixed distributions, such as in McGuire [29], but those studies did not appreciate the significantly greater modeling flexibility the introduction of  $p$  permitted. For instance, if we set  $p = 0$ , then the result is the familiar Poisson square wave process discussed by Parzen [31]. On the other hand, let  $p$  have as its complement  $q = 1 - p$ . Then, if the Poisson renewal rate is  $\nu$ , the arrival rate for nonzero renewals is  $q\nu$ . Holding times between renewals are exponentially distributed with means of  $1/\nu$  each. Hypothetical realizations of such a process are illustrated in figure 1.4.

Previous attempts (at M.I.T. and elsewhere) to represent infrequent loads with random durations had focused on less convenient "three parameter" models, in which the load durations are arbitrarily distributed, independent random variables. These models were non-Poisson, and hence less tractable. Examples are provided in the collection by Grigoriu [21].

In order to study the problem of summing the processes, Bosshard adopted a discrete state Markov approach. Each process is allowed to take on only a discrete set of values, and the states of the chain correspond to

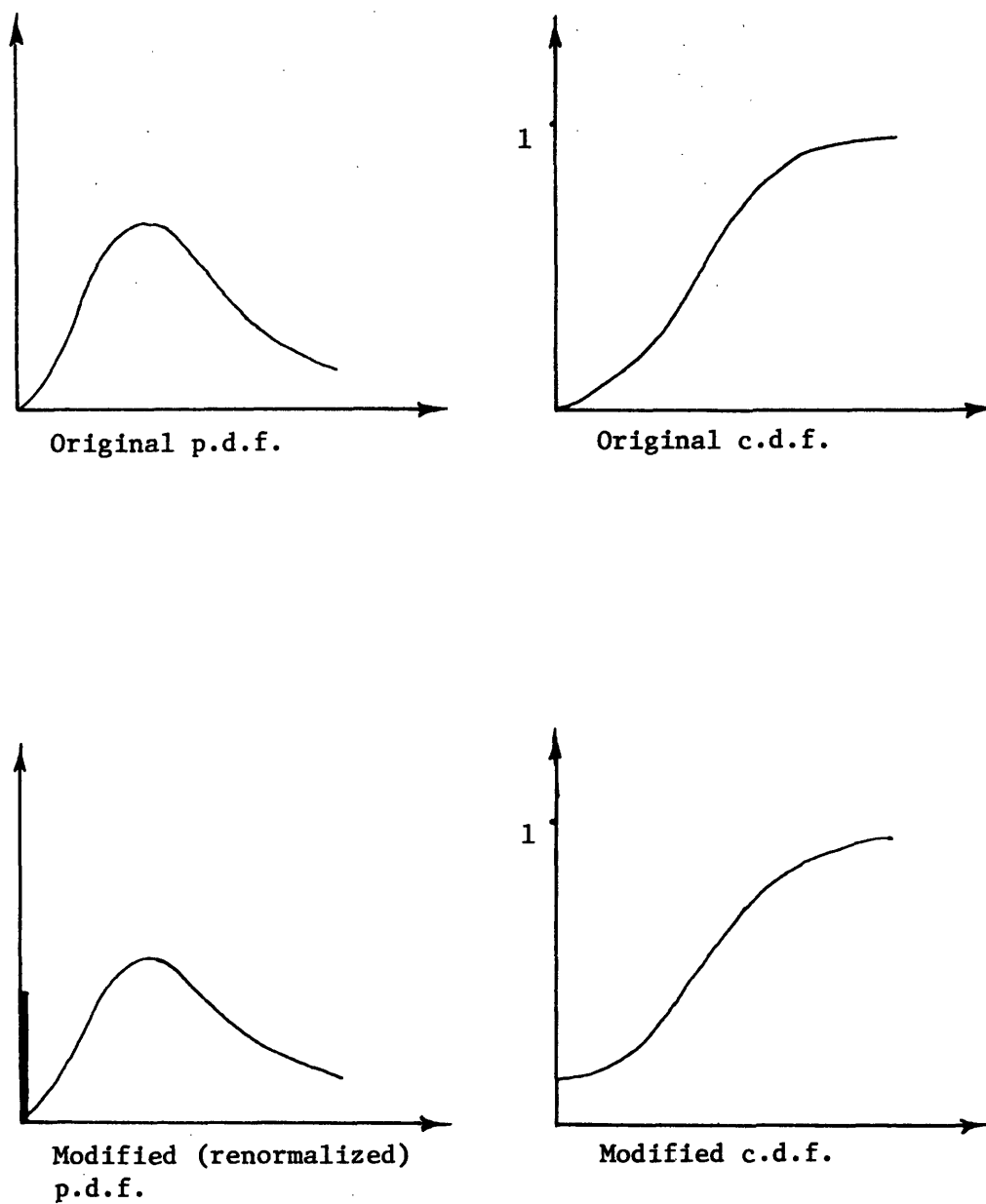


Figure 1.3: Effect of adding a probability mass at the origin of a distribution function.



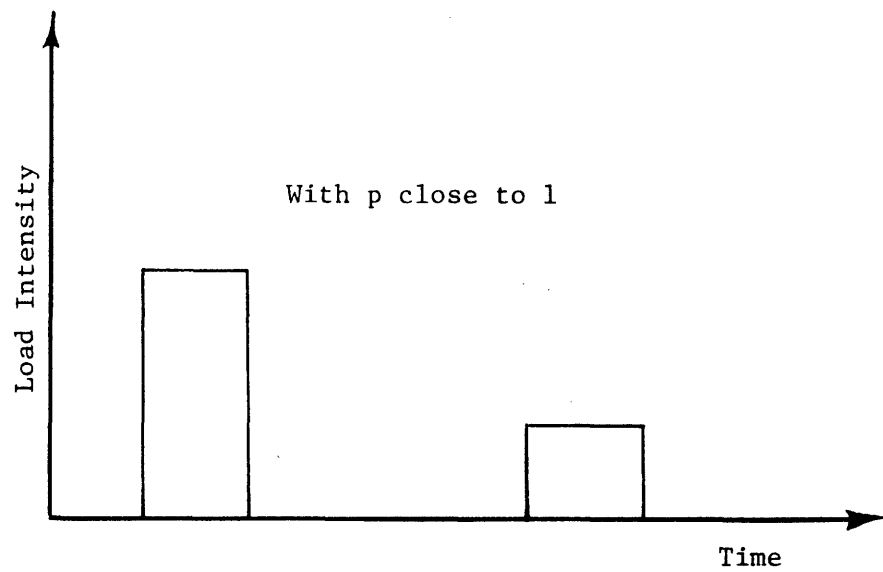
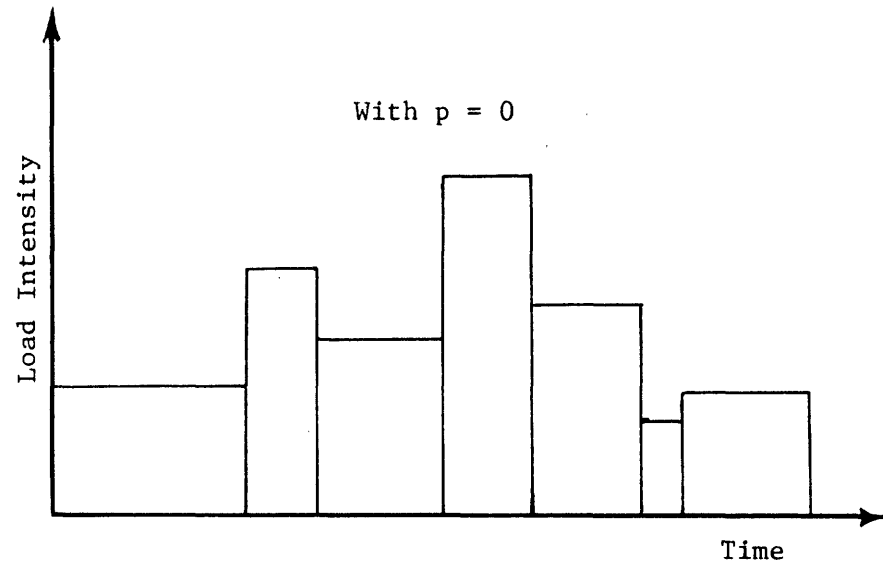


Figure 1.4: Hypothetical realizations of modified square wave processes.

all possible combinations of these two sets. Bosshard showed how this chain could be used to find the (discretized) extreme value distribution for the sum of two processes over a given reference period. Using simple two level discretizations on two processes, he studied then the coincidence problem, or the probability that the two processes will combine, each non-zero, during a reference period. Although his Fortran program would allow studies utilizing the full power of his approach, such as extreme value distributions for cases with more interesting distributions on the individual processes, such studies were not carried out. In part, this is because the approach is computationally expensive (as some limited experience with his program by researchers at M.I.T. has indicated).

Veneziano, Grigoriu, and Cornell have studied combinations of independent smooth Gaussian processes [40]. Results are given for the mean rate of outcrossing from a "safe" region in  $n$  dimensions. Simplifications are found for spheres and polygonal regions. These results have an important role in this work, and deserve to be presented in detail not appropriate to this section. Instead, they are presented in section 2.2.

While the above three references represent recent work specifically addressed to load combinations problems, there are earlier studies which have laid the foundations for them. Gumbel wrote a treatise on asymptotic extreme value distributions which is now considered to be a classic [23]. Rice did fundamental work dealing with mean-crossing rates for Gaussian processes [34]. Ditlevsen [16], and Crandall and Mark [14] are other excellent references on extremes of Gaussian processes.

In summary, note the three approaches to problem formulation that have been pursued in these studies: extreme value distributions, mean rates of

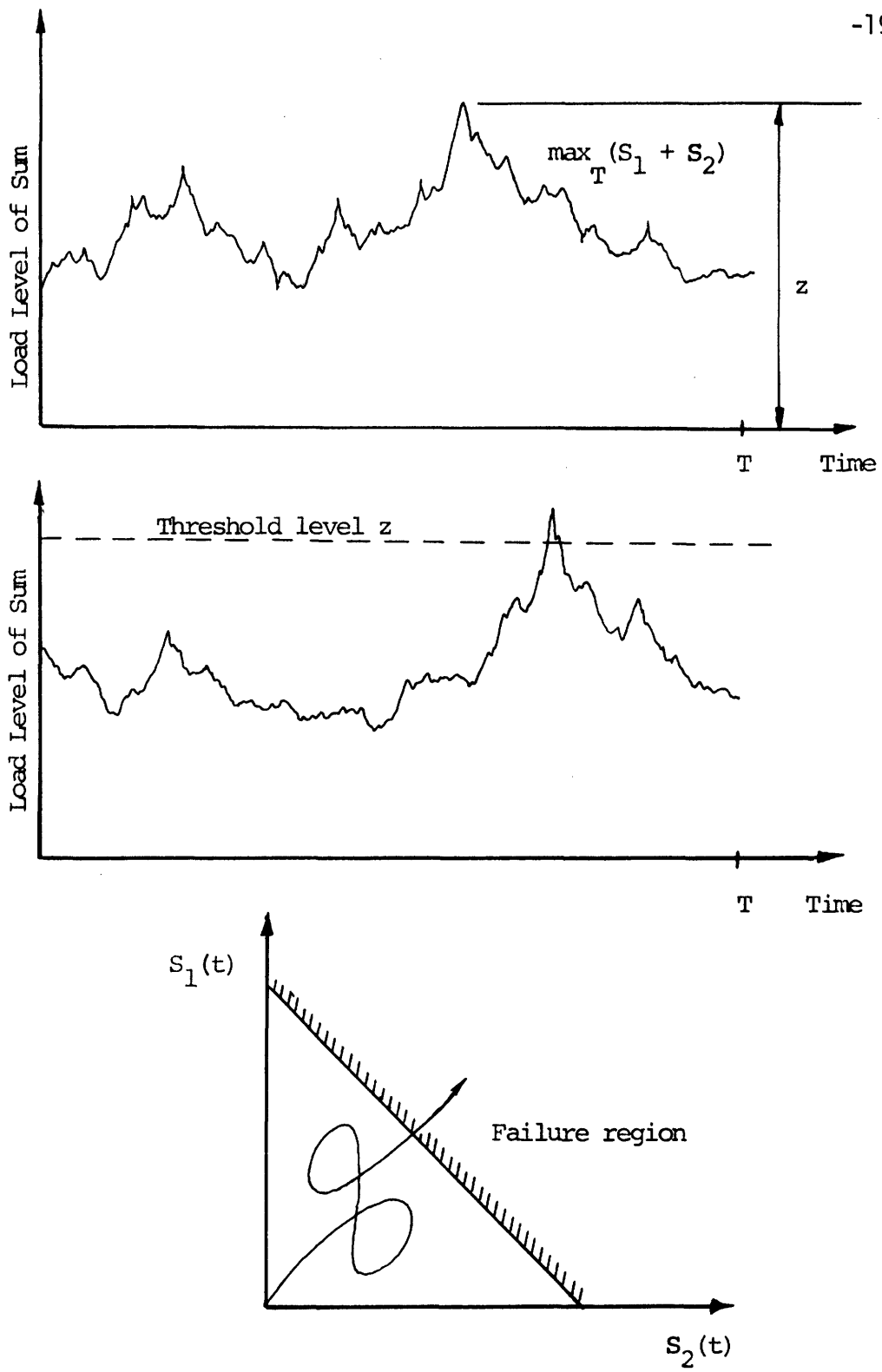


Figure 1.5: Three equivalent load combination formulations.

upcrossing above a threshold level, and mean rates of outcrossing from a safe region (e.g., in two dimensions). These are all illustrated in figure 1.5. Actually, these approaches are equivalent. First of all, the probability that the extreme value distribution of the combination is less than a given level is exactly the same as the probability that there are no upcrossings of this threshold:

$$P \left[ \max_T (S_1 + S_2) = z \right] = P \left[ \text{no upcrossings of the threshold } z, \text{ before time } T \right]$$

Further, since the safe region in the last illustration is linear, the problem is again of the form  $S_c = S_1 + S_2$ , and so is equivalent to an upcrossing problem. This equivalence is discussed with more precision and detail in section 2.4.

Other work bearing on load combinations has grown out of other research topics in civil engineering reliability. Two examples are presented here.

C. J. Turkstra has studied the decisions involved in structural design [36]. In the course of his work, he considers probabilistic design formats, including combinations of dead, occupancy, wind, and snow loads. The annual maximum total load, or its scalar load effect, is sought. He proposes that:

A reasonably simple expression for nominal maximum annual total loads  $S_T$  is obtained if it is assumed that on the day when one  $Q$  load reaches its annual maximum, other loads are chosen at random from the populations of their daily maximum loads....

Then, he proposes that the parameters of the total load on any of the critical days are of the form:

$$E(S_{T_j}) \cong E(S_j \text{ max}) + \sum_{i \neq j} E(S_i \text{ daily max}) \quad (1.2a)$$

$$\text{Var}(S_{T_j}) \cong \text{Var}(S_j \text{ max}) + \sum_{i \neq j} \text{Var}(S_i \text{ daily max}) \quad (1.2b)$$

Or, as Turkstra wrote them:

$$E(S_{T_j}) \cong E(S_j \text{ max}) + \sum_{i \neq j} a_i E(S_i \text{ max}) \quad (1.3a)$$

$$\text{Var}(S_{T_j}) \cong \text{Var}(S_j \text{ max}) + \sum_{i \neq j} b_i \text{Var}(S_i \text{ max}) \quad (1.3b)$$

where  $S_i \text{ max}$  and  $S_j \text{ max}$  refer to annual maxima of loads  $i$  and  $j$ , and  $a_i$  and  $b_i$  are constants depending upon the location and use of the structure, with  $a_i \leq 1$ . This is to say, he proposed that the parameters of the loads related to daily maximum values be related to annual extreme value information. In either set of equations, note also that individual loads are to be "rotated", each in turn assuming the leading position where the annual maximum is considered.

Clearly, the approach tends to be unconservative, in that it does not account for possible maximum values resulting from combinations where none of the loads is at an individual maximum. However, consider the effect of another assumption. Denote by  $P(S_{T_j} \leq z)$  the probability that the total maximum effect is less than  $z$ , with load  $j$  at an annual maximum. Assume that these probabilities are independent, even though it is generally not true. Then, we may approximate the result relating to the maximum total  $S_T$ , regardless of the relative values of individual loads:

$$P(S_T \leq z) = \prod_{\text{all } i} P(S_{T_i} \leq z) \quad (1.4a)$$

The assumption of independence tends to be conservative. In situations where a single load is dominant, the approximation should improve; this was reported by McGuire [29]. A result complimentary to equation 1.4a simply sums exceedance probabilities:

$$P(S_T > z) = \sum_{\text{all } i} P(S_{T_i} > z) \quad (1.4b)$$

which as an approximation to 1.4a is conservative.

Turkstra's approach has the advantage that it is easily translated into design rules for practical structural codes, each critical case being represented by a deterministic load combination checking condition. In fact, it is the basis for rules in both U.S. and European proposals, as will be discussed in Chapter 4.

Hasofer considered the extreme value distribution resulting from the superposition of a Poisson square wave with a Poisson event process, that is, a process with no time duration. The research grew out of a study dealing with floor live loads [24]. It is made more interesting by the fact that it is an exact result. Further, it demonstrates how mathematically difficult an exact (versus approximate) result may become, since it requires the solution of two integral equations; Hasofer did this numerically.

Of course, there are other studies which dealt with load combinations or related topics. However, the goal here is not to provide a complete and detailed review. Instead, the work that has been reviewed in detail represents that which has had a direct impact on this thesis.

#### 1.4 Issues of Modeling

Load combinations has been a little explored field until recently. As a result, basic issues concerning mathematical modeling of load combinations remain. This section will address some of these issues, and then will select and define the features of a model to be used in the rest of this thesis. The implications of the features selected will also be explored, with particular regard to the limitations they impose.

Three basic model qualities are desirable:

1. The model must be useful for dealing with codified design.
2. The model must not demand any more information than can reasonably be supplied.
3. The accuracy of any approximations in mathematical methods used must be subject to verification.

To deal with codified design means that both the input and output of the model must bear directly upon the design process. For example, if loading codes define wind loading in terms of pressures, the model should also deal in terms of pressures, not spectral density curves that must be further translated. On the other hand, the output must contain useful information for some safety checking scheme. So, for example, it is not enough to know the probability that earthquake forces and snow loads will act concurrently upon a structure exactly once during its life. Information about intensities is also necessary. The distribution of the lifetime maximum moment in a particular member due to the superposition of the two load processes would be an alternative of greater value.

The quality that the model must not demand too much information is

dictated by the limitations of practical situations. There is simply very little data on the processes, natural or man-made, that contribute to structural loading. Estimates can be made, according to engineering judgement. Such estimates contain valid information, and the model sets up a formal framework for using it. However, a deeper discussion of this issue leads into the realm of decision theory, such as Grigoriu dealt with [22].

Accuracy, in the context of this discussion, can only be defined in a relative sense. We do not know the true state of nature. So, we cannot state the true probability that the moment in a beam produced by two loads in combination exceeds a given level at a given time. Yet, given some assumptions, we may be able to get a closed form result, an "exact" result for our purposes. Then, if a simpler approach is adopted for the purpose of codification, it can be judged by the former standard.

Therefore, a premise advanced here is that simplicity is a helpful, perhaps necessary model quality. Simplicity also has an advantage inasmuch as it helps to clarify, rather than obscure what is actually occurring. Long span bridge loading provides an example. Asplund used a very simple model to study the reduction of lane loads with increasing bridge length [4]. His model neglects consideration of the number or spacing of axles on trucks, truck size distributions, vehicle headway, and other aspects considered in more recent research. However, his paper showed clearly why lane loads should be reduced with increasing span length, and thus verified an intuitive notion previously held by engineers.

In his work on model selection, Grigoriu also recognized the value of model simplicity [22]. He studied the question in a more formal manner than adopted here, attaching a penalty for increasing model complexity.



Taking all of the above into consideration, the following model features are selected:

1. The model will consider the combination of only two load processes.
2. Each load will be modeled as a modified square wave, as proposed by Bosshard.
3. The reliability information will be expressed in terms of mean crossing rates.

Let us now detail the implications of these features.

First, combinations of three or more loads cannot be directly considered. This is because the sum of two processes, with either  $p \neq 0$ , is no longer a Poisson renewal process, the only renewal process for which superpositions are also renewal processes; see Karlin and Taylor [26]. However, combinations of lateral wind and floor live load, of interest for many buildings, may still be considered.

Second, the use of the model as formulated by Bosshard poses the question of how to model individual load processes as a series of distinct events. This places a burden on researchers who are attempting to model individual load processes. They must model loads in terms of  $p$ ,  $v$ , and a single distribution function relating to intensities. For example, imagine that figure 1.6 represents the measured wind speed before, during, and after a thunderstorm. The bold lines indicate the way that the storm must be modeled. Questions to answer include when does the storm begin, when does it end, and what is its representative wind speed? Let us see how such questions may be approached.

One might say that the storm begins when an upward trend in wind speed is first detected, and ends when the downward trend at the tail of the

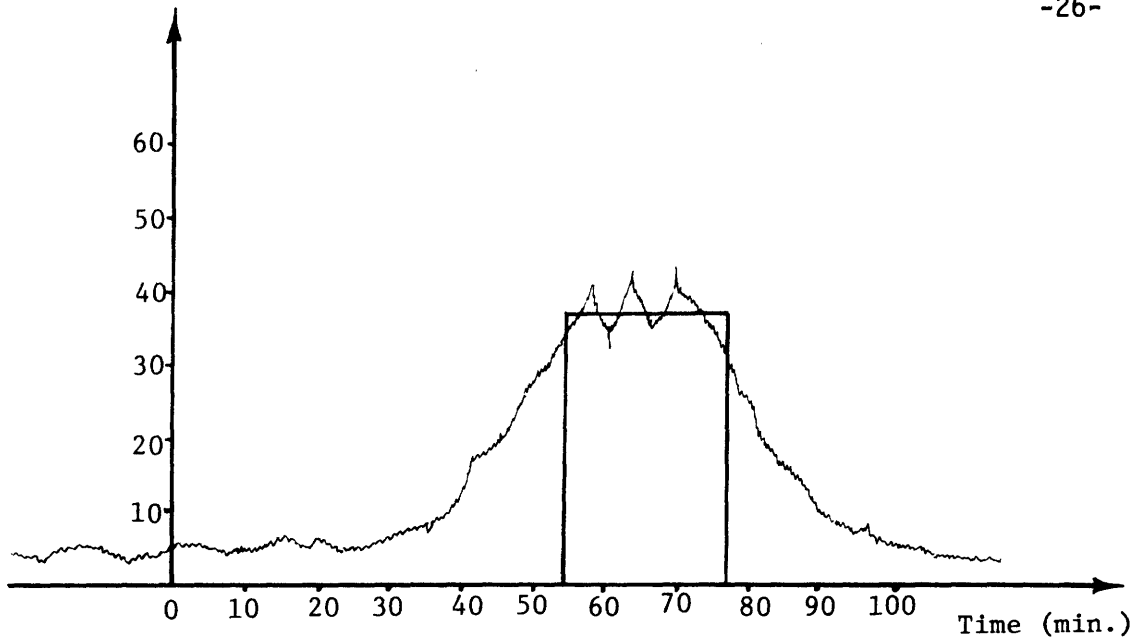


Figure 1.6: Event representation of a thunderstorm.

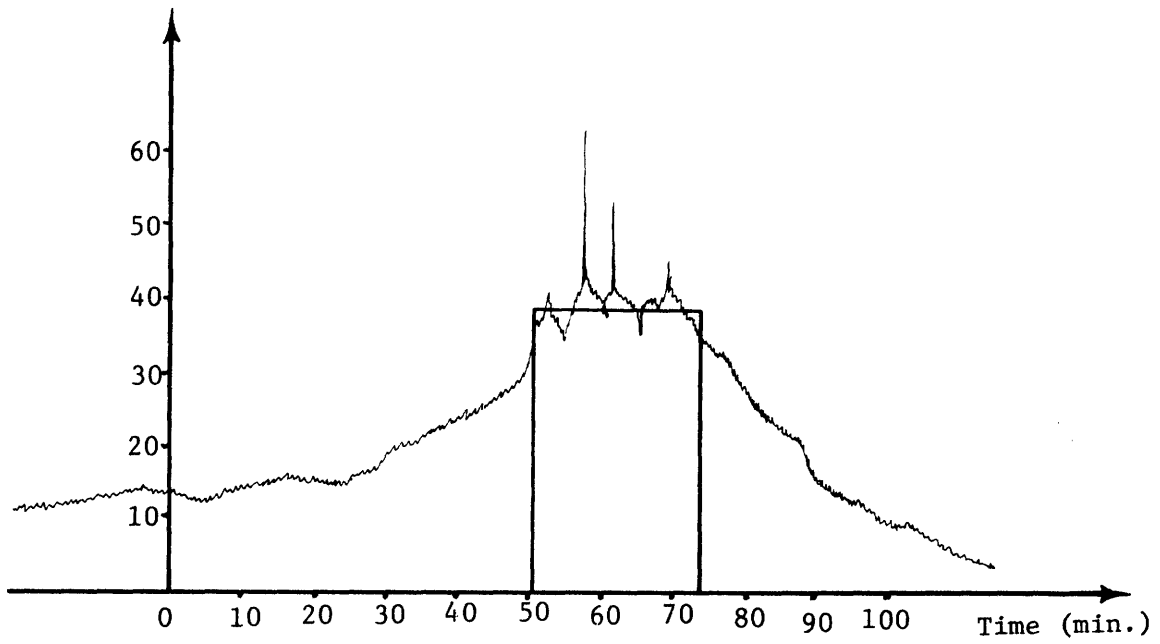


Figure 1.7: Event representation of a severe thunderstorm.

storm ends. For figure 1.6 we might judge that the storm begins between minutes 30 and 40, and ends somewhere after minute 100. However, the wind speeds are still low at these points, not of interest to structural engineers. Instead, let us focus attention on wind speeds above 35 miles per hour. Then, say that the event representation of the storm begins when sustained speeds of greater than 35 m.p.h. begin, and end when such speeds are no longer sustained. By sustained, we may mean that the velocity must remain above the reference level for all but short periods of time, say 20 seconds. Then, the representative velocity might well be taken as the mean velocity during this period of event representation.

The problem then becomes the selection of the reference (threshold) level of wind velocity. In the example illustrated by figure 1.6, 35 m.p.h. would seem a good choice, because it is close to the chosen representative velocity.

However, some problems may be more difficult. Figure 1.7 illustrates what may happen during a severe thunderstorm, with short gusts of more than 50 or 60 m.p.h. Again, 35 m.p.h. was chosen as a reference level, and again the representative value is not much greater. Yet, due to gusts there is a much greater variability about the representative velocity. We may attribute this variability to a secondary stochastic process; whereas the primary stochastic process describes the arrival of storms with representative velocities, the secondary process describes the gustiness about this velocity. This secondary process may even be required to account for the possibility of long waves, of perhaps 20 to 30 minute periods. The total static structural effect during any event is then due to the random but constant-in-time primary value, plus that due to the random, time varying

secondary process. The proposal here implies that only the primary component of the process will be properly represented in the analysis of temporal combinations with other loads. The constant-in-time (i.e., the square wave) assumption greatly facilitates this analysis.

It is important, for the purpose of the accuracy of this model, that the secondary stochastic process contain relatively little variability compared to the primary process. This condition reduces the probability that (in the case of our example) the maximum lifetime wind velocity or its structural effect occurs during an event other than the one with the maximum representative velocity, a situation illustrated in figure 1.8. It also reduces the probability that the maximum effects due to the combination of wind with other loads occurs at a time other than that which the model would suggest. Criteria for comparing variability in the primary and secondary processes might take the form of keeping an acceptably low ratio of the variances of the two processes. Unfortunately, formation of such criteria goes beyond the scope of this work.

Structural interaction must also be considered. Figure 1.9 illustrates a possible realization of the secondary stochastic process for thunderstorms, and the resulting bending moment in a particular member of a structure subjected to the storm. Even if we do not consider the dynamic characteristics of the building, there may be a filtering effect. Such filtering may be due to one or more of many reasons.

Again using wind for example, filtering may be due to the fact that it takes time for a gust to envelope a building; and by the time the gust is beginning to have an effect, it is dying down. Such interaction requires dynamic analysis, to be fully accounted for. However, ordinary design pro-

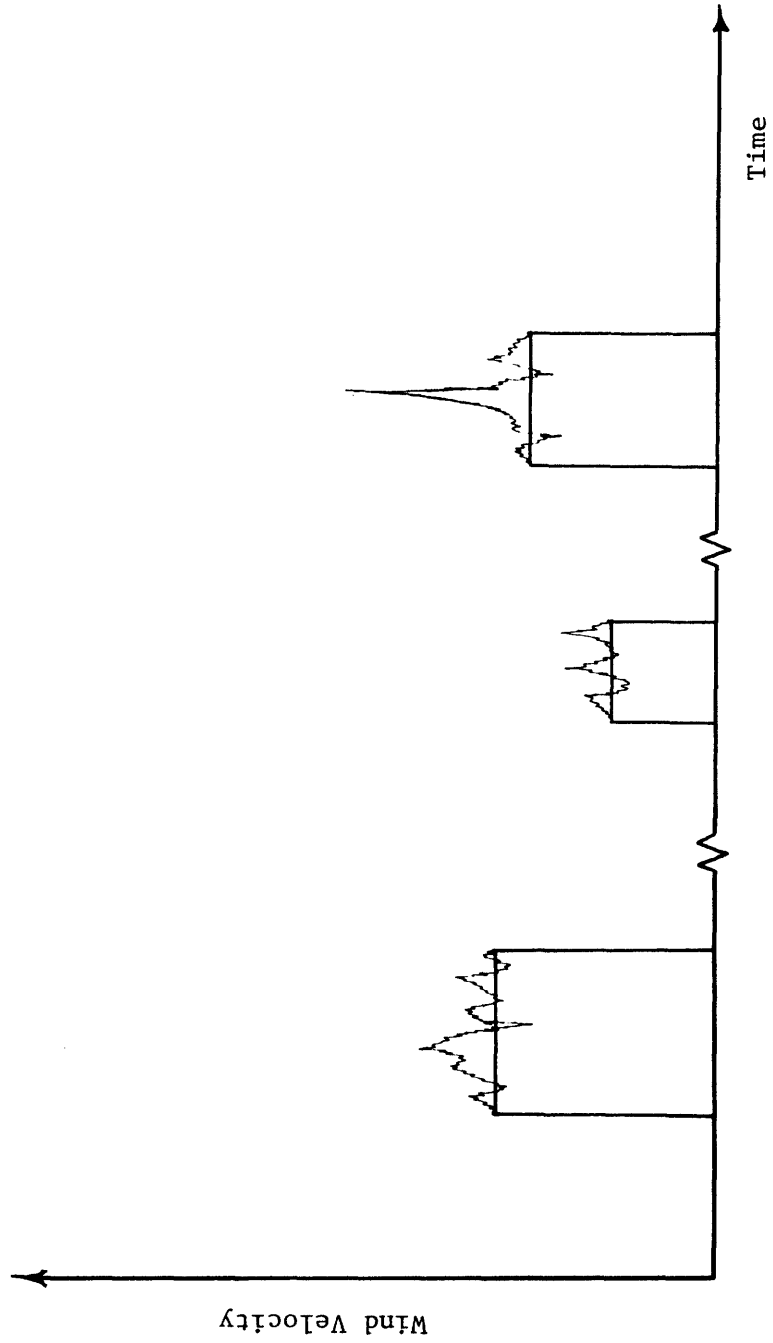


Figure 1.8: Effect of excessive variability in the secondary process.

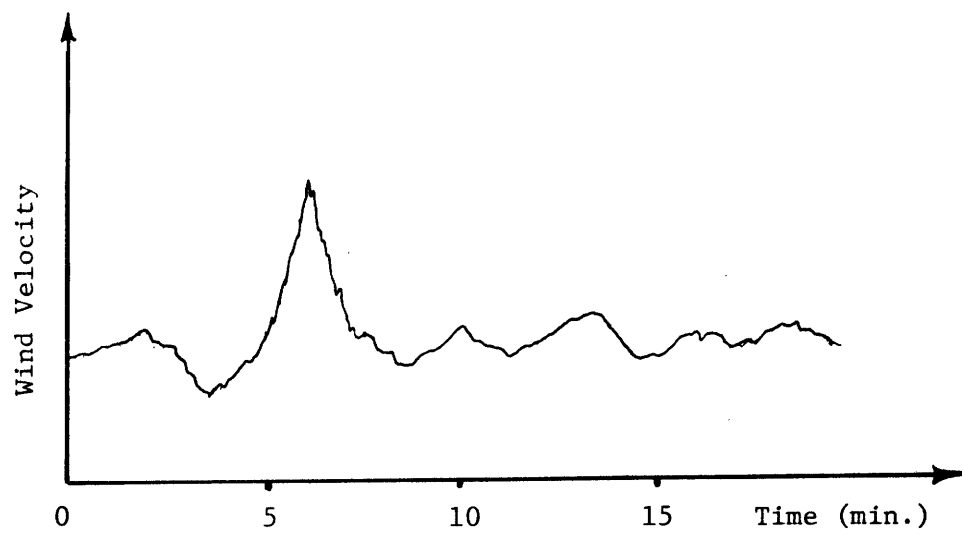
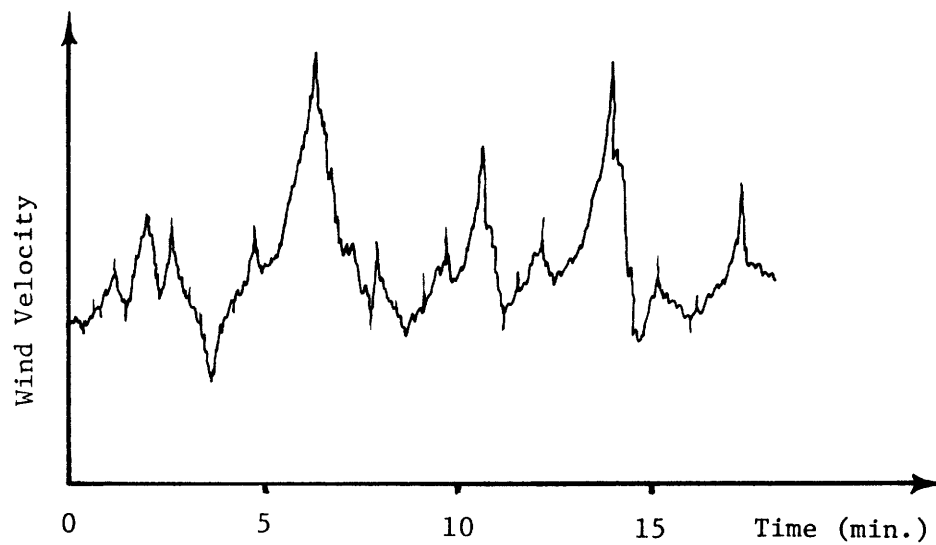


Figure 1.9: The effect of filtering.

cedures involve only pseudo-static analysis. Therefore, it is left to code committess and researchers modeling storms to select a transfer function typical of the class of buildings being designed, to check and see that the residual variability of the secondary process, left after filtering, is acceptable.

There may be too much variability left after filtering. In such a case, it may be an alternative to model storms as consisting of either sustained winds or peaks. This is similar to the idea of using sustained and extraordinary load processes in floor live load modeling [32]. Yet, there would be a significant difference. In the case of wind loading, the two processes would be mutually exclusive, and so would not create a load combination problem within the modeling of a single load type.

Consideration of structural interaction leads also to the topic of variable space. When we speak of the space of variables, we are simply referring to the physical meanings of the quantities represented. Load space variables deal directly with load phenomena, such as wind pressure, the weight of furniture on a floor or snow on a roof, etc. On the other hand, load effect variables refer to the results that loads subject a structure to, such as bending moment or axial force. It is the behavior of the structure itself in translating loads to effects that defines a mapping between the two spaces. We must decide which space we wish to work in.

There are advantages to working with either loads or effects. Usually, fewer effects are considered than loads. For instance, live floor loads, wind and earthquake loads, and snow loads may be considered; however, at the same time, at most only axial and bending effects may be significant. Also, safety checking is usually performed in terms of effects,

such as ultimate moment capacity. However, loading codes deal in terms of loads, not effects. Furthermore, it is usually assumed that loads act independently. In terms of modeling, this assumption becomes one of stochastic independence. Yet, effects are usually not independent. For an elementary example, consider the case of a reinforced concrete column subjected to both gravity and wind loading.

Let us assume linear elastic structural behavior, for simplicity. Further, assume the fixed spatial loading pattern of uniform loads. Then, adopting the same approach as Borges and Castenheta, relate the floor and wind loading to the moment and axial effects, M and P, by a matrix:

$$\begin{Bmatrix} M \\ P \end{Bmatrix} = \begin{bmatrix} c_{WM} & c_{LM} \\ c_{WP} & c_{LP} \end{bmatrix} \begin{Bmatrix} W \\ L \end{Bmatrix} \quad (1.5)$$

An interpretation of the coefficients of this matrix is illustrated in figure 1.10.

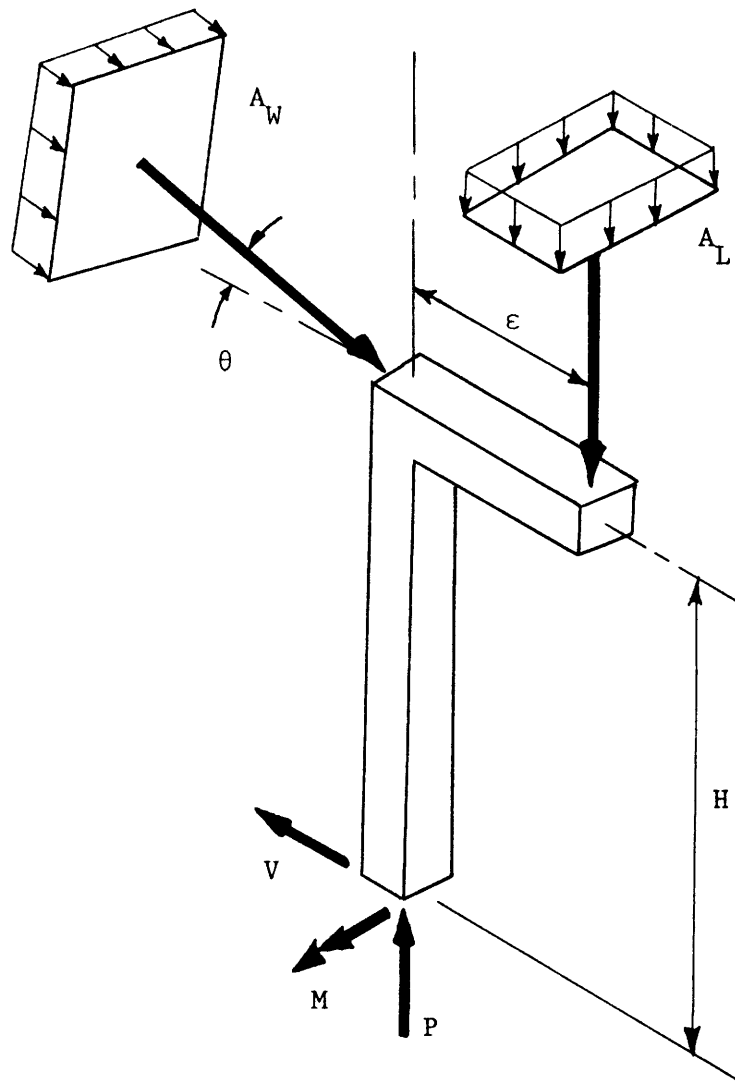
Consider a point in time at which it is known that both wind and live loads are acting at random levels. Assume knowledge only of means and variances, and that the loads are not correlated. Then, the covariance between effects is found by simple linear operations:

$$\text{Cov}(M,P) = c_{WM}c_{WP}\sigma_W^2 + c_{LM}c_{LP}\sigma_L^2 \quad (1.6)$$

which is generally nonzero.

The method adopted here is to invert the matrix [C], and translate the description of the safe region into load space. Denote the inverse by [D]. Any point on the failure surface in load effect space is mapped back to a





$$C_{WM} = A_W \cos \theta H$$

$$C_{WP} = A_W \sin \theta$$

$$C_{LM} = A_L \epsilon$$

$$C_{LP} = A_L$$

Figure 1.10: Interpretation of influence coefficients.

$$\begin{Bmatrix} W_u \\ L_u \end{Bmatrix} = \begin{bmatrix} d_{MW} & d_{PW} \\ d_{ML} & d_{PL} \end{bmatrix} \begin{Bmatrix} M_u \\ P_u \end{Bmatrix} \quad (1.7)$$

Proceeding point by point, we can define a new diagram in terms of the loads themselves. Using this new diagram, safety analyses can be carried out, in terms of the load processes only.

No matter what space of variables is selected, the failure surface may be irregular and difficult to describe analytically. In such cases, it may be desirable to replace the surface by simple approximations, such as spherical or circular segments, planes or straight lines. Especially with the latter approximations, considerable mathematical simplifications may be achieved, as will be demonstrated in the next two chapters.

Finally, let us examine the usefulness of mean outcrossing rates as reliability information. Structural failures are rare events. Due to this fact, and also because we focus on high load and load effect levels, it may be assumed that these rates pertain to Poisson processes. Then, the probability of the total load outcrossing the safe region (or exceeding a threshold), denoted  $p_f$ , is

$$p_f = 1 - P(\text{No outcrossing in } [0, T]) = 1 - \exp(-v_+T) \quad (1.8)$$

where  $v_+$  is the outcrossing rate. By taking the first term in the Taylor series expansion for the exponential function, we obtain:

$$p_f \leq v_+T \quad (1.9)$$

which for small  $p_f$ , is a good, while conservative approximation when taken as an equality. Note that  $v_+T$  is also the expected number of outcrossings.

### 1.5 Purpose and Scope of Research

As implied by the title of this thesis, its main goal is not only to study models of load combinations, but also the effect of approximations on them. Toward this end, each succeeding chapter will contain more approximations than the one before. At the same time, progress will be made toward findings of practical value.

In Chapter 2, load combinations will be studied as mean outcrossing rate problems. The outcrossing rate problem for the modified square wave process will first be solved. Then, as an approximation, the continuous process results of Veneziano, Grigoriu, and Cornell will be presented. Comparisons made in the form of case studies will show that the continuous process results often well approximate those of the modified square wave. Additional insight is also gained by their use.

Also in Chapter 2, it will be shown how two dimensional failure boundaries may be linearly approximated. This offers the great advantage of reducing the two dimensional outcrossing problem to a scalar (one dimensional) upcrossing rate problem. A method to perform these linearizations in load space is presented, and the resulting error and limitations discussed in a series of case studies dealing with reinforced concrete columns. A more direct method for performing such linearizations, in terms of load effects, is also suggested.

Advantages gained from adopting a scalar boundary are exploited in Chapter 3. The mean upcrossing rate for the sum of two modified square wave processes is found. A Markovian approach similar to but distinct from that taken by Bosshard helps interpret the results and provide in-

sight. Even further simplifications, useful in certain special cases, are also presented.

Code procedures for dealing with load combinations is the subject of Chapter 4. Past and present development of practice is summarized. Moreover, the theoretical objectives modern code writing authorities hope to achieve are presented, which links this chapter to the previous ones. Lastly, it is shown how the stochastic model results of Chapter 3 can be used to evaluate the degree to which simple codified formats are meeting these objectives. A brief example of such a study is actually given.

Finally, Chapter 5 will offer general conclusions based upon the entire body of this work. Recommendations for future research will also be made.

## LOAD COMBINATIONS AS MEAN OUTCROSSING RATE PROBLEMS

2.1 Outcrossing Rate Results for Modified Square Wave Processes

The result for the mean outcrossing rate for the combination of two modified square wave processes is found by a conceptually straightforward argument. It is valid, however, only for processes that are independent both in terms of temporal characteristics and in values of load intensities associated with renewals.

A hypothetical realization of a two dimensional combination of a modified square wave process is shown in figure 2.1. This illustration emphasizes the principle that the probability of simultaneous change is negligible. Therefore, the problem can be split into two parts, consisting of finding the mean rates of outcrossing associated with changes in loads 1 and 2 separately. Let us focus on the mean rate of outcrossing associated with changes in load 1 first. The result relating to load 2 is then similar.

Before proceeding, though, let us introduce some less precise but shorter language. Though one must be mindful of their nature as expected values, let us refer to rates of outcrossing, rather than mean rates. Further, when referring to outcrossings associated with changes in a given load, we shall simply allude to outcrossings "due" to that load. These conventions will be used in the sections that follow.

Symbolically, denote the rate of outcrossings due to load 1 by  $v_{1+}$ . The rate  $v_{1+}$  is related to the rate  $v_1$  by the probability that any particular renewal of process 1 results in an outcrossing, or:

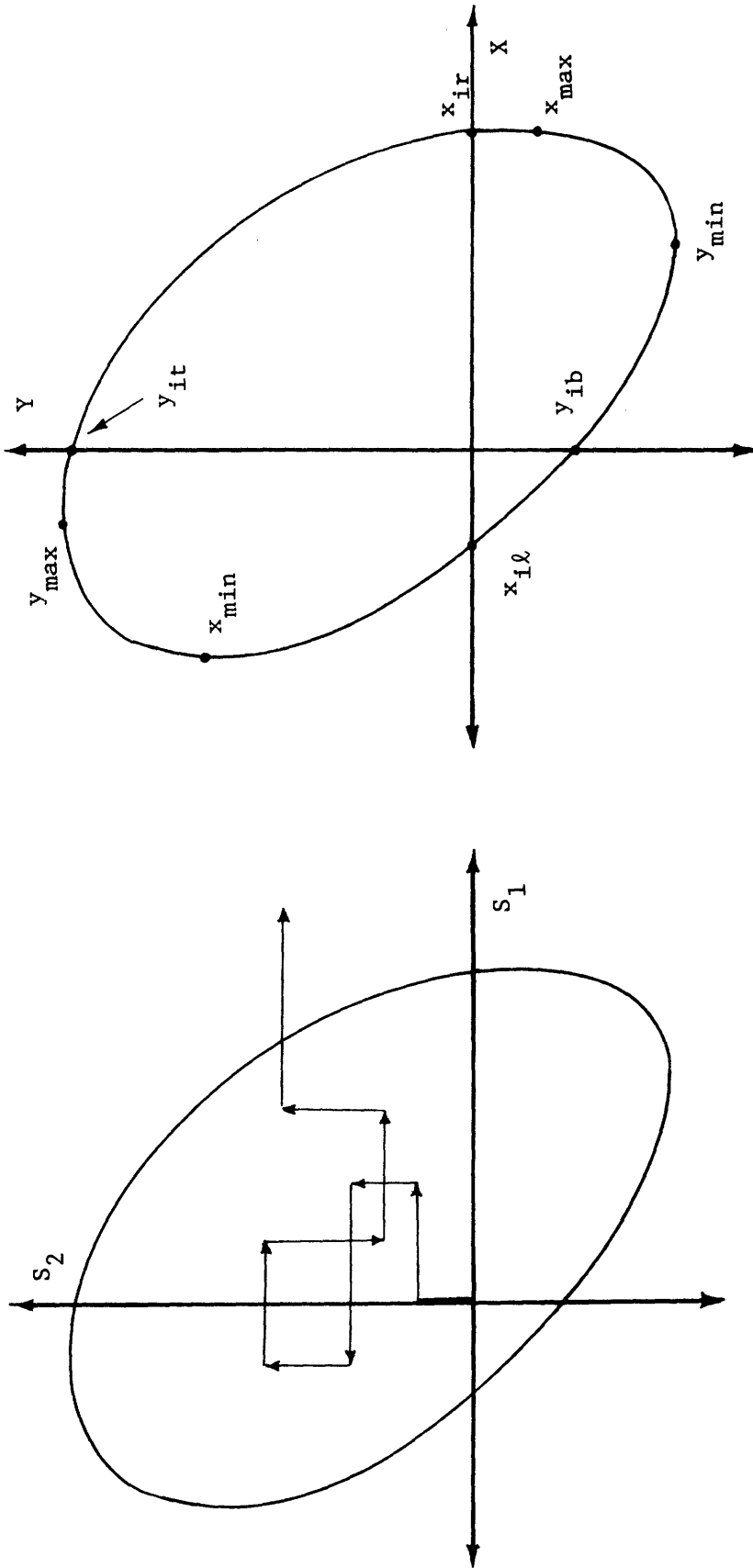


Figure 2.1: Hypothetical realization of a two dimensional square wave process.

Figure 2.2: Important points on the failure boundary.

$$v_{1+} = v_1 P \left\{ \begin{array}{l|l} \text{There is an} & \text{There is a change} \\ \text{outcrossing} & \text{in load 1} \end{array} \right\}$$

Further, since the two load processes are independent, it is convenient to condition upon the level of load 2. So, using this fact:

$$v_{1+} = v_1 \int_{\Omega} P \left\{ \begin{array}{l|l} \text{There is an} & \text{There is a change in} \\ \text{outcrossing} & \text{load 1, and } S_2 = s_2 \end{array} \right\} P\{S_2 = s_2\} ds_2$$

To make the above result more explicit, we need to consider the forms of the distributions relating to the intensities of loads 1 and 2. Let us denote with a prime the modified and renormalized distributions obtained from considering  $F_1(s_1)$ ,  $F_2(s_2)$ ,  $P_1$ , and  $P_2$ :

$$F_1'(s_1) = p_1 + q_1 F_1(s_1) \quad (2.1a)$$

$$F_2'(s_2) = p_2 + q_2 F_2(s_2) \quad (2.1b)$$

(Recall that the effect of including a probability mass  $p$  was illustrated in figure 1.3.) It should be emphasized that these primes have no relation to the operation of differentiation.

Also, we must consider the form of the boundary in order to write an explicit result. Let us make a slight notational change at this point (to reduce multiple subscripts). Instead of labeling the load variables for loads 1 and 2 by  $s_1$  and  $s_2$ , simply call them  $x$  and  $y$ , respectively. There are then 8 important points on the boundary to consider. These include the extrema,  $x_{\max}$ ,  $y_{\max}$ ,  $x_{\min}$ , and  $y_{\min}$ , along with the intercepts  $x_{i\ell}$ ,  $x_{ir}$ ,  $y_{it}$ , and  $y_{ib}$ . All of these points are illustrated in figure 2.2.

For the purposes of integrating with respect to  $y$ , we now consider

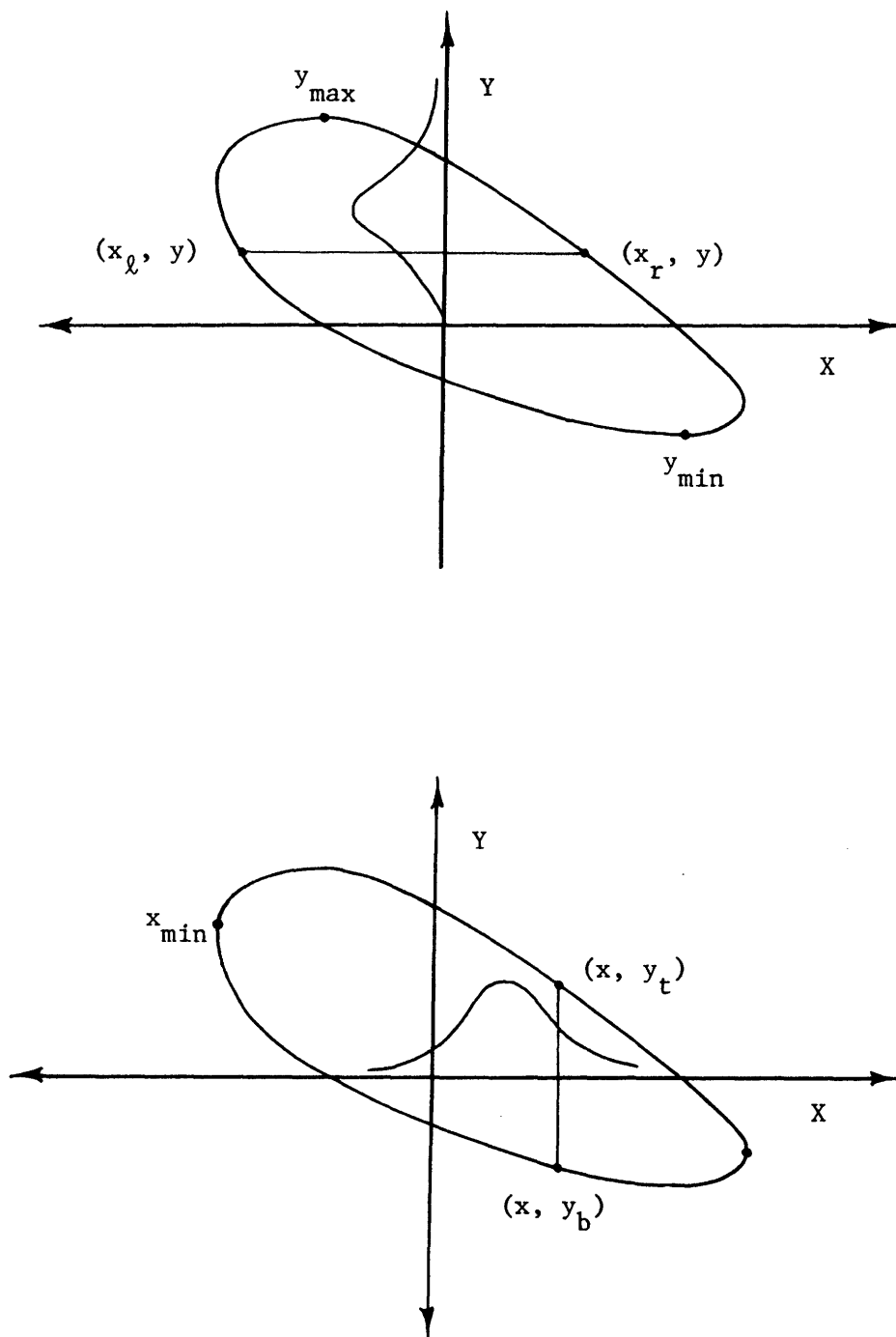


Figure 2.3: Integrations involved in the two dimensional modified square wave formulation.



two paths from  $y_{\min}$  to  $y_{\max}$ , running to the left and right, containing  $x_{i\ell}$  and  $x_{ir}$ , respectively. Denote the ordinates relating to a given value of  $y$  as  $x_\ell$  and  $x_r$ , respectively.

So, using this notation, for a given value  $y$ , the probability of being within the safe region is:

$$P\{\text{Safe}|y\} = F'_1(x_r) - F'_1(x_\ell) = p_1 + q_1[F_1(x_r) - F_1(x_\ell)] \quad (2.2)$$

Unity minus the right hand side of 2.2 is the probability of being out of the safe region, given  $y$ . Since an outcrossing event involves the transition from a safe to an unsafe state, and recalling the independence of successive renewals,  $v_{1+}$  is:

$$v_{1+} = v_1 \int_{y_{\min}}^{y_{\max}} \{p_1 + q_1[F_1(x_r) - F_1(x_\ell)]\} \{q_1 - q_1[F_1(x_r) - F_1(x_\ell)]\} dF'_2(y) \quad (2.3)$$

Accounting for the probability  $p_2$ , equation 2.3 becomes:

$$v_{1+} = v_1 q_1 p_2 \{p_1 + q_1[F_1(x_r) - F_1(x_\ell)]\} \{1 - [F_1(x_r) - F_1(x_\ell)]\} + v_1 q_1 q_2 \int_{y_{\min}}^{y_{\max}} \{p_1 + q_1[F_1(x_r) - F_1(x_\ell)]\} \{1 - [F_1(x_r) - F_1(x_\ell)]\} f_2(y) dy \quad (2.4)$$

where  $f_2(y)$  now relates to the p.d.f. of renewals of load 2. Considering a symmetric result for load 2, the final (total) result is obtained:

$$v_+ = v_1 q_1 p_2 \{p_1 + q_1[F_1(x_r) - F_1(x_\ell)]\} \{1 - [F_1(x_r) - F_1(x_\ell)]\} + v_2 p_1 q_2 \{p_2 + q_2[F_2(y_t) - F_2(y_b)]\} \{1 - [F_2(y_t) - F_2(y_b)]\}$$

$$\begin{aligned}
& + v_1 q_1 q_2 \int_{y_{\min}}^{y_{\max}} \{p_1 + q_1 [F_1(x_r) - F_1(x_\ell)]\} \{1 - [F_1(x_r) - F_1(x_\ell)]\} f_2(y) dy \\
& + v_2 q_1 q_2 \int_{x_{\min}}^{x_{\max}} \{p_2 + q_2 [F_2(y_t) - F_2(y_b)]\} \{1 - [F_2(y_t) - F_2(y_b)]\} f_1(x) dx \quad (2.5)
\end{aligned}$$

Except for extremely simple cases of little practical interest, equation 2.5 must be evaluated numerically. The form of these two integrations are indicated in figure 2.3.

## 2.2 Outcrossing Rate Results for Gaussian Processes

As mentioned previously, the results outlined in this section are taken from reference [40]. Only slight changes in notation to resolve certain conflicts with other results have been made.

The general formulation is as follows. Let  $\vec{X}(t)$  be a stationary, continuously differentiable process with  $n$  components, and  $\Omega$  be a region in  $R^n$ , defined by:

$$\Omega = \{\vec{X}: g(\vec{X}) \leq z\} \quad (2.6)$$

That is,  $\Omega$  is the safe region defined by the function  $g$ .

Analogously with upcrossing events of scalar functions, a sample function  $\vec{x}(t)$  is said to outcross the boundary  $B_\Omega$  at a time  $t_0$  if  $\vec{x}(t_0)$  is on  $B_\Omega$  and:

$$\dot{\vec{x}}_n(t_0) = \vec{n}(t_0) \cdot \dot{\vec{x}}(t_0) > 0 \quad (2.7)$$

where  $\vec{n}(t_0)$  is the unit vector normal to  $B_\Omega$  at  $\vec{x}(t_0)$ , with the positive

direction towards the exterior of  $\Omega$ . Intuitively, this means that at  $t_0$ , the sample function is just on the boundary  $B_\Omega$ , and has an outward velocity.

The approach used to find the outcrossing rate is a generalization of Rice's argument [34]. It is expressed as:

$$v_+ = \int_{B_\Omega} \int_0^\infty \dot{x}_n f_{\vec{X}, \dot{X}_n}(\vec{x}, \dot{x}_n) d\dot{x}_n d\vec{x} = \int_{B_\Omega} E_0^\infty[\dot{X}_n | \vec{X} = \vec{x}] f_{\vec{X}}(\vec{x}) d\vec{x} \quad (2.8)$$

where  $E_0^\infty[\cdot]$  denotes a partial (or positive tail) expectation.

We will study a particular class of cases. First, assume that we restrict ourselves to stationary Gaussian processes, then  $X_i(t)$  and  $\dot{X}_i(t)$  are independent. Further, if we assume  $X_i(t)$  and  $X_j(t)$  to be independent,  $i \neq j$ , it also follows that  $\dot{X}_i(t)$  and  $\dot{X}_j(t)$  are independent, and no covariance information is needed at all. Then, the partial expectation in 2.8 becomes a constant independent of  $x$ :

$$E_0^\infty[\dot{X}_n | \vec{X} = \vec{x}] = E_0^\infty[\dot{X}_n] \quad (2.9)$$

So, 2.8 becomes simply

$$v_+ = E_0^\infty[\dot{X}_n] f(B_\Omega) \quad (2.10)$$

where  $f(B_\Omega)$  is the probability density that  $\vec{X}(t)$  is on the boundary at any given time  $t$ .

Using the above assumptions makes a tractable equation for polyhedral regions in  $R^n$  possible. First, reduce all coordinates by dividing each component  $x_i$  through with the appropriate standard deviation  $\sigma_i$ . Let the failure boundary have  $m$  (hyperplanar) faces. Denote the  $i^{\text{th}}$  face as  $B_i$ ,

with a unit exterior normal  $\hat{n}_i$ . The  $j^{\text{th}}$  component of this normal is denoted here as  $n_{ij}$ . It can be shown that for this case, we may write the density  $f(B_i)$  as:

$$f(B_i) = \phi(r_i)\phi_{n-1}(B_i) \quad (2.11)$$

where  $r_i$  is the distance from the mean point  $E[\vec{X}]$  to the face  $B_i$  and  $\phi(r_i)$  is the standard normal density evaluated at this distance. Further,  $\phi_{n-1}(B_i)$  is the integral over  $B_i$  of the conditional density of  $\vec{X}$  given that  $\vec{X}$  is on the (infinite) hyperplane of which  $B_i$  is a part. This is in the form of an  $(n-1)$ -dimensional standard normal density with its mean at the orthogonal projection of the mean  $E[\vec{X}]$  on the hyperplane. This reduction of dimension is particularly useful in the solution of two dimensional problems, such as illustrated in figure 2.4.

Further consideration of face  $B_i$  yields another useful result. The partial expectation for this single face becomes:

$$E[\dot{X}_n]_i = \frac{\sigma_{ni}}{\sqrt{2\pi}} \quad (2.12)$$

where

$$\sigma_{ni}^2 = \sum_{j=1}^n n_{ij}^2 \sigma_{jj}^2$$

and where

$$\sigma_{jj}^2 = \text{Var}(\dot{X}_j)$$

that is, the variance of the  $j^{\text{th}}$  component of the derivative process.

Application of equations 2.10, 2.11, and 2.12 now leads to the desired result. Summing the rates of outcrossing through the individual faces:

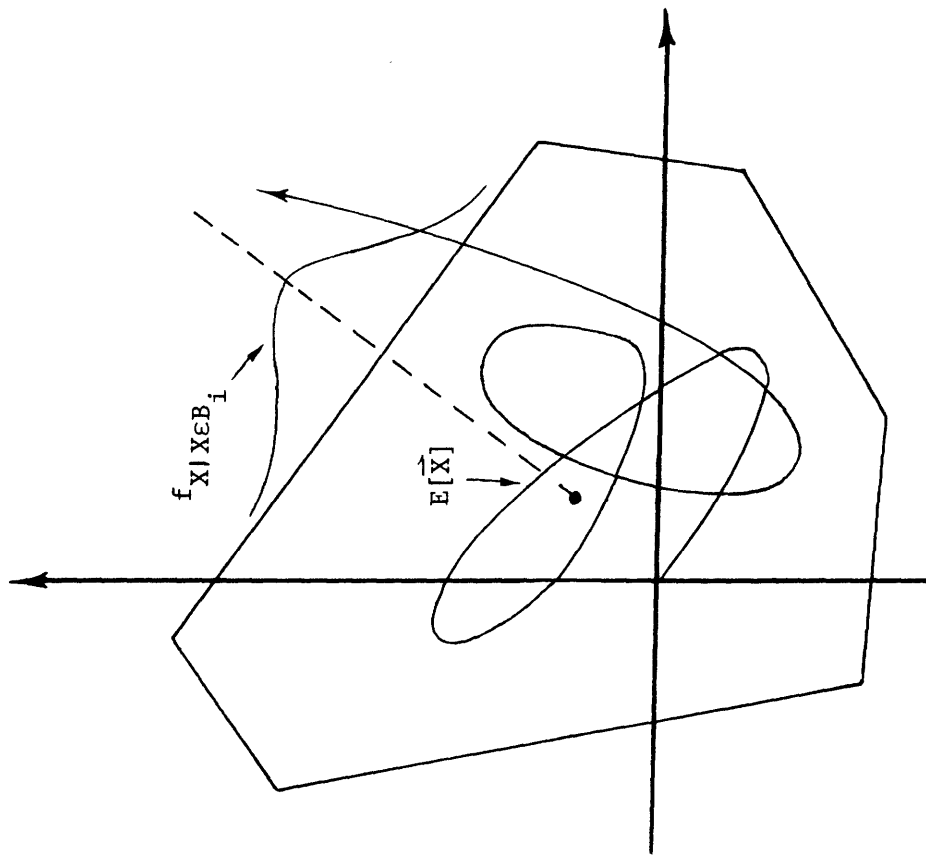


Figure 2.4: Outcrossing of a two dimensional Gaussian process.

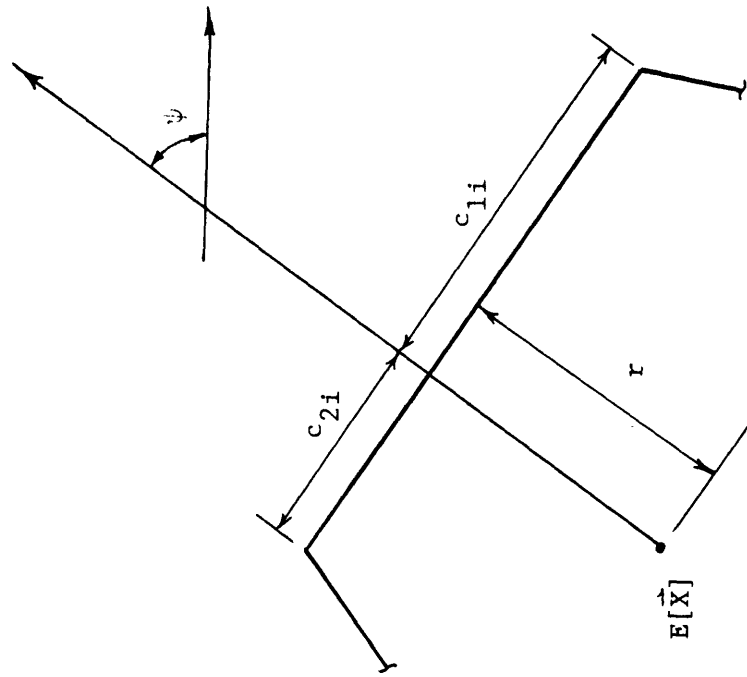


Figure 2.5: Details of the segment  $B_i$ .

$$v_+ = \frac{1}{\sqrt{2\pi}} \sum_{i=1}^m \left\{ f(B_i) \sqrt{\sum_{j=1}^n n_{ij} \sigma_{jj}^2} \right\} \quad (2.13)$$

This is simplified further if attention is focused on the two dimensional problem. In this case denote the components of  $\vec{n}_i$  as:

$$n_i = \begin{Bmatrix} \cos \psi_i \\ \sin \psi_i \end{Bmatrix}$$

and let  $O_i$  be the point on  $B_i$  closest to the mean  $E[\vec{X}]$ . Then,  $B_i$  may be split into two segments, from each vertex of  $B_i$  to  $O_i$ , as illustrated in figure 2.5 (unless  $O_i$  is itself at a vertex). Let the algebraic distances from the vertices of  $B_i$  to  $O_i$  be  $c_{1i}$  and  $c_{2i} > c_{1i}$ . Using these symbols, equation 2.13 becomes:

$$v_+ = \frac{1}{2\pi} \sum_{i=1}^m [\Phi(c_{2i}) - \Phi(c_{1i})] (\sigma_{11}^2 \cos^2 \psi_i + \sigma_{22}^2 \sin^2 \psi_i)^{1/2} \exp(-r_i^2/2) \quad (2.14)$$

This is the result of this section that is used later in this chapter to actually calculate outcrossing rates.

We would like to use these results to study the modified square wave process. However, to apply the result 2.14, we must supply stochastic process information in the form of  $\sigma_{11}$  and  $\sigma_{22}$ . These parameters have no direct analogues in the square wave process, since the derivative of the square wave process does not exist. Yet, we may still attempt to achieve comparable results by selecting  $\sigma_{11}$  and  $\sigma_{22}$  in some reasonable way. We choose to do this by matching the mean rate of crossings of the mean level of each load process, acting individually, for both the modified square

wave and Gaussian process formulations. For process 1 and the modified square wave formulation:

$$v_+ = [p_1 + q_1 F_1(\mu)][q_1 - q_1 F_1(\mu)]v_1 = [p_1 q_1 + (q_1^2 - p_1 q_1)F_1(\mu) - q_1^2 F_1^2(\mu)]v_1 \quad (2.15)$$

Assume  $F_1(\mu)$  to refer to the mean of a normal distribution; then, it is simply evaluated as 0.50. So, equation 2.14 becomes:

$$v_+ = (0.50 p_1 q_1 - 0.25 q_1^2)v_1 \quad (2.16)$$

Use equation 2.13 with  $m = 1$ ,  $\psi_i = 0$ , and  $\Phi(c_{2i}) - \Phi(c_{1i}) = 1$ , to account for an infinite straight line parallel to the x axis. With  $r_i = 0$  to place this line through the mean:

$$v_+ = \frac{1}{2\pi} \sigma_{11} \quad (2.17)$$

Equating the right hand sides of 2.15 and 2.16, we get:

$$\sigma_{11} = \pi(p_1 q_1 - 0.50 q_1^2)v_1 \quad (2.18)$$

A similar result holds for process 2.

All of the mathematics necessary to this chapter are now at hand. The following sections will deal with their application.

### 2.3 Case Studies: Reinforced Concrete Columns

Let us consider an example of a reinforced concrete column subject to wind, live floor, and gravity dead loads. Assume the structural interaction defined by equation 1.9, but with L replaced by D + L. Treat D as a constant in any particular case, a nominal (mean) value in the same sense that the interaction diagram defines the nominal resistance of the column.

Less explicitly, the same end could be sought by raising the mean live load,  $\mu_L$ , by an appropriate amount. However, the chosen approach has the advantage of limiting the variability in the floor load to that actually imposed by the live load process, therefore leaving the dead load both deterministic and constant in time, as it is commonly assumed to be. Flexibility in choosing a dead to live load ratio is also maintained.

Consideration of random (though constant in time) dead load is conceptually straightforward. Equations 2.5 and 2.14, for either the jump or continuous process formulations can be viewed as conditional results, given a particular value of dead load. In each case then, replace the left hand side,  $v_+$ , with  $v_{+|D}$ . Assuming the dead load to be independent of the other load processes, denote its distribution as  $f_D(s)$ . Then:

$$v_+ = \int_0^{\infty} v_{+|D} f_D(s) ds \quad (2.19)$$

is the true mean rate of outcrossings, accounting for random dead load.

We shall explore this example three times. Each particular combination of an interaction diagram and a matrix  $[C]$  will be referred to here as a study. Each study will consist of at least three cases, which here refer to sets of parameters characterizing the individual load processes. The purpose of these studies is twofold. First, we shall examine the behavior of equations 2.5 and 2.13 by comparing the rates obtained for different cases. Then, we shall proceed to the main tasks of finding out whether and how a failure boundary may be linearized.

### 2.3.1 Parameter Selection

The studies have been chosen in such a way as to represent situations



that may be encountered in practice, as far as possible. Interaction diagrams used here are from a paper dealing with column strength [18], and may also be found in reference and text books, such as [41].

These diagrams have been presented in nondimensional form, based on ratios of parameters. Parameters that have not been previously introduced here are listed below:

$e$  = ratio of ultimate moment to ultimate axial force,  $M_u/P_u$

$b$  = section width

$h$  = total section depth

$\theta h$  = depth between reinforcing layers

$f'_c$  = concrete (crushing) strength

and

$$\rho\mu = \frac{A_s f_y}{0.85\theta b h f'_c}$$

where

$A_s$  = reinforcing steel area

$f_y$  = yield strength of reinforcing

Geometrical parameters are illustrated in figure 2.6.

Since the columns are symmetric, each interaction diagram may be reflected about its vertical axis. This describes behavior in the region of (positive) axial force and negative bending moment. Furthermore, assume no net tensile strength, therefore restricting each diagram to the region of positive axial force. This convention serves to close each diagram into a convex polygon.

The interaction diagrams and [C] matrices used in this work are pre-

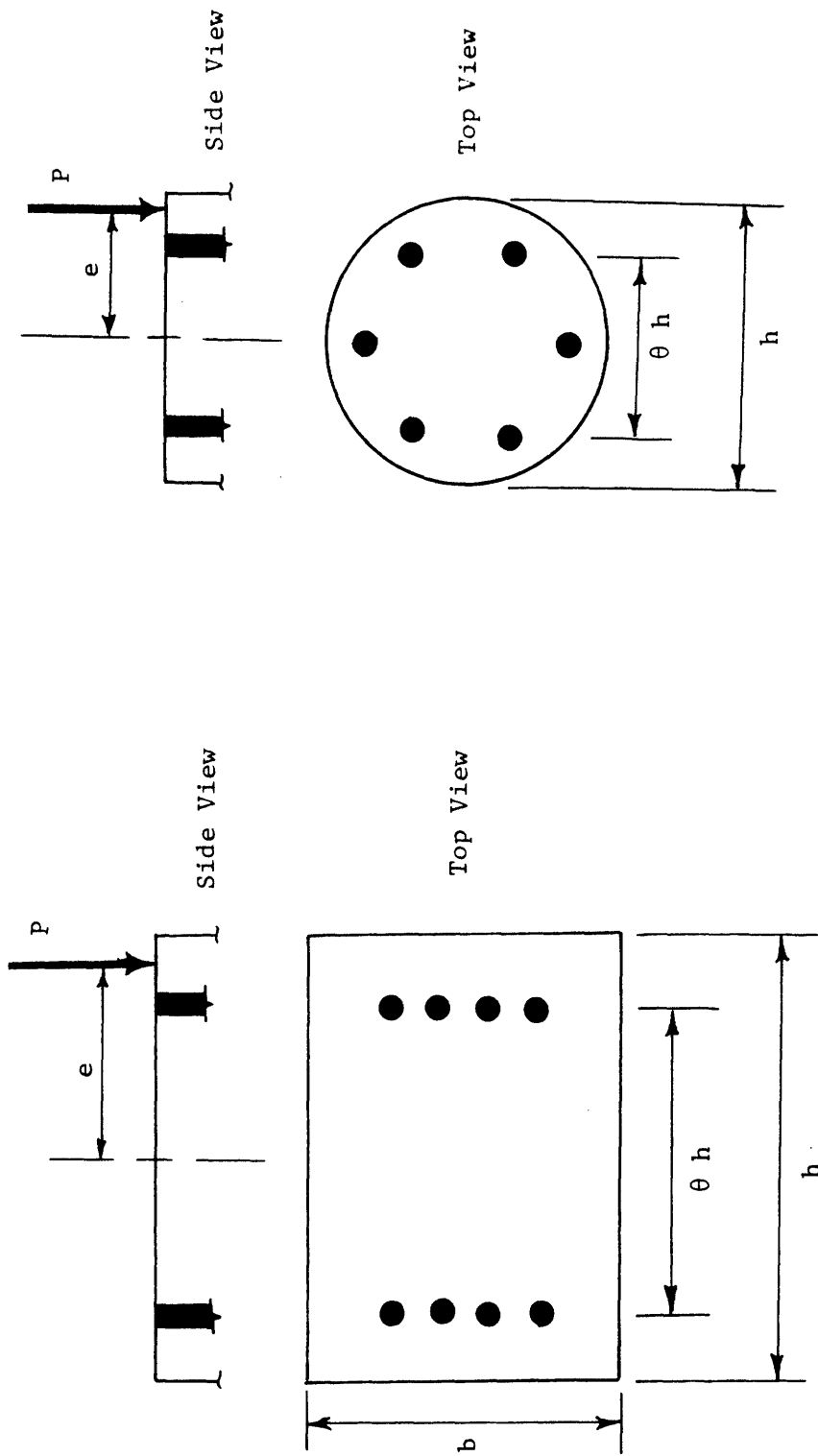


Figure 2.6: Reinforced concrete column parameters.

sented at the beginning of each individual study, along with the reasoning behind their selections.

Load parameter values that define individual cases were suggested in part by McGuire's report [29]. Floor live load was modeled as the "sustained" live load in the report. To represent a building without vacancies,  $p$  was chosen as zero. Also, the renewal rate of the live load process was chosen as  $v_L = 0.125$  (per year), the value used in the report. Finally, a value of 57% for the coefficient of variation of the live load was used in the report, and is used in most cases here.

Judgement had to be exercised in the selection of reasonable values for other parameters, however. For the dead load  $D$ , values of 150, 100, and 75 (lbs. per ft.<sup>2</sup>) were chosen to represent normal, lightweight, and very lightweight construction, respectively. Dead to mean live load ratios of 3:1 or 2:1 were used. The parameter  $p_w$  was chosen in all cases as 0.9977. So, with  $v_w = 2190$ , we have a mean rate of

$$(1 - 0.9977)2190 = 5$$

storms per year. With  $v_w = 1314$ :

$$(1 - 0.9977)1314 = 3$$

storms per year is the mean rate of arrival. Further, the storms have mean durations of:

$$(1/2190)(8760 \text{ hrs./yr.}) = 4.00 \text{ hours}$$

$$(1/1314)(8760 \text{ hrs./yr.}) = 6.67 \text{ hours}$$

in these respective cases, or a total of 20 hours per year, either way. Mean wind pressures of 10 to 35 (lbs. per ft.<sup>2</sup>) were used; with a stan-

standard deviation of 5.0, this corresponds to coefficients of variation from 14% to 50%.

The values used for the stochastic load process parameters are presented in tabular form with each study.

### 2.3.2 Computational Procedures

Before proceeding, the computational procedures necessary to carry out the case studies will be briefly discussed.

Equation 2.5 for modified square wave processes has been evaluated using Simpson's rule by a Fortran computer program. We shall refer to this program as the Outcrossing Rate Program, O.R.P. for short. A listing and a summary of O.R.P.'s input formats is given in the appendix.

As input, O.R.P. accepts the following:

1. The matrix [C].
2. The column interaction diagram, in a point-by-point form.
3. The parameters  $v_w$ ,  $p$ ,  $\mu_w$ ,  $\sigma_w$ ,  $v_L$ ,  $\mu_L$ ,  $\sigma_L$ , and D.

Furthermore, either normal or gamma distribution functions can be specified for either load process.

As output, O.R.P. yields:

1. The transformed interaction diagram in terms of wind and floor loads, and the extrema pertaining to this diagram.
2. The four paths from extrema to extrema, as illustrated in figure 2.3, and the x and y axis intercepts.
3. The value of the mean outcrossing rate (including the individual contributions due to each load process as well as the sum).

One precaution should be taken when using the program with linear

boundaries. By specifying the identity matrix for [C], such boundaries may be input directly; that is, the transformation will not change the diagram. This boundary should not take the form of vertical or horizontal lines, such as the axes, however. Either zero or infinite slopes along portions of the failure boundary may confuse the routines that search for extremum points and result in invalid output.

Equation 2.14 for continuous Gaussian processes may be evaluated by hand. When doing so, it is helpful to proceed in the following manner:

1. Reduce the coordinates of the transformed interaction diagram (from O.R.P. or hand calculations) by division by the appropriate standard deviations; so the points  $W^*$  and  $L^*$  become  $W^*/\sigma_W$  and  $L^*/\sigma_L$ .
2. Find the reduced means, corresponding to  $\mu_W/\sigma_W$  and  $(D + \mu_L)/\sigma_L$ .
3. Find the points  $O_i$ , and the distances to the mean,  $r_i$ .
4. Find the distances  $c_{1i}$  and  $c_{2i}$ , and then use standard tables to evaluate  $\Phi(c_{1i})$  and  $\Phi(c_{2i})$ .
5. Having tabulated all of the above, compute the crossing rate due to each segment, and then sum all of these rates.

Step 3 amounts to an elementary exercise in analytic geometry. However, for the purpose of checking for errors, it is useful to make plots or geometric constructions as one proceeds.

### 2.3.3 Study 1

The first column chosen has a rectangular section with  $\theta = 0.90$  and  $\rho\mu = 0.50$ . This section is deep and well suited to bending, and moderately reinforced. Assume the following interaction matrix:

$$\begin{bmatrix} 6.0 \times 10^{-3} & 1.5 \times 10^{-4} \\ 6.0 \times 10^{-4} & 2.25 \times 10^{-3} \end{bmatrix}$$

(all in units of  $\text{ft.}^2/\text{lb.}$ ). This corresponds to a situation such as follows. Most of the axial effects are due to the vertical loading and most of the bending to the wind, but there are significant effects due to the off diagonal terms. Column eccentricity translates vertical loads into bending effects. Wind load adds to axial forces, such as may be the case when the column is not near the centroid of the building.

The interaction diagram, showing the mean load effects for cases A, B, and C as well, is shown in figure 2.7. After it has been mapped to load space, it assumes the form of figure 2.8. Since the off diagonal terms of  $[C]$  are about an order of magnitude less than those on the diagonal, the diagram has not been badly distorted.

To facilitate evaluation of  $v_+$  by equation 2.14, the coordinates on the latter diagram were reduced by division with  $\sigma_w$  and  $\sigma_L$ . The resulting diagram is shown in both figures 2.9 and 2.10. It was noted that the segment closest to the mean made the greatest single contribution to the outcrossing rate in each case, with the next largest contribution owing to an adjacent segment. This suggested that linearizations of the failure surface be made by simply extending the segment closest to the mean in any given case. This minimization of  $r$  corresponds to the criterion suggested in the papers by Hasofer and Lind [25] or Ditlevsen and Skov [17]. Figures 2.9 and 2.10 also illustrate the linearizations.

Outcrossing rate results for the different methods are plotted versus  $r$  and shown in figure 2.11. The top curve shows the results of equation 2.14, and the points below it the results based on the same continuous process but with the failure surface linearized. The lower curve shows the results for the jump process (equation 2.5) assuming normal distributions

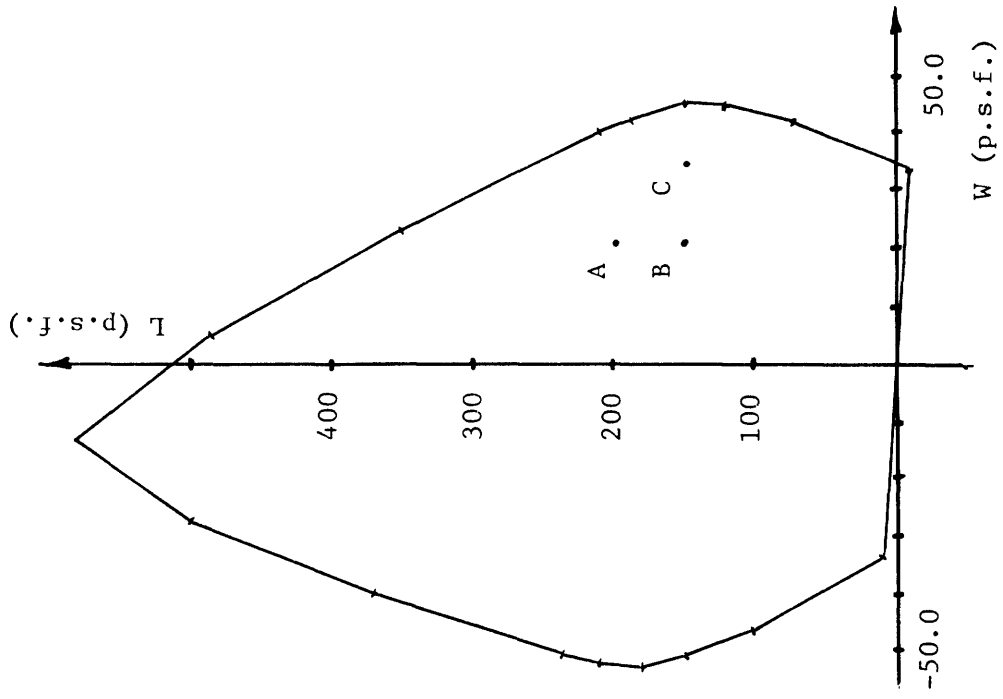


Figure 2.8: Interaction diagram in load space, study 1.

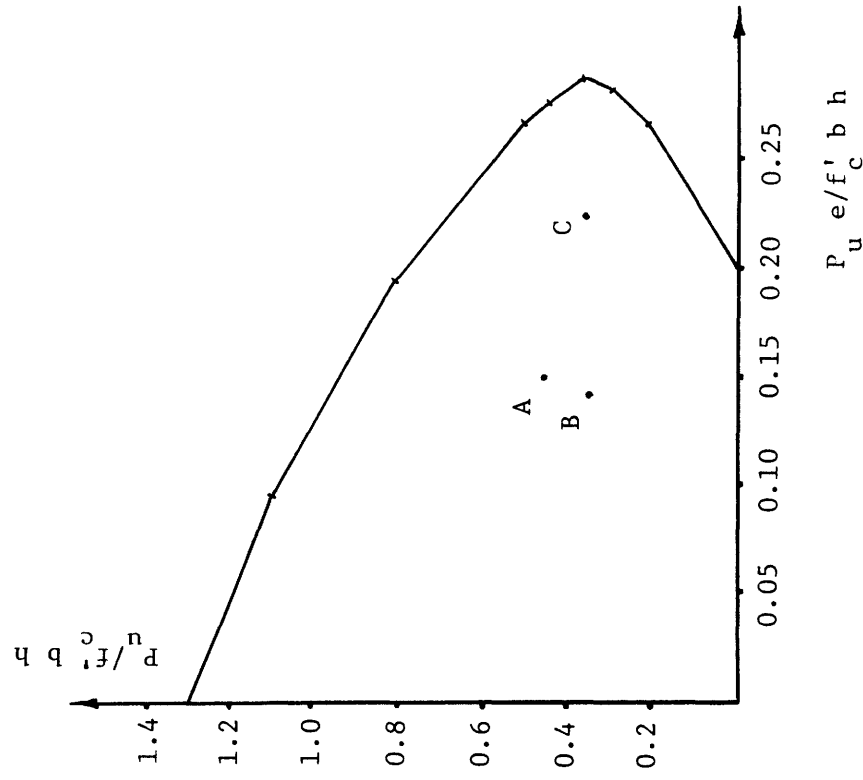


Figure 2.7: Interaction diagram in load effect space, study 1.

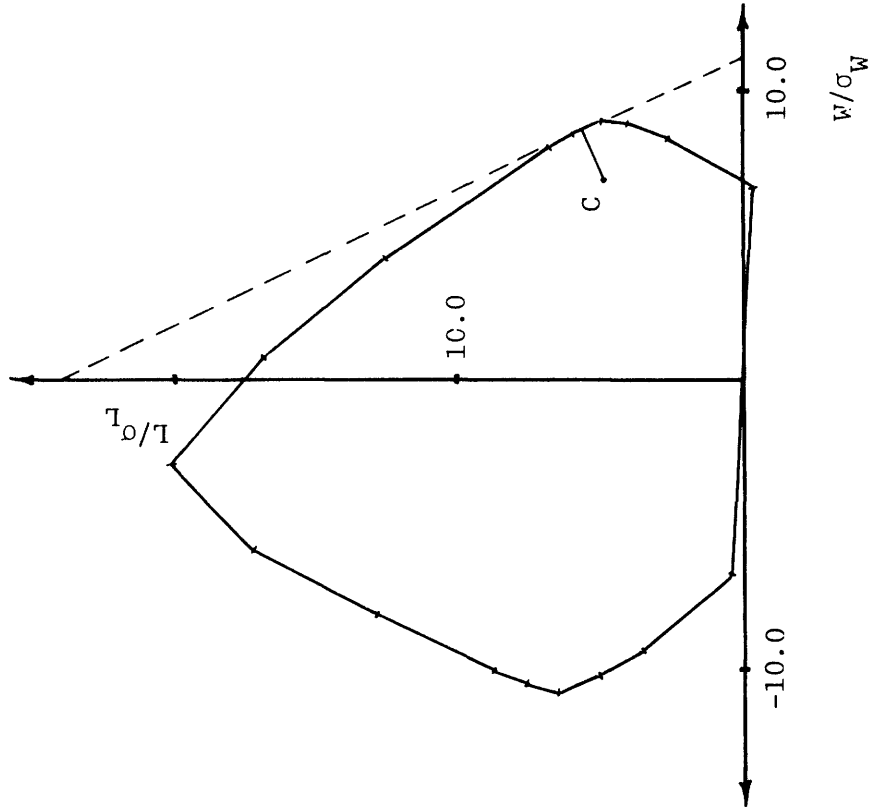
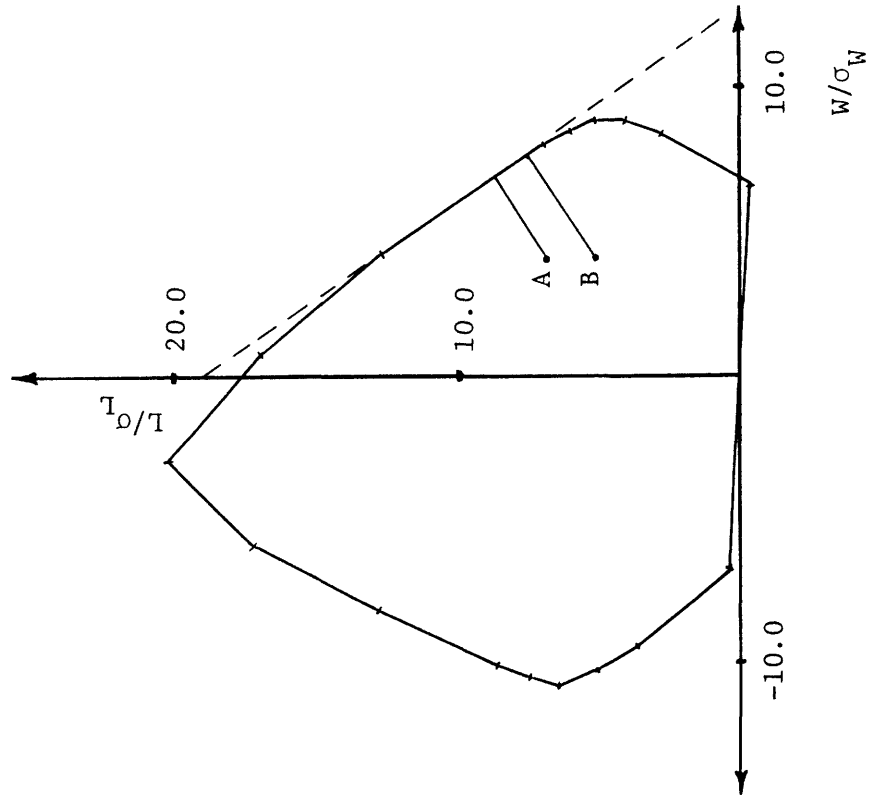


Figure 2.9: Reduced space diagram, cases 1A and 1B.

Figure 2.10: Reduced space diagram, case 1C.



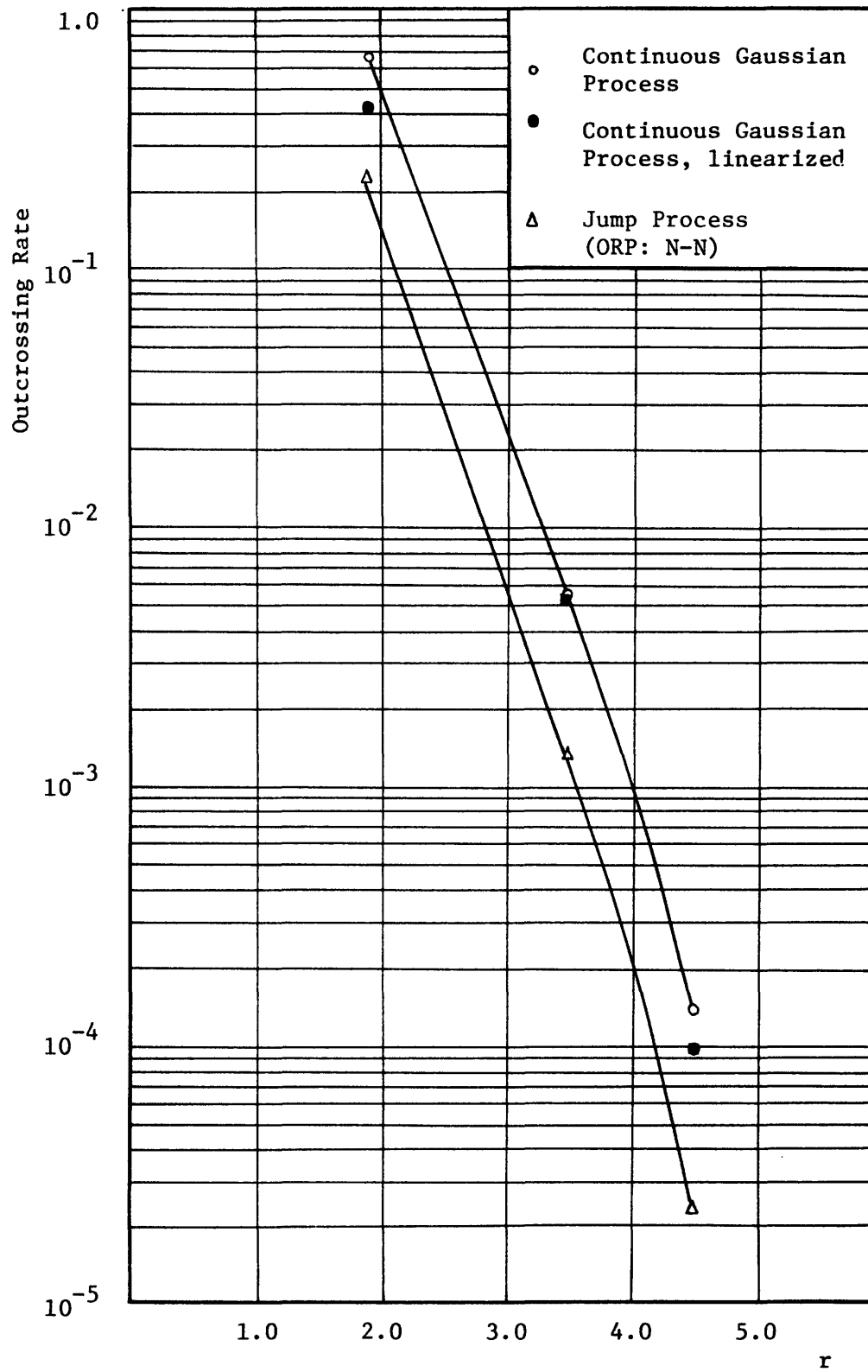


Figure 2.11: Continuous and jump process results, study 1.

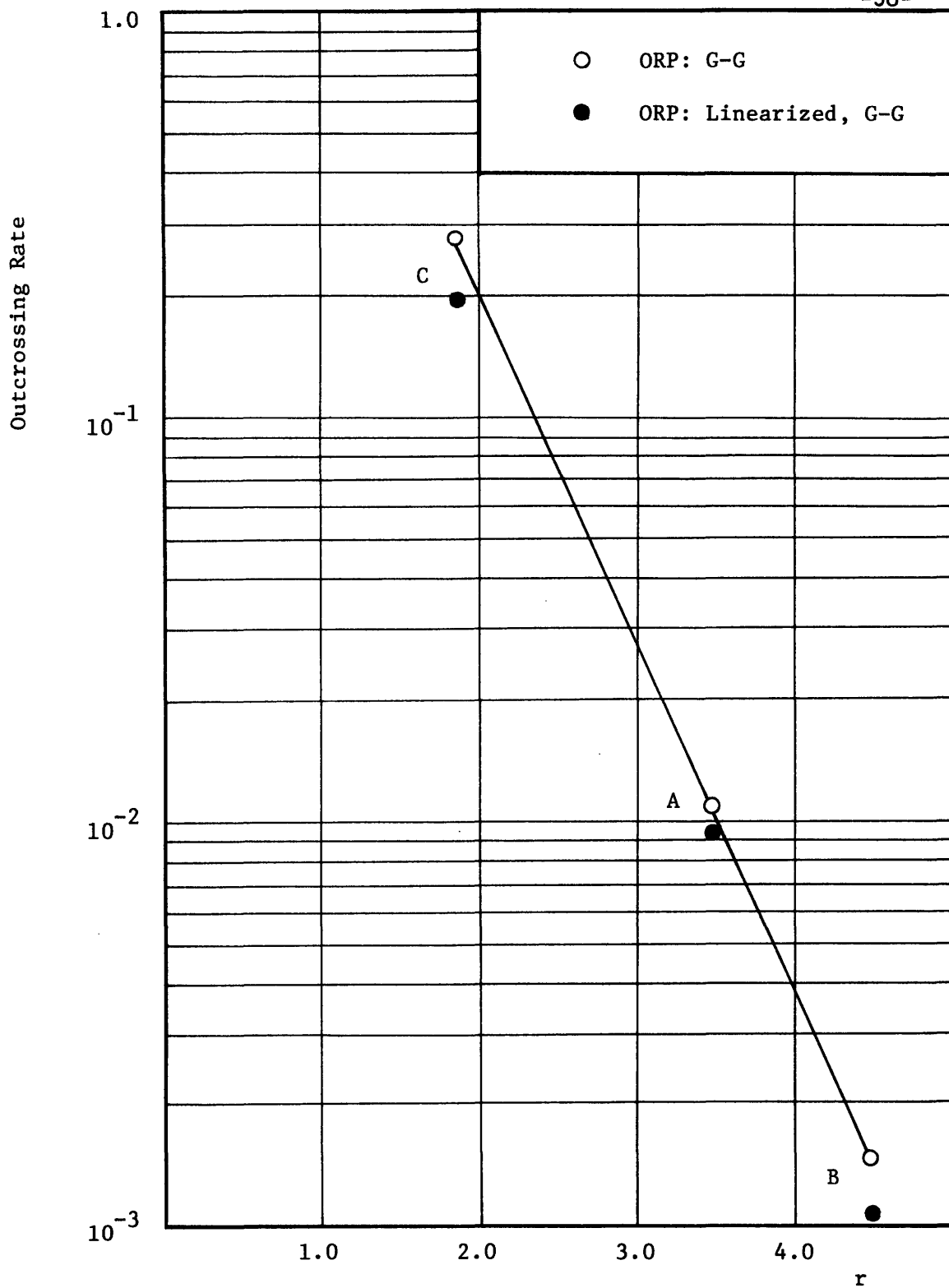


Figure 2.12: Linearizations of the jump process, study 1.

on each load. All of the plots are smooth curves that are almost straight lines on semilog paper. The curvature that does exist might be attributed to the fact that the tail of a normal distribution decays at a greater than exponential rate.

The linearizations were in error by 37%, 4.8%, and 30% for cases C, A, and B (listed with respect to increasing  $r$ ). All of these errors are in the form of underestimates. This is due to the nature of the failure diagram; it is convex, and therefore, the linear segments are always on or beyond its boundary. No relationship between the magnitude of the error and  $r$  has been found in this or in the other studies. Instead, the reason case A gave the least error seems to be that it is nearer the center of the segment (that A and B are both closest to) and this segment is much longer than the closest segment to C. However, using this concept does not help to formulate an objective criterion to predict or judge the magnitude of the error.

Then, the jump process was used to find the outcrossing rates for both the full and linearized boundaries, assuming gamma distributions on both load processes. These results are plotted on figure 2.12. Note that the results based on the full boundary now fall on a straight line, due apparently to the nearly exponential nature of the gamma tail. However, the errors caused by linearization have become 28%, 12%, and 30% respectively. The only apparent conclusion is that for these cases use of gamma distributions made the error less sensitive to the position of the mean point than use of normal distributions.

All of the results are summarized in table 2.1.

Although the method of linearization is unconservative, it was judged

Table 2.1: Parameter Values and Results for Study 1

Case	$\nu_w$	$p$	$\mu_w$	$\sigma_w$	$\nu_L$	$\mu_L$	$\sigma_L$	$D$
A	2190	0.9977	20.0	5.0	0.125	50.0	28.6	150.0
B	2190	0.9977	20.0	5.0	0.125	50.0	28.6	100.0
C	2190	0.9977	35.0	5.0	0.125	50.0	28.6	100.0

Case	$r$	Equation 2.14			Outcrossing Rate Program		
		Full $\Omega$	Line	N-N	G-G	Line (G-G)	
A	3.47	$5.24 \times 10^{-3}$	$5.06 \times 10^{-3}$	$1.33 \times 10^{-3}$	$1.07 \times 10^{-2}$	$9.46 \times 10^{-3}$	
B	4.46	$1.39 \times 10^{-4}$	$9.71 \times 10^{-5}$	$2.47 \times 10^{-5}$	$1.48 \times 10^{-3}$	$1.06 \times 10^{-3}$	
C	1.84	$6.68 \times 10^{-1}$	$4.17 \times 10^{-1}$	$2.22 \times 10^{-1}$	$2.77 \times 10^{-1}$	$1.94 \times 10^{-1}$	

to be acceptable for this study. The reason is that it still gives estimates within the proper order of magnitude, which may be all that is required, and that it works about as well for either gamma or normal distributions. However, both A and B fell near a long linear segment. It was decided to test this method again with an interaction diagram with a more constant curvature. This is done in study 2.

#### 2.3.4 Study 2

The column chosen for this study is circular in section, with a value of  $\theta = 0.60$  only. Such a section is efficient only for withstanding axial force, not well suited to bending. Interaction was assumed as:

$$\begin{bmatrix} 3.5 \times 10^{-3} & 8.0 \times 10^{-5} \\ 0.0 & 2.40 \times 10^{-3} \end{bmatrix}$$

This corresponds to reducing the coefficients that result in bending moment from the levels assumed in the first study. The zero term expresses that axial effects due to wind load have been neglected. A slight increase in the transformation from vertical load to axial effect has also been made.

The interaction diagram in load effect space is shown in figure 2.13. It is typical of diagrams for circular columns, with the nearly constant curvature desired of the failure boundary.

The diagram in reduced space and its linearizations are shown in figure 2.14. Results are summarized in table 2.2, and plotted on figures 2.15 and 2.16.

In one aspect, study 2 resembles study 1 with respect to results for  $v_+$ . The curve for the continuous Gaussian process and the curve for the jump process with normally distributed loads are similar. Again, the

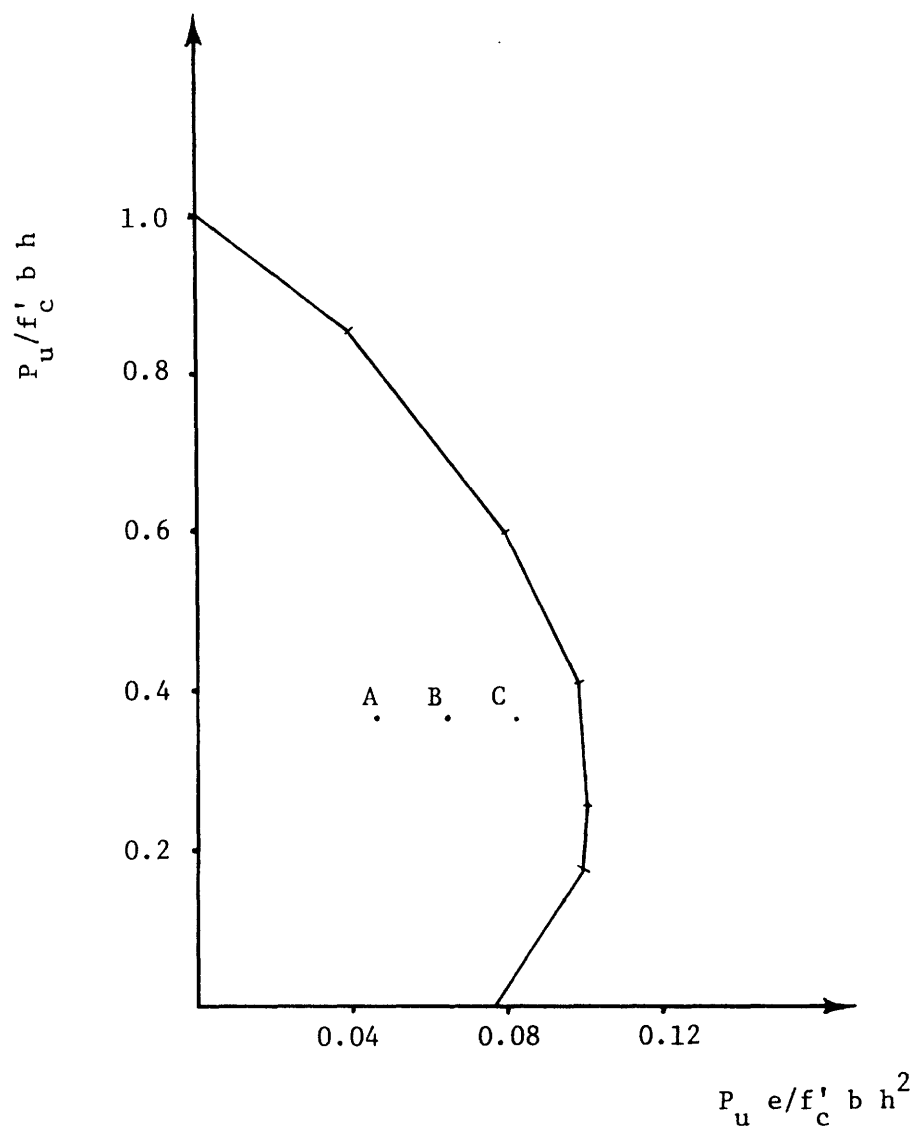


Figure 2.13: Interaction diagram in load effect space, study 2.

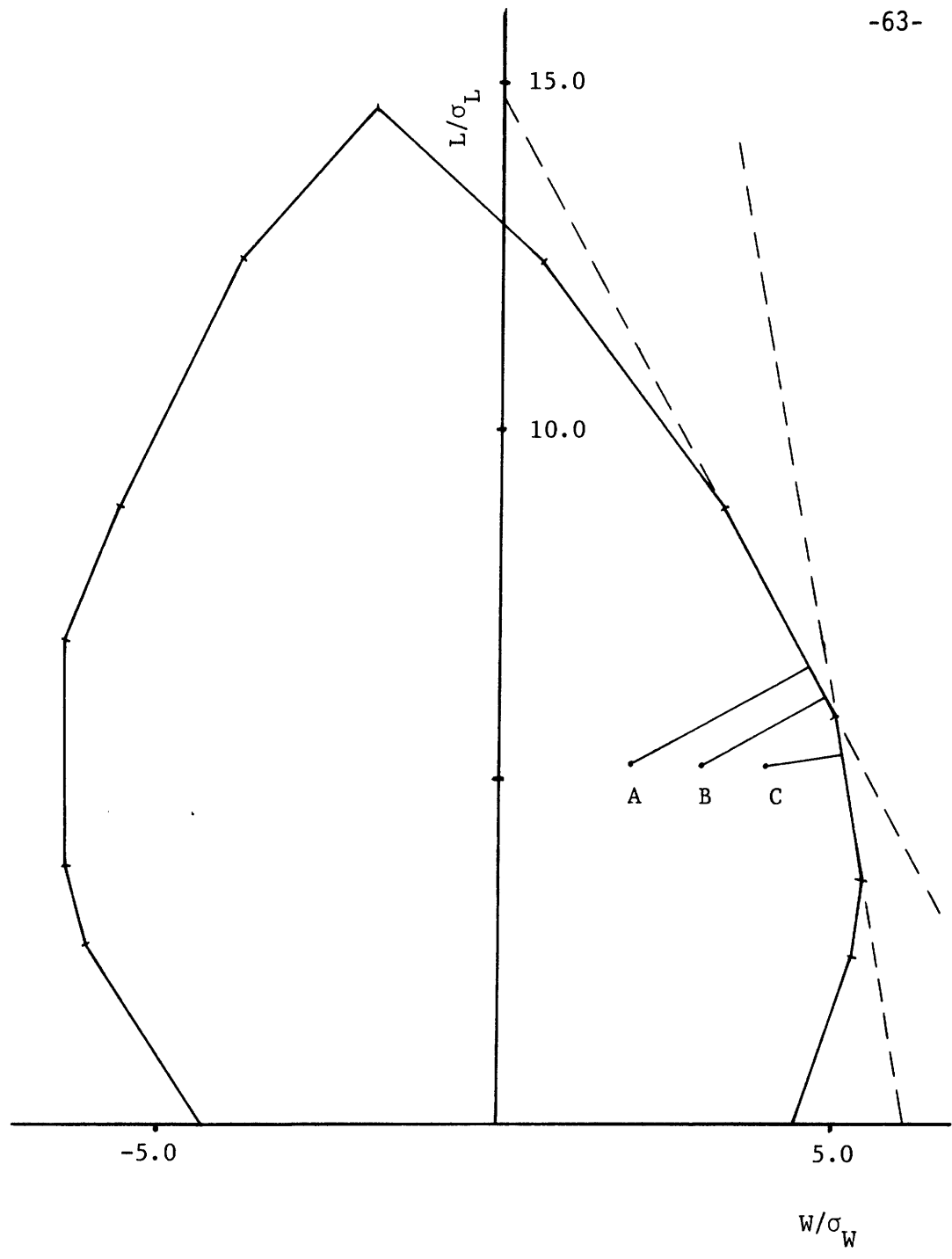


Figure 2.14; Reduced space diagram, study 2.

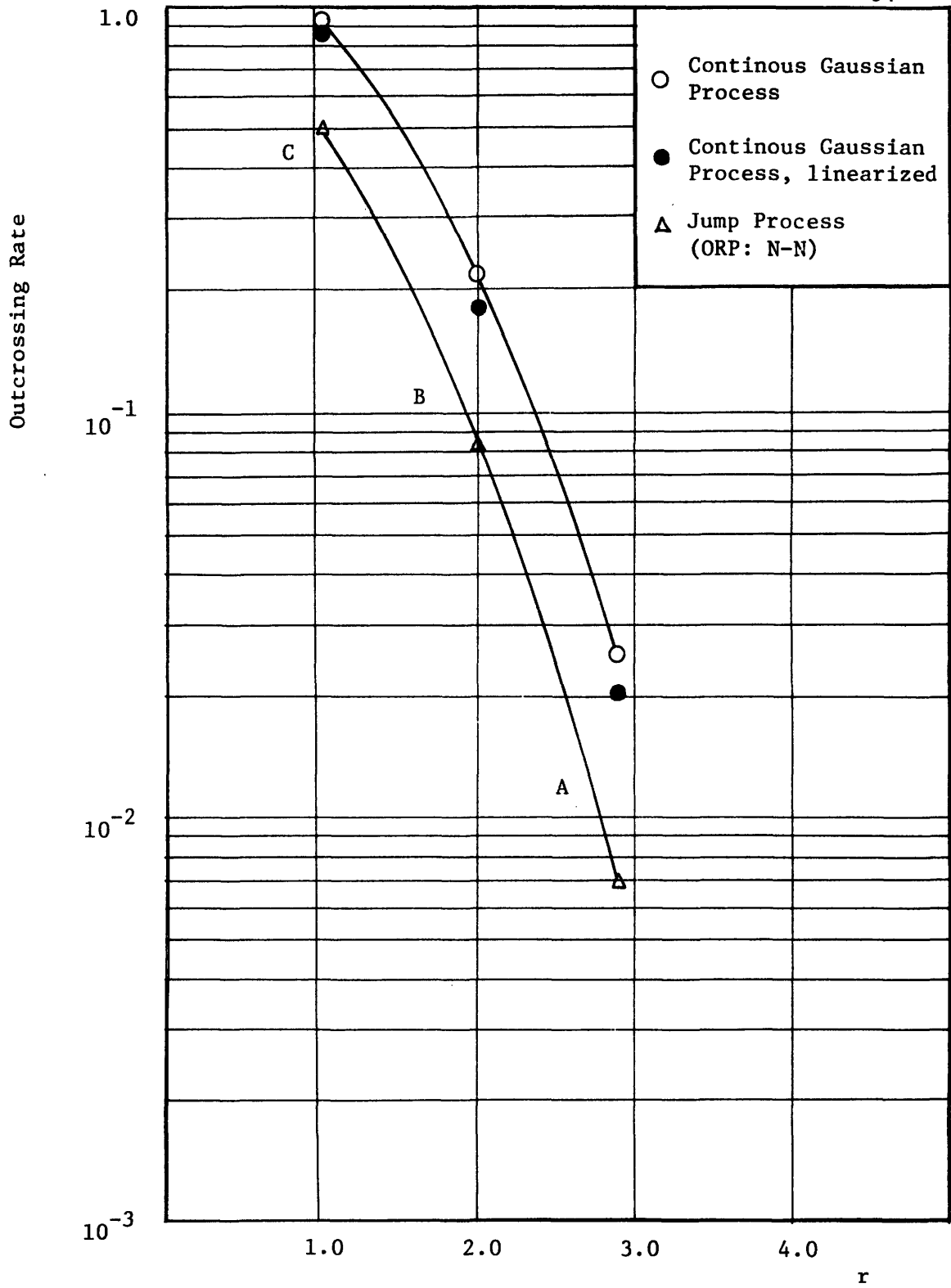


Figure 2.15: Continuous and jump process results, study 2.



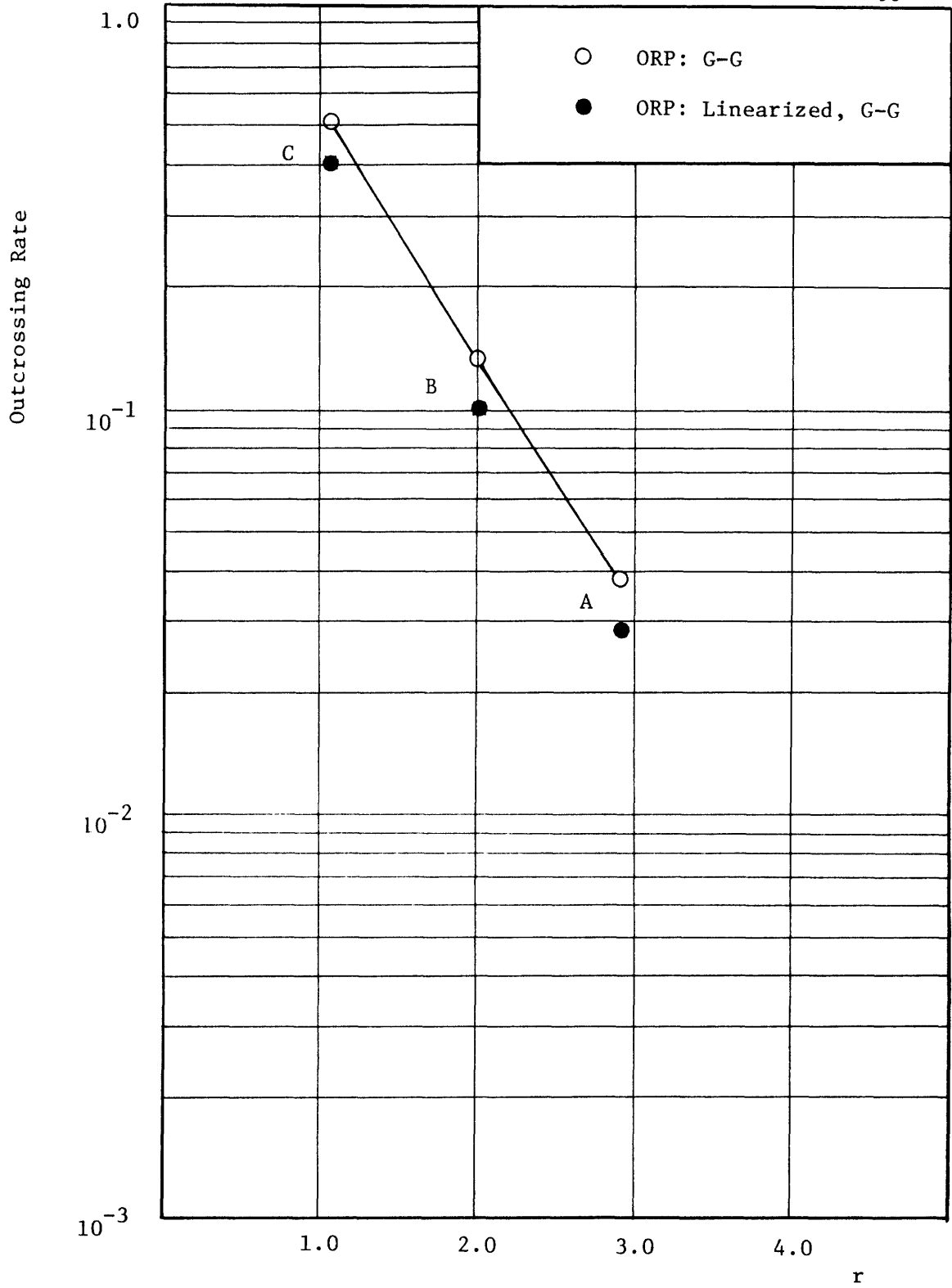


Figure 2.16: Linearizations of the jump process, study 2.

Table 2.2: Parameter Values and Results for Study 2

Case	$\nu_w$	$p$	$\mu_w$	$\sigma_w$	$\nu_L$	$\mu_L$	$\sigma_L$	$D$
A	1314	0.9977	10.0	5.0	0.125	50.0	28.6	100.0
B	1314	0.9977	15.0	5.0	0.125	50.0	28.6	100.0
C	1314	0.9977	20.0	5.0	0.125	50.0	28.6	100.0

Equation 2.14

Outcrossing Rate Program

Case	$r$	Equation 2.14			Outcrossing Rate Program		
		Full $\Omega$	Line	N-N	G-G	Line (G-G)	
A	2.89	$2.52 \times 10^{-2}$	$2.07 \times 10^{-2}$	$6.81 \times 10^{-3}$	$3.79 \times 10^{-2}$	$2.88 \times 10^{-2}$	
B	2.00	$2.17 \times 10^{-1}$	$1.79 \times 10^{-1}$	$8.40 \times 10^{-2}$	$1.33 \times 10^{-1}$	$1.01 \times 10^{-1}$	
C	1.05	$9.42 \times 10^{-1}$	$8.70 \times 10^{-1}$	$4.99 \times 10^{-1}$	$5.03 \times 10^{-1}$	$4.28 \times 10^{-1}$	

latter curve gives the appearance of having been translated down a constant distance from the former curve. Perhaps if another criterion (rather than equation 2.18) were used to match the processes, the curves could be brought into coincidence.

Error of linearization ranged from 7.6% to 24% in this study. Generally, errors are smaller than in study 1.

There was an even weaker link between the results assuming gamma versus normal distributions, however. While case C gave the least error for the Gaussian process result, only 7.6%, it gave nearly the worst of any errors due to linearization, 15%, assuming gamma distributions. So, while the continuous process formulation has suggested a method of failure surface linearization that has so far been effective for jump processes and gamma distributions, it cannot predict the error associated with linearization for the latter process.

The first two studies have still failed to find many limits of usefulness of this method of linearization. A third study was therefore carried out.

### 2.3.5 Study 3

Again, a rectangular section was chosen, this time with  $\theta = 0.70$ . This section is not as deep as that used for study 1; in fact, it may be assumed to be a square section. Structural interaction was assumed as:

$$\begin{bmatrix} 6.0 \times 10^{-3} & 0.0 \\ 5.0 \times 10^{-3} & 2.0 \times 10^{-3} \end{bmatrix}$$

The zero term indicates that bending effects due to floor loads are entirely negligible. This may be the result of pinned connections to the rest

of the structural system, and balanced loading on all spans that frame into the column. However, all of the other terms in the matrix are of the same magnitude, which means that axial effects due to wind are especially important in this study.

The interaction diagram in load effect space is shown in figure 2.17. The locations of points corresponding to mean effects for cases A through E are scattered over a wide portion of the diagram.

However, the plot in reduced space shows A, B, C, and D at relatively similar locations. In fact, all four are linearized in the same way as shown on figure 2.18.

Case E, with very light vertical load, is entirely different. This is illustrated by figure 2.19. The segment closest to E has a positive slope. It corresponds to an entirely different mode of failure. Whereas all previous failure modes represented linearly corresponded to overloads, this mode instead corresponds to a tensile failure, caused by removal of axial load.

Results are summarized in table 2.3. The footnotes to the last column will shortly be explained.

The results based upon continuous Gaussian processes or modified square waves with normal distributions are given in figure 2.21. Note that the last points, corresponding to E, behave strangely. Both curves show upturns because of E. This is due to the fact that all four of the segments nearest to E make significant contributions to the outcrossing rate, instead of only one or two as with cases A through D. However, this leads to an especially inaccurate linearization. The error based on the continuous process is 65%, because only one segment is linearized. In fact, this

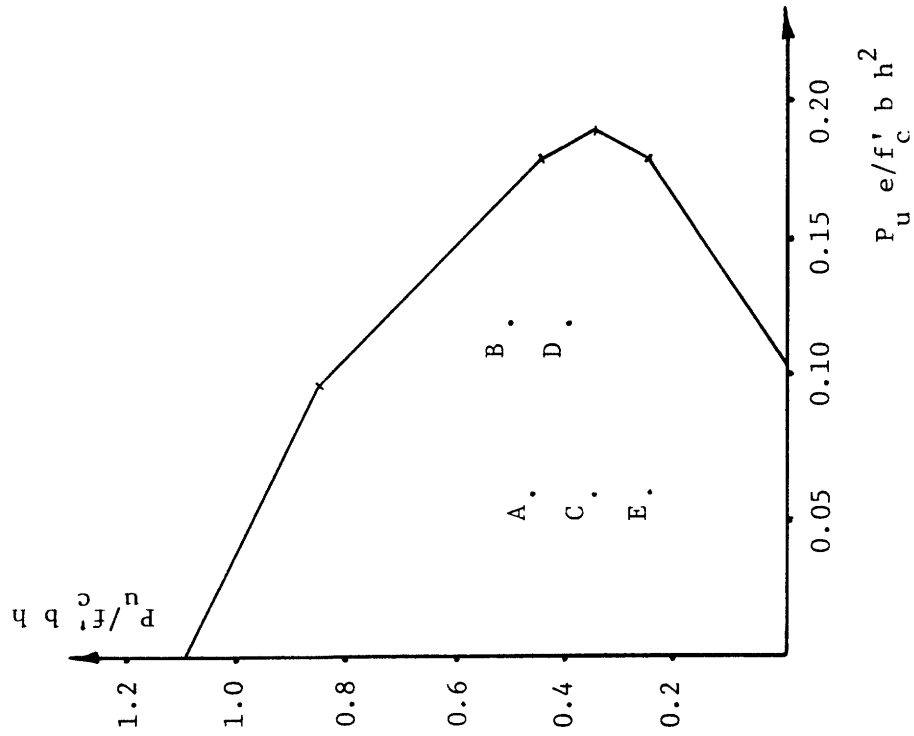


Figure 2.17: Interaction diagram in load effect space, study 3.

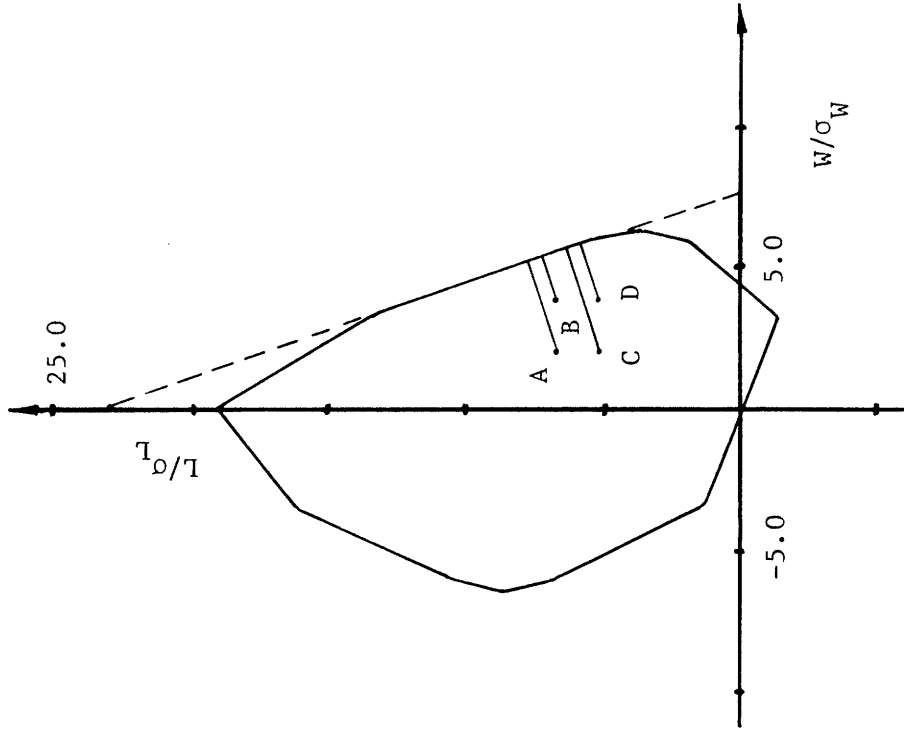


Figure 2.18: Reduced space diagram, study 3, cases A - D.

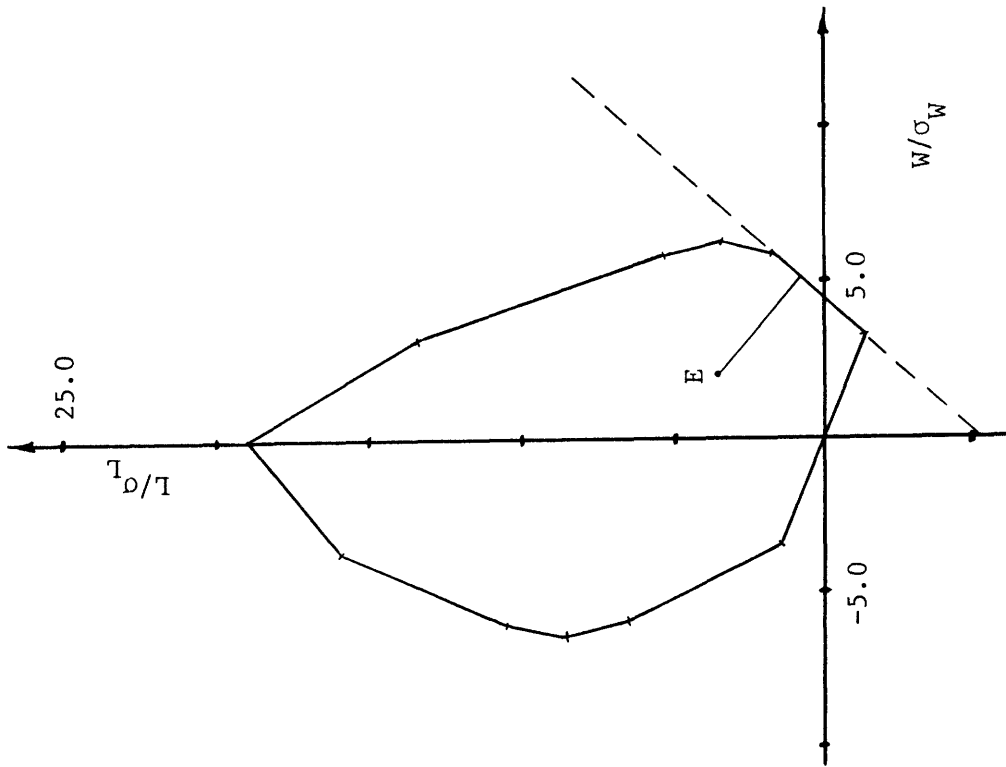


Figure 2.19: Reduced space diagram, case 3E.

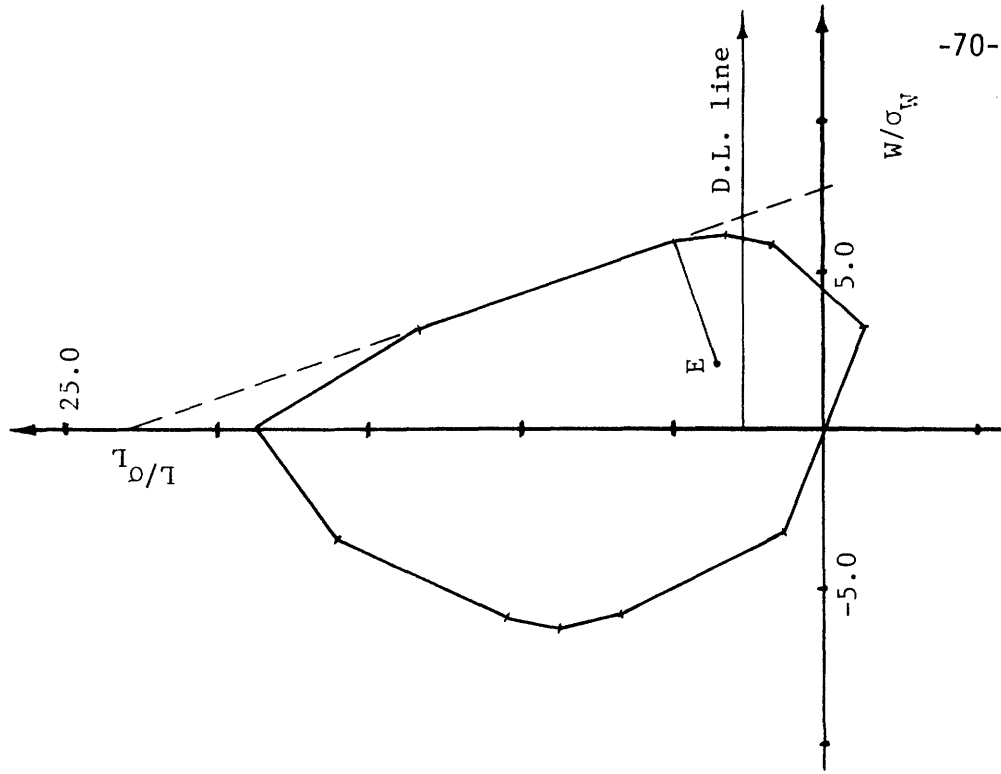


Figure 2.20: Reduced space diagram and amended linearization, case 3E.

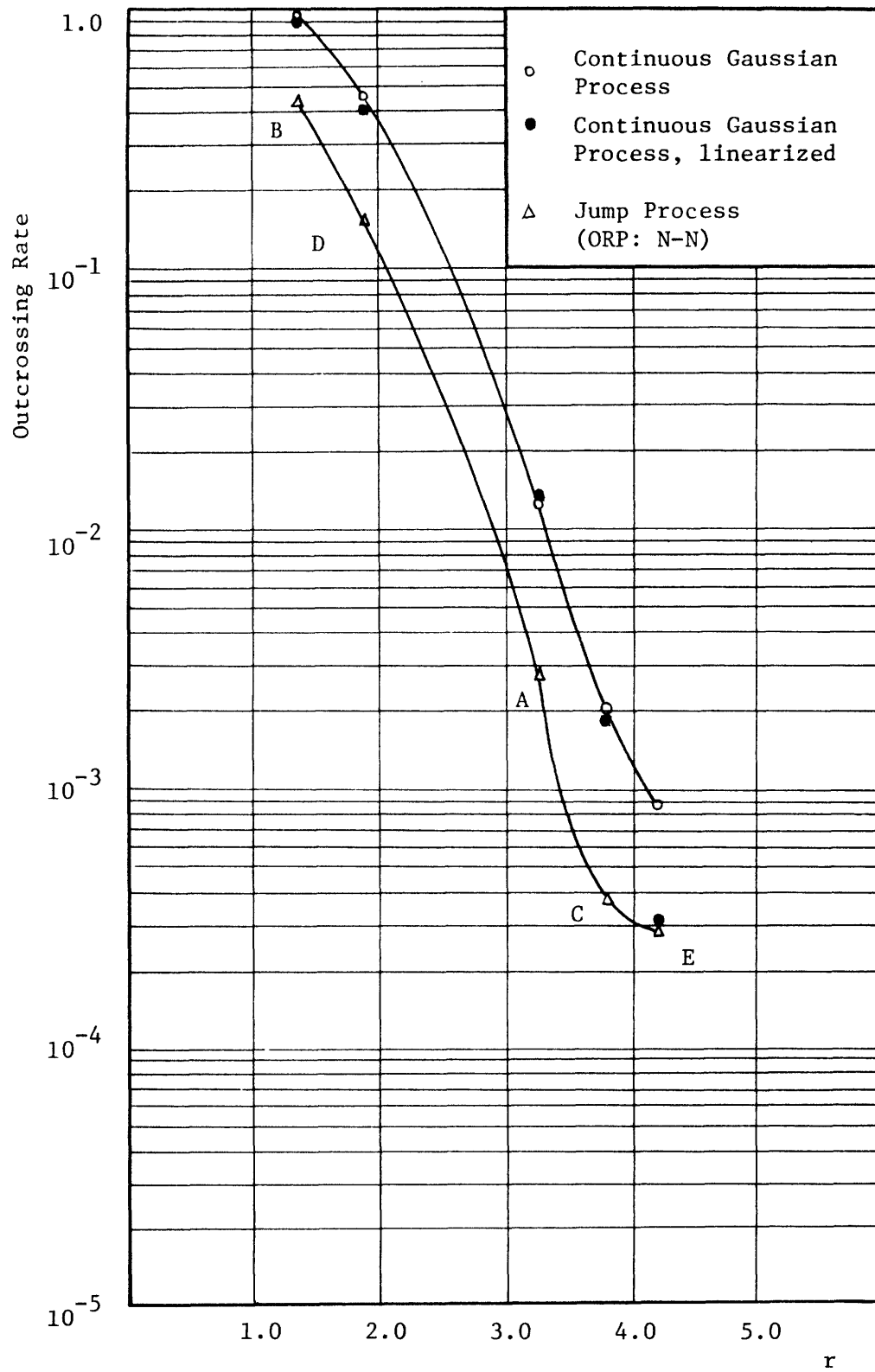


Figure 2.21: Continuous and jump process results, study 3.

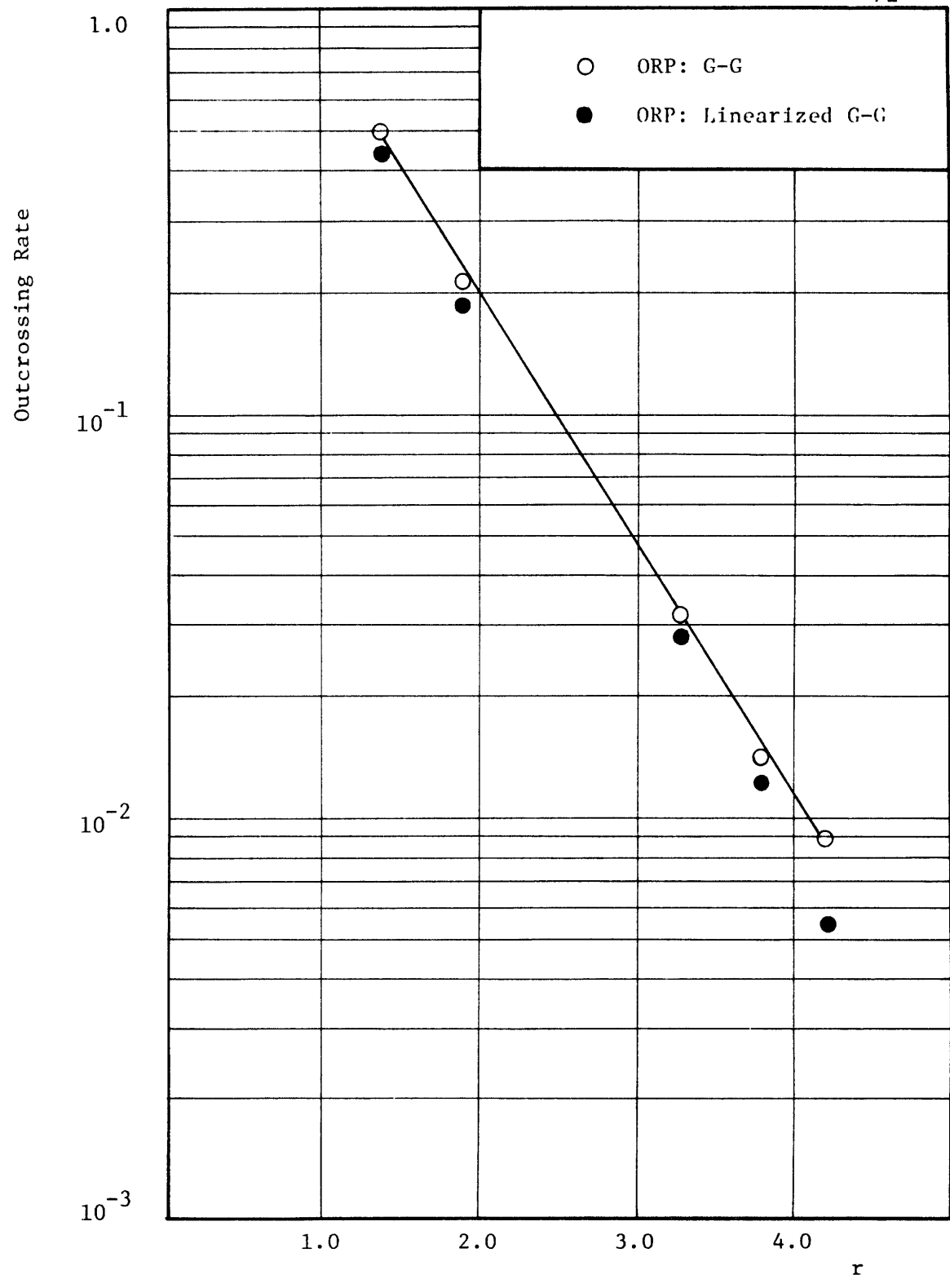


Figure 2.22: Linearizations of the jump process, study 3.



Table 2.3: Parameter Values and Results for Study 3

Case	$\nu_w$	$p$	$\mu_w$	$\sigma_w$	$\nu_L$	$\mu_L$	$\sigma_L$	D
A	2190	0.9977	10.0	5.0	0.125	50.0	28.6	150.0
B	2190	0.9977	20.0	5.0	0.125	50.0	28.6	150.0
C	2190	0.9977	10.0	5.0	0.125	50.0	28.6	100.0
D	2190	0.9977	20.0	5.0	0.125	50.0	28.6	100.0
E	2190	0.9977	10.0	5.0	0.125	25.0	28.6	75.0

Equation 2.14

Outcrossing Rate Program

Case	r	Equation 2.14			Outcrossing Rate Program		
		Full $\Omega$	Line	N-N	G-G	Line (G-G)	
A	3.24	$1.23 \times 10^{-2}$	$1.24 \times 10^{-2}$	$2.82 \times 10^{-3}$	$3.17 \times 10^{-2}$	$2.95 \times 10^{-2}$	
B	1.37	$9.66 \times 10^{-1}$	$9.42 \times 10^{-1}$	$4.40 \times 10^{-1}$	$4.77 \times 10^{-1}$	$4.46 \times 10^{-1}$	
C	3.79	$2.05 \times 10^{-3}$	$1.83 \times 10^{-3}$	$3.76 \times 10^{-3}$	$1.41 \times 10^{-2}$	$1.25 \times 10^{-2}$	
D	1.89	$4.66 \times 10^{-1}$	$4.02 \times 10^{-1}$	$1.54 \times 10^{-1}$	$2.13 \times 10^{-1}$	$1.87 \times 10^{-1}$	
E	4.19	$8.54 \times 10^{-4}$	$2.96 \times 10^{-4}$	$3.25 \times 10^{-4}$	$8.89 \times 10^{-3}$	$\left\{ \begin{array}{l} 2.92 \times 10^{-4}^* \\ 5.50 \times 10^{-3}^{**} \end{array} \right.$	

\*see figure 2.19

\*\*see figure 2.20

amounts to accounting only for tensile failures, and ignoring all others.

Figure 2.22 shows the results based upon gamma distributed loads. No upturn for case E is evident, as when normal distributions were assumed. Nevertheless, the linearization (as illustrated by figure 2.19) is inaccurate by more than an order of magnitude, completely out of the range of figure 2.22 and so not plotted.

What is plotted is instead the result of linearizing for E in the same way as for A through D. The error is thereby reduced to only 38%. Referring to figure 2.20, the reason will now be given. The D.L. line on the figure indicates the portion of the vertical load that is permanent and constant. Since the gamma distribution only considers positive random variables, this line shows the minimum vertical load that is consistent with the assumptions. By this formulation, the segment linearized in figure 2.19 represents an impossible failure mode. Yet, it is not an impossible mode when normal distributions are assumed, so the error due to the linearizations was not nearly as extreme when used for computations relating to continuous Gaussian processes.

Clearly, one could now construct numerous cases exemplifying the same behavior. By selecting a failure mode that is impossible to attain with positive random loads and suitably choosing parameters, practically any degree of inaccuracy could be produced. However, such exercises would be useless, and so are not engaged in here. Instead, let us draw some general conclusions from all three studies that have been performed.

#### 2.3.6 Conclusions drawn from Case Studies

It would be difficult to judge the merit of any individual conclusion

advanced here. Therefore, let us proceed to list conclusions roughly in the order in which they were reached, regardless of their relative importance.

First, the continuous process formulation of equation 2.14 provides a good approximation to the jump process formulation of equation 2.5. Comparable results are obtained for outcrossing rates when the parameters  $\sigma_{11}$  and  $\sigma_{22}$  are selected reasonably. Matching the mean rate of crossings of the mean level of each individual load process led to equation 2.18. Outcrossing rates obtained in this way appear conservative, since in every case the rate calculated using the continuous time formulation exceeded the rate calculated using the jump process formulation.

Outcrossing rates are related to the location of the mean point  $E[\vec{X}]$  relative to the failure boundary. Part of this sensitivity is expressed by the relationship between the outcrossing rate and  $r$ . On a semilog scale, the rate  $v_+$  decays approximately linearly with increasing  $r$ , which corresponds to a second-moment safety index.

Linearizations were also made in each case with regard to  $r$ , by constructing a tangent at the point on the failure surface closest to  $E[\vec{X}]$ . Typically, errors due to linearization of the continuous process formulation were less than that involved with matching to the jump process by use of equation 2.18, especially when loads are assumed to be normally distributed. Therefore, although these errors were in the form of underestimates, overestimation associated with the matching leads to a result which is on the whole generally conservative. To assure this conservatism, a functional relationship between  $r$  and linearization error would be desirable. However, none was found. Other elements must be considered, two of which have

been identified.

The shape of the diagram must be accounted for. Shape is difficult to quantify. More conveniently, charts could be made, plotting ratios of the outcrossing rates based on one boundary and approximations to it. This was done by Veneziano, Grigoriu, and Cornell; two of their figures are reproduced here.

In figure 2.23, a circular boundary  $\Omega$  of radius  $r$  is replaced both by an inscribed circle centered on the coordinate axes and a tangential vertical line. The mean point  $E[\vec{X}]$  is at the origin of the (reduced) coordinate system, and  $\sigma_{11} = \sigma_{22}$ .

Using the parameter  $\lambda$ , the rate  $v_+$  for an offset disk  $\Omega$  can be compared to that for a centered circular boundary of smaller radius. With careful selection of the ratio  $\lambda/r$ , the dashed curves allow for consideration of a broad range of circles with  $r$  in the practical range of 1 to 5. Then the solid curves yield the desired information regarding linearization error. Note that all of these encompass only one order of magnitude. The principle relationship is seen to be between the outcrossing rate ratio (error) and the degree of offset  $\lambda/r$ . On the other hand, the curves for the five radii are virtually indistinguishable for most of their length.

Figure 2.24 compares an elliptical region  $\Omega$  to another two approximations. The dashed curves again indicate an inscribed circle, the solid curves a pair of lines forming a double boundary (often referred to as a D-type barrier). Since symmetry holds, the outcrossing rate for the set is simply twice that would be noted for a single line. Again, note the lack of sensitivity to  $r$  displayed by the solid curves, except for  $r = 1.0$ . Also, note the convergence of these curves to unity as  $\gamma$  goes to zero and

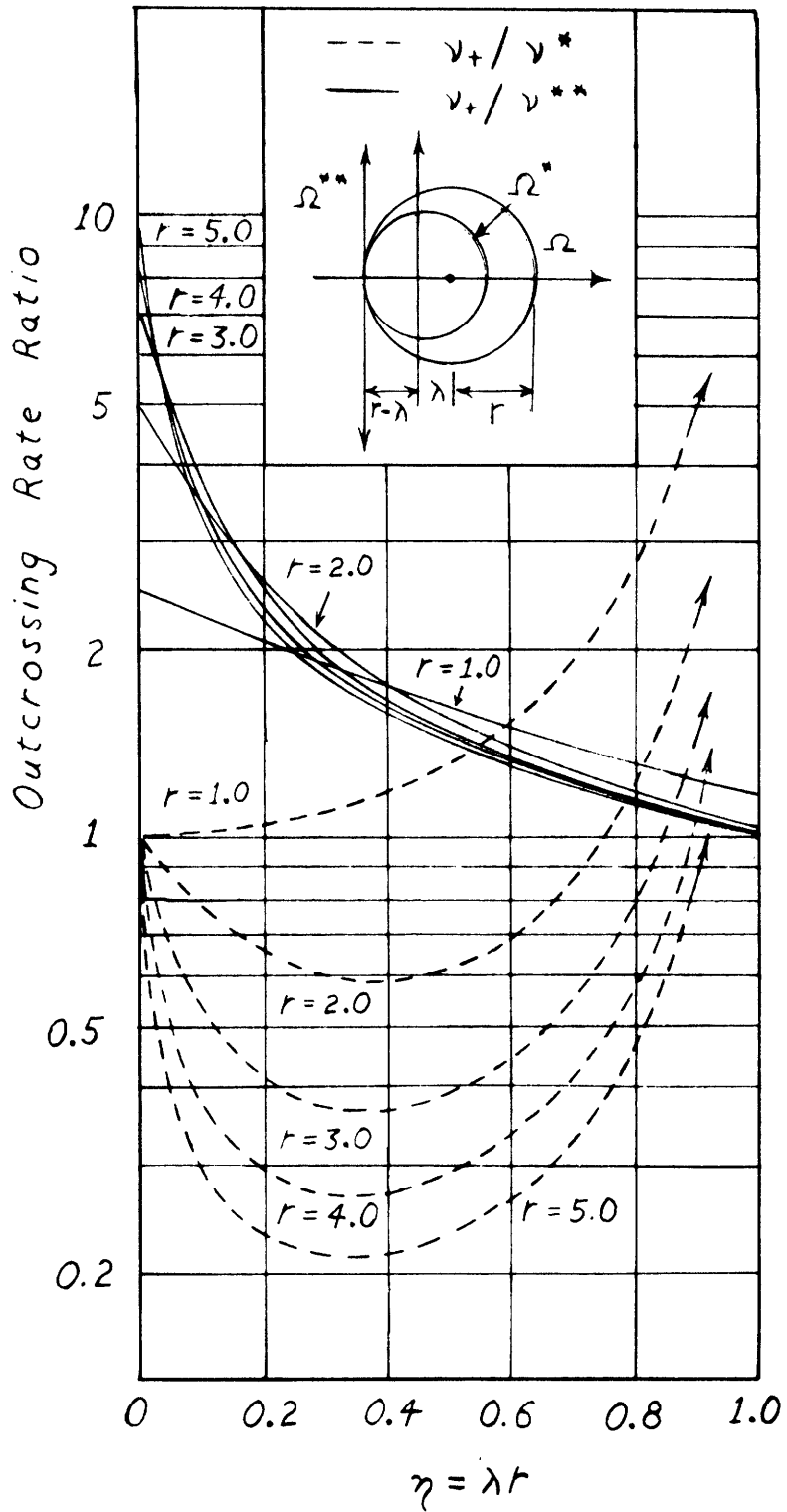


Figure 2.23 (After Veneziano, Grigoriu, and Cornell):  
Approximations of circular boundaries by a line.

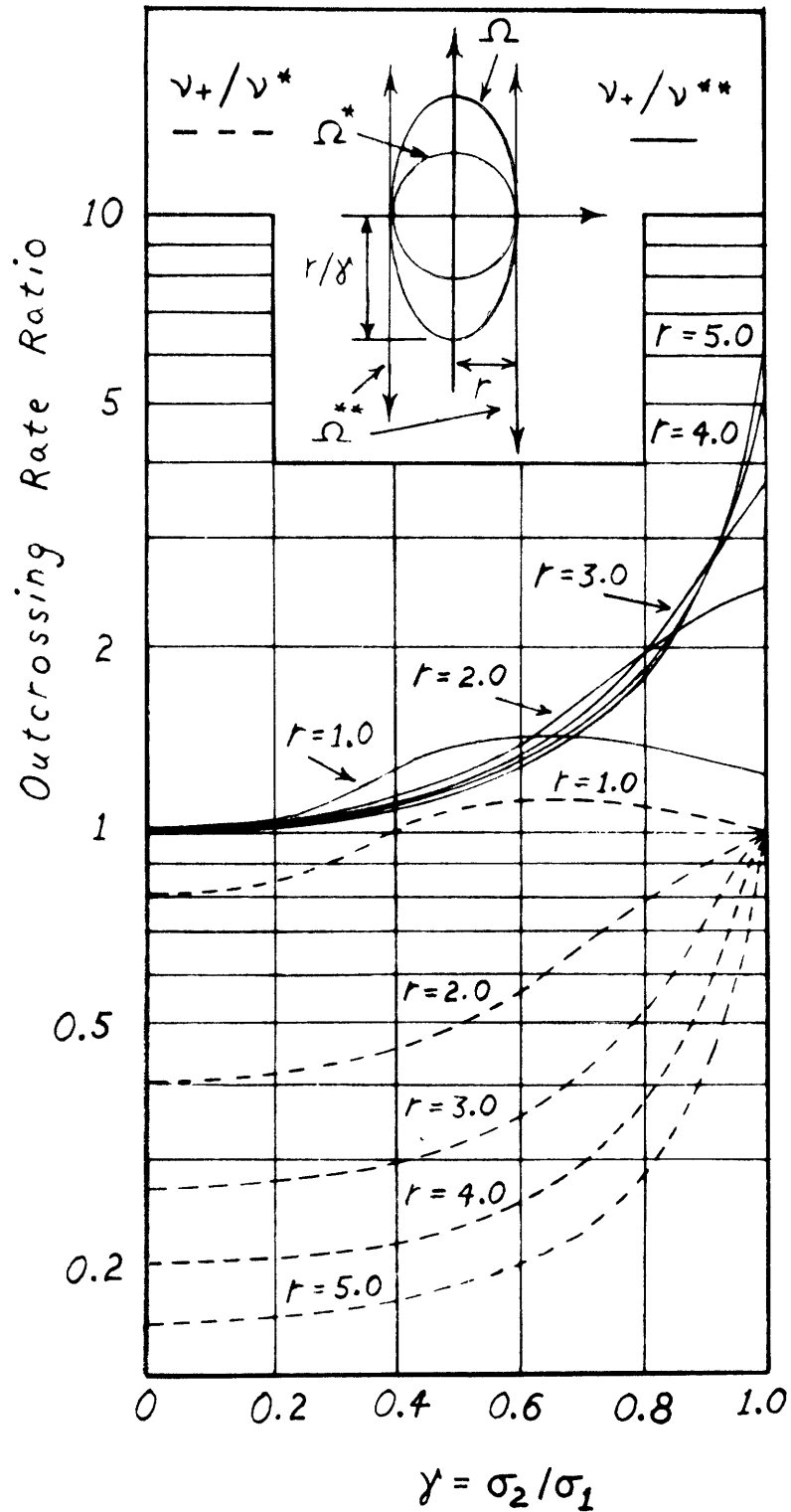


Figure 2.24 (After Veneziano, Grigoriu, and Cornell):  
Approximation of an elliptical boundary by a line.

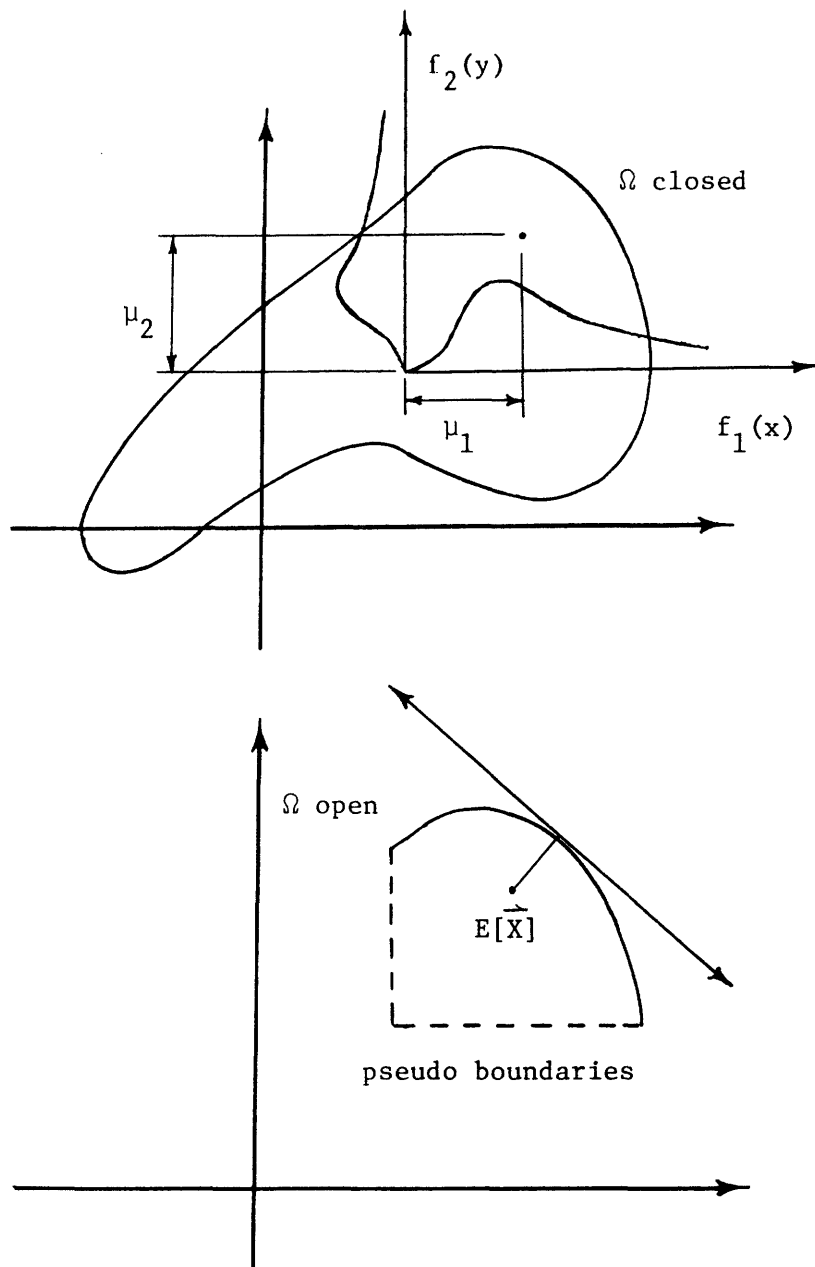


Figure 2.25: Transformation of the failure region into an open domain.

the ellipse becomes increasingly elongated.

The second element that has been identified as a cause of linearization error but has defied quantification is skewness in the load distributions. This manifested itself in case 3E, when blind adherence to the minimum-r linearization criterion resulted in a linearization corresponding to an impossible failure mode. In cases where skewness arises because the random variables are restricted to positive values, such as with gamma distributions, regions of the failure surface corresponding to negative values should be deleted. This transforms the failure region into an open domain, as illustrated in figure 2.25. For the purpose of evaluating equation 2.5, however, a closed region is required. This is satisfied by adopting pseudo boundaries, as illustrated. With this change, computations of  $v_+$  and failure surface linearizations can then proceed as before. Plots of linearization error, similar to figures 2.23 and 2.24, but relating to various open regions would then serve as useful guides.

In any case (no matter what the distribution assumptions, etc.) engineering judgement should still be exercised before linearizations are made. Clearly, linearizations made corresponding to unlikely or impossible failure modes should be expected to lead to large errors. For this reason, it would be desirable to carry out linearizations in load effect space, which structural designers are more familiar with. A method for doing this is suggested in the next section.

#### 2.4 Linearizations in Load Effect Space

The method suggested in this section was motivated by Veneziano's discussion of various second-moment methods [39]. Schemes similar to the



minimum- $r$  in reduced space criterion of the last section were considered. They were characterized mainly by their search for a single best direction from  $E[\vec{X}]$  and a resulting single point on the failure surface. On the other hand, Veneziano's own scheme [38] searches in a number of fixed directions and approximates the failure surface by semicircular segments. This is illustrated in figure 2.26. If the number of search directions is large enough, such a method becomes asymptotically invariant, in the sense defined by Veneziano [37].

The method, as adapted here, retains the feature of searching in a number of fixed directions. However, linearizations are to be made at only the single point, intercepted on the failure boundary, closest to  $E[\vec{X}]$ . So, the method here is not intended to approach invariance, but instead to simply approximate minimization of  $r$ . Whereas a mathematically strict minimization scheme demands that both a direction and a distance be found, this approximation reduces the problem to simply comparing a number of different values for  $r$ . As a result, it is no more difficult to deal with a continuous boundary than its discrete approximation. Most importantly, it can be implemented equally well in any chosen variable space.

The suitable number of searches and their directions depend upon the problem considered. For an illustration here, a reinforced concrete column is again used as an example, and three search directions are chosen. In reduced space, these directions would correspond to  $\psi = 0^\circ$ ,  $\psi = 90^\circ$ , and  $\psi = 45^\circ$ .

Given the failure diagram, the method could be carried out by means of a graphical construction, such as in figure 2.27. The construction proceeds as follows:

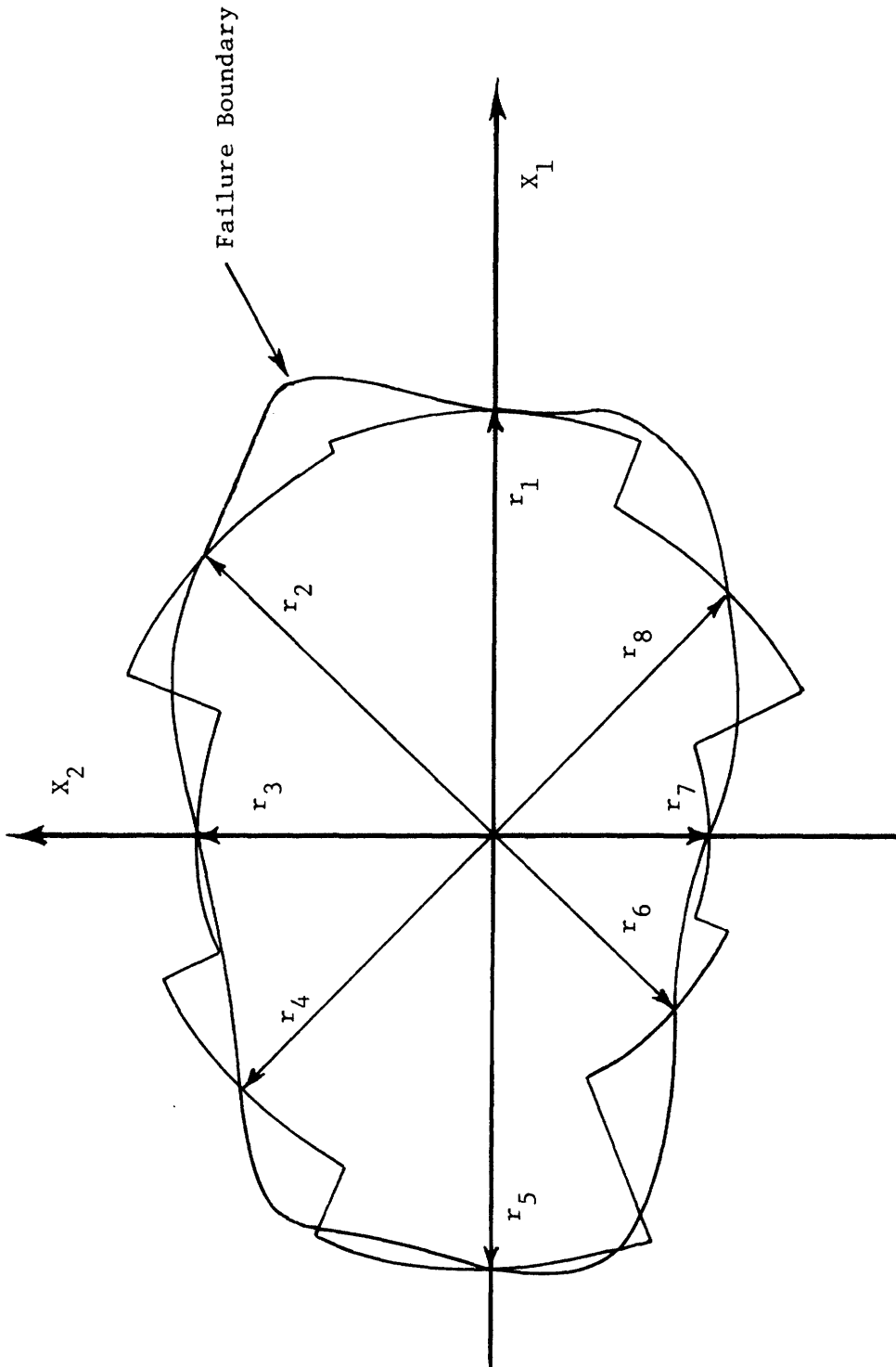


Figure 2.26: Veneziano's searching scheme.

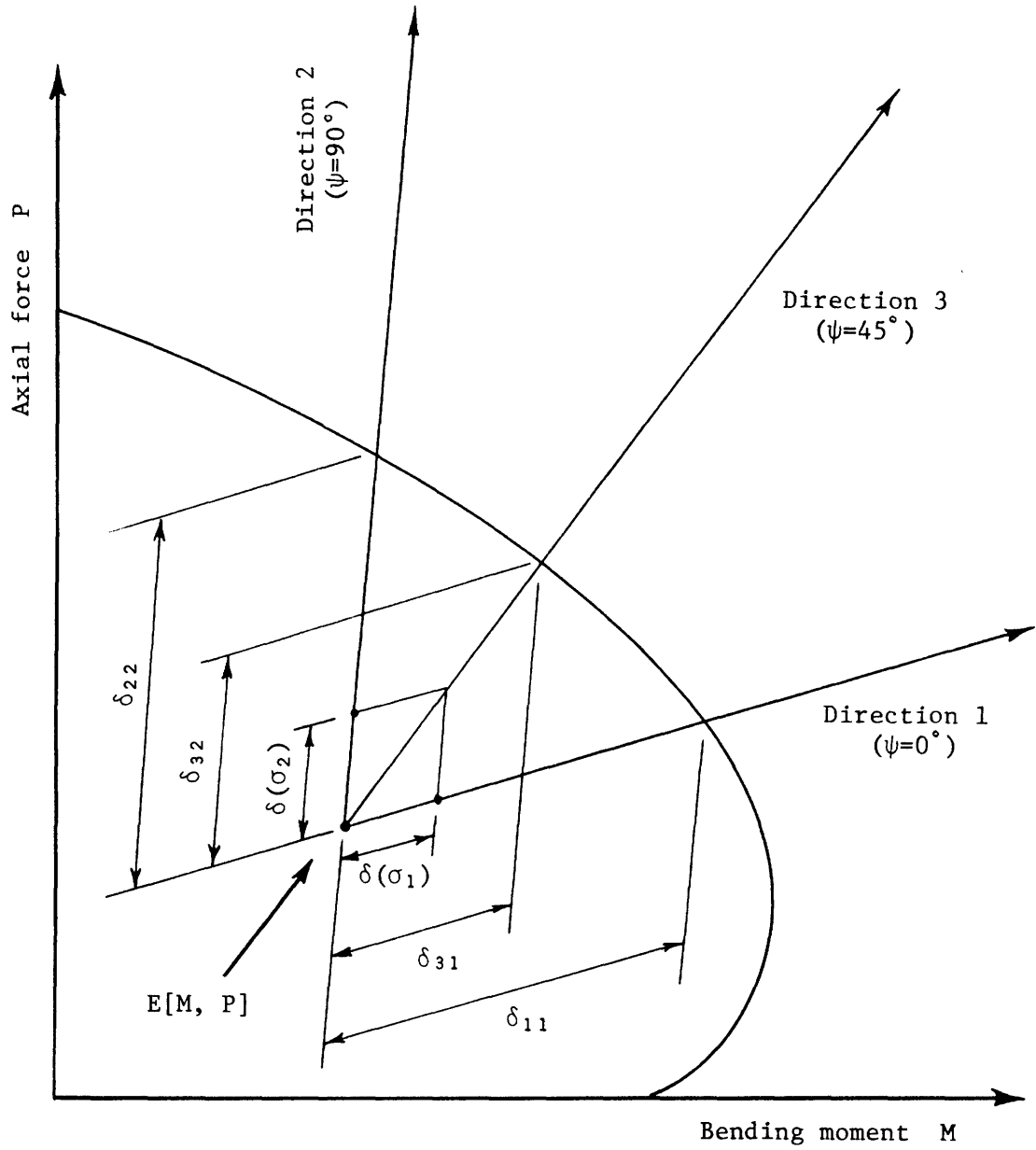


Figure 2.27: Linearizations in load effect space.

1. Plot the point of expected load effect,  $E[M, P]$ . For linear structural behavior, this is the same as the load effect at the mean loads.
2. Plot the point corresponding to the load effect arising when the first load is  $S_1 = \mu_1 + \sigma_1$ , the second load being  $S_2 = \mu_2$ . A ray from  $E[M, P]$  passes through this point at a distance  $\delta(\sigma_1)$ , and defines direction 1. Similarly, plot the load effect produced by  $S_1 = \mu_1$  and  $S_2 = \mu_2 + \sigma_2$ , thereby defining  $\delta(\sigma_2)$  and direction 2. These correspond to  $\psi = 0^\circ$  and  $\psi = 90^\circ$ , respectively.
3. By laying off segments from the two points plotted in step 2, construct a parallelogram with sides of length  $\delta(\sigma_1)$  and  $\delta(\sigma_2)$ . The ray from  $E[M, P]$  through the opposite vertex defines direction 3, equivalent to  $\psi = 45^\circ$ .
4. Measure the distances from  $E[M, P]$  to the failure boundary in directions 1 and 2 as  $\delta_{11}$  and  $\delta_{22}$ , respectively. Then, measure the distances from  $E[M, P]$  to the boundary that are projected onto the other two rays,  $\delta_{31}$  and  $\delta_{32}$ .
5. The reduced space distances corresponding to the three directions can now be found. Corresponding to directions 1 and 2, these are:

$$r_1 = \delta_{11}/\delta(\sigma_1)$$

$$r_2 = \delta_{22}/\delta(\sigma_2)$$

Since in reduced space directions 1 and 2 are orthogonal, the Pythagorean theorem applies and:

$$r_3 = \sqrt{[\delta_{31}/\delta(\sigma_1)]^2 + [\delta_{32}/\delta(\sigma_2)]^2}$$

Compare the values  $r_1$ ,  $r_2$ , and  $r_3$ . The least of these, along with its corresponding angle  $\psi$ , is used for the linearization.

In the case of the example, figure 2.27, careful scaling reveals that  $r_1 = 3.85$ ,  $r_2 = 3.40$ , and  $r_3 = 2.80$ . So, one would choose  $\psi = 45^\circ$  and  $r = 2.80$ , as is illustrated.

Given this (or any other) method of finding the point at which to linearize, many alternative methods could be adopted to define the line itself. Two procedures are presented here.

Both methods define the line as the tangent to the boundary at the point of linearization. Consider the situation where the boundary is given analytically in terms of some function, say  $P = g(M)$ . Then, differentiating  $g$  yields the slope at the point of linearization, and so the equation of the line desired can be found. However, it may be the case that the engineer has no analytical expression for the boundary. For instance, this situation would arise when a column interaction diagram is obtained from a standard handbook. In this case, the alternative is to simply fit the tangent by eye.

Any method of linearization of a two-dimensional boundary allows the problem to be cast in the same form as a scalar load effect problem. First of all, define a non-dimensional equivalent load effect:

$$E = \frac{M}{M'} + \frac{P}{P'} \quad (2.20)$$

where  $M'$  and  $P'$  are the intercepts of the linearization on the load-effect axes. Clearly, a value of  $E < 1$  indicates the safe region,  $E > 1$  indicates failure, and  $E = 1$  defines the boundary. Assuming once again the example of linear structural interaction of equation 1.5, substitution into equation 2.20 yields:

$$E = \left[ \frac{C_{WM}}{M'} + \frac{C_{WP}}{P'} \right] W + \left[ \frac{C_{LM}}{M'} + \frac{C_{LP}}{P'} \right] L \quad (2.21)$$

for the equivalent problem.

More generally, considering two loads  $S_1$  and  $S_2$ , the coefficients can be lumped into constants  $a_1$  and  $a_2$  to yield:

$$E = a_1 S_1 + a_2 S_2 \quad (2.22)$$

which can be treated in the same manner as a problem of the form, say:

$$M = c_{1M} S_1 + c_{2M} S_2 \quad (2.23)$$

where  $M$  denotes bending moment. Whereas in this latter case,  $M$  possesses a physical meaning and  $E$  is simply a convenient device, the two problems are mathematically alike. This formal correspondence will be exploited in the next chapter.

To close this section, let us illustrate these concepts with a specific example. Figure 2.28 depicts the linearization of the same problem considered in case study 1A. However, the diagram in figure 2.28 is shown in its original smooth form, versus the piecewise linear form it was originally presented in (figure 2.7). This is because it no longer needs to be digitized for input to a computer program.

The figure shows that  $r_3 = 3.61$  was chosen, corresponding to  $\psi = 45^\circ$ . This is slightly higher than the  $r = 3.47$  found in the reduced space linearization of the earlier study, and would therefore lead to a somewhat lower value (by 36%) for  $v_+$  by use of equation 2.14.

In this example, the tangent was fit by eye. The corresponding values for the intercepts  $M'$  and  $P'$  are shown on the figure. Using these

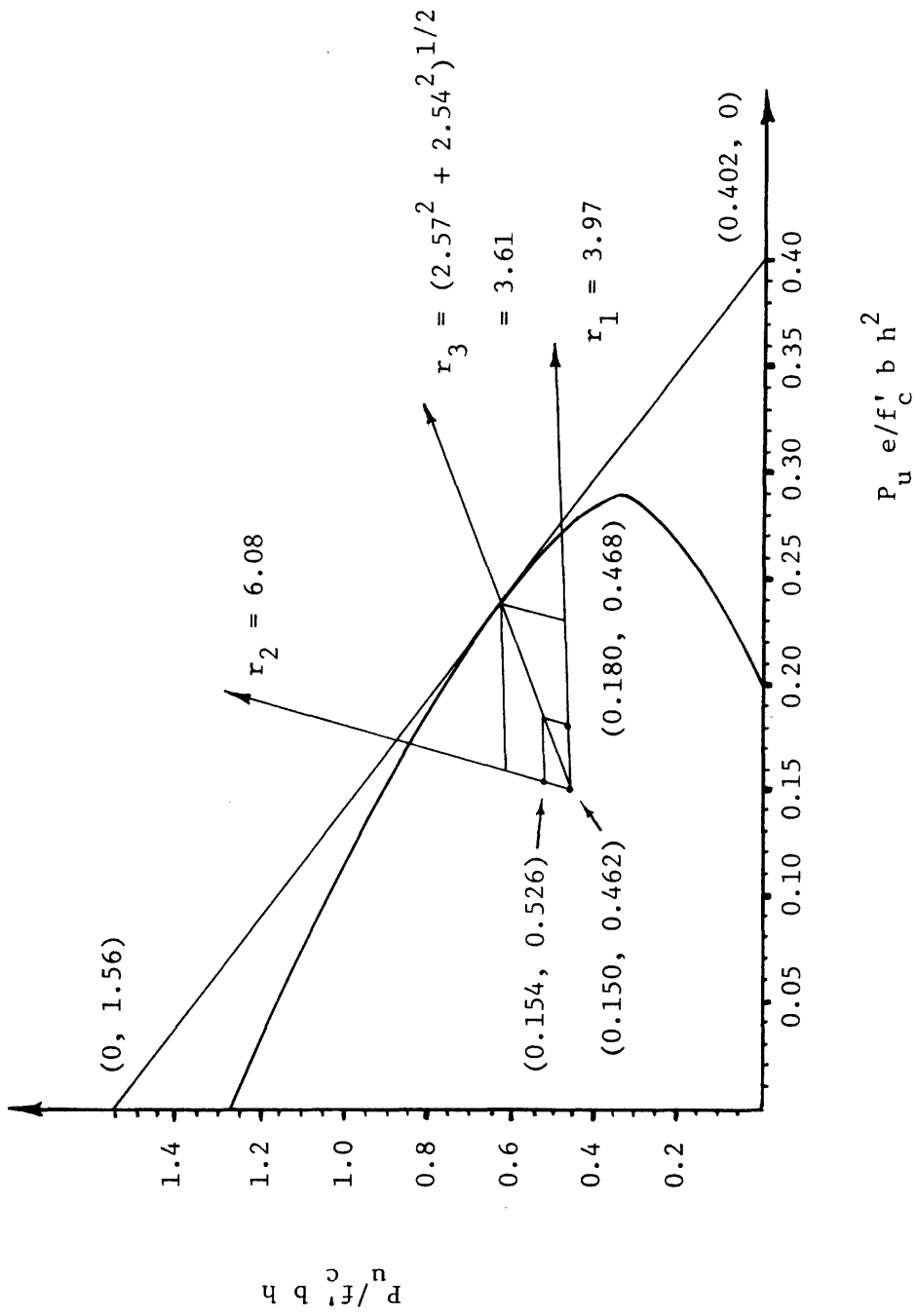


Figure 2.28: Linearization example in load effect space.

values, the coefficients of equation 2.22 are found to be  $a_1 = 1.54 \times 10^{-2}$  and  $a_2 = 1.81 \times 10^{-3}$ . So, the problem is now transformed into an equivalent scalar problem such as considered in the next chapter.



## SCALAR LOAD COMBINATIONS PROBLEMS

3.1 Upcrossing Rates for Scalar Sums of Processes

As stated in Chapter 1, and then demonstrated in section 2.4, the virtue of linearizing a two dimensional problem is that such an approximation reduces an outcrossing rate problem to a scalar problem. Hence, the focus of this chapter will be on problems of the form:

$$M = c_{1M}S_1 + c_{2M}S_2 \quad (2.23)$$

Simplifications resulting from this form are exploited here. Further simplifications result from the fact that only non-negative random variables are used in this chapter.

Recognizing that only two points are necessary to determine a line, and again placing all the work here in non-dimensional form, let us write in place of equation 2.23:

$$Z = c\bar{S}_1 + (1-c)\bar{S}_2 \quad (3.1)$$

where:

$$\bar{S}_1 = \frac{S_1}{\mu_1}, \quad \bar{S}_2 = \frac{S_2}{\mu_2}$$

using mean values for convenience. The corresponding scalar coefficient  $c$ , and scalar level  $Z$  are:

$$c = \frac{c_{1M}\mu_1}{c_{1M}\mu_1 + c_{2M}\mu_2}$$

and

$$Z = \frac{M}{c_{1M}\mu_1 + c_{2M}\mu_2}$$

Alternatively, one may have originally started with a two-dimensional diagram, reduced to the equivalent load effect of equation 2.21. In such a case, it is a straightforward exercise to show:

$$c = \frac{\left[ \frac{c_{WM}}{M'} + \frac{c_{WP}}{P'} \right] \mu_W}{\left[ \frac{c_{WM}}{M'} + \frac{c_{WP}}{P'} \right] \mu_W + \left[ \frac{c_{LM}}{M'} + \frac{c_{LP}}{P'} \right] \mu_L}$$

and so on. From this point on, no distinctions will be drawn according to the origins of a problem, since it does not matter for the purposes of this chapter. Furthermore, the bar denoting the reduction of the problem to this form will be omitted; that is, we shall write  $S_1$  and  $S_2$ , not  $\bar{S}_1$  and  $\bar{S}_2$ . While this helps keep the notation brief, it should be borne in mind that the non-dimensional form of equation 3.1 is actually implied.

Note also that all previously defined notation with regard to distribution functions will be followed here. So,  $F_1(x)$  still refers to load 1, and to consider the inclusion of  $p_1$ , we write  $F'_1(x)$ , etc. However, arguments of these functions will no longer be explicit. Since we intend to refer to  $c_1 S_1$  and  $c_2 S_2$  throughout, we would have to include the coefficients in the arguments. Instead, we simply use  $x$ , and so the following are implied:

$$F_1(x) = F_1(c_1 s_1) \text{ with } x = c_1 s_1$$

and

$$F_2(x) = F_2(c_2 s_2) \text{ with } x = c_2 s_2$$

The meaning of  $x$  as a dummy variable should be clear in all contexts.

Additionally, we introduce the shorthand notation for convolution:

$$F_{1*2}(z) = \int_0^z F_1(z-x)dF_2(x) = \int_0^z F_2(z-x)dF_1(x) \quad (3.2)$$

The derivation of the mean upcrossing rate for the scalar sum is similar to that which led to equation 2.5. Again, let us seek the rate  $v_{1+}$ , conditioning on the level of the (factored) load  $c_2 S_2$ . However, matters are made simple by the fact that if  $x$  is the conditional level, then the remaining load necessary to reach the threshold is just  $z-x$ . So, by the same sort of arguments that led to equation 2.11, we get:

$$v_{1+} = v_1 \int_0^z [p_1 + q_1 F_1(z-x)][q_1 - q_1 F_1(z-x)]dF_2'(x) \quad (3.3)$$

Accounting now for  $p_2$ :

$$\begin{aligned} v_{1+} &= v_1 p_2 [p_1 + q_1 F_1(z)][q_1 - q_1 F_1(z)] \\ &+ v_1 \int_0^z [p_1 + q_1 F_1(z-x)][q_1 - q_1 F_1(z-x)]f_2(x)dx \quad (3.4) \end{aligned}$$

Rearranging, and recalling that  $1 - F_1(\cdot) = G_1(\cdot)$ :

$$\begin{aligned} v_{1+} &= v_1 q_1 p_2 G_1(z)[p_1 + q_1 F_1(z)] + v_1 p_1 q_1 q_2 [F_2(z) - F_{1*2}(z)] \\ &+ v_1 q_1^2 q_2 \int_0^z F_1(z-x)G_1(z-x)f_2(x)dx \quad (3.5) \end{aligned}$$

Again using symmetry, the total result is found to be:

$$v_+ = v_1 q_1 p_2 G_1(z)[p_1 + q_1 F_1(z)] + v_2 p_1 q_2 G_2(z)[p_2 + q_2 F_2(z)]$$

$$\begin{aligned}
 & + v_1 p_1 q_1 q_2 [F_2(z) - F_{1*2}(z)] + v_2 p_2 q_1 q_2 [F_1(z) - F_{1*2}(z)] \\
 & + v_1 q_1^2 q_2 \int_0^z F_1(z-x) G_1(z-x) f_2(x) dx + v_2 q_1 q_2^2 \int_0^z F_2(z-x) G_2(z-x) f_1(x) dx \quad (3.6)
 \end{aligned}$$

### 3.2 A Markovian Approach

It is possible to derive equation 3.6 in other ways than that adopted in the last section. One such approach, using a Markov chain, is outlined here. It is not carried through to completion because it is very laborious, and the desired result is in hand anyway. Yet, it provides a term by term insight into equation 3.6 that would otherwise be difficult to acquire.

An alternative way to regard the processes is that they are intermittently being activated and then stopped. At every renewal, the probability of being activated is  $q$ ; and, if the process is already activated, it may be stopped with probability  $p$ , or reactivated with probability  $q$ . So, the expected amounts of time that processes 1 and 2 are active in the span  $[0, T]$  are  $q_1 T$  and  $q_2 T$ , respectively. Roughly speaking, the necessary condition every Markov chain must meet is that the probability of being in any future state, when the present is known, is not affected by any additional knowledge of past states. These conditions are met because the Poisson square wave processes assumed for loading are independent, and each possesses the so-called memoryless property [5]. Then, define the states of the chain as follows:

- State 0: Neither process is active
- State 1:  $\begin{cases} \text{Process 1 is active} \\ \text{Process 2 is stopped} \end{cases}$

State 2:  $\begin{cases} \text{Process 1 is stopped} \\ \text{Process 2 is active} \end{cases}$

State 1\*2: Both processes are active

This continuous time Markov chain has an associated transition intensity matrix, [Q]:

$$\begin{bmatrix} -(q_1 v_1 + q_2 v_2) & q_1 v_1 & q_2 v_2 & 0 \\ p_1 v_1 & -(p_1 v_1 + q_2 v_2) & 0 & q_2 v_2 \\ p_2 v_2 & 0 & -(q_1 v_1 + p_2 v_2) & q_1 v_1 \\ 0 & p_2 v_2 & p_1 v_1 & -(p_1 v_1 + p_2 v_2) \end{bmatrix}$$

The construction and interpretation of such matrices is discussed in detail by Parzen [31].

The stationary distribution is found by solving the matrix equation:

$$\{\Pi_0 \Pi_1 \Pi_2 \Pi_{1*2}\} [Q] = \{0 \ 0 \ 0 \ 0\} \quad (3.7)$$

and imposing the condition

$$\Pi_0 + \Pi_1 + \Pi_2 + \Pi_{1*2} = 1$$

It then turns out that the stationary distribution for the chain does not depend upon the rates  $v_1$  or  $v_2$ :

$$\Pi_0 = p_1 p_2$$

$$\Pi_1 = q_1 p_2$$

$$\Pi_2 = p_1 q_2$$

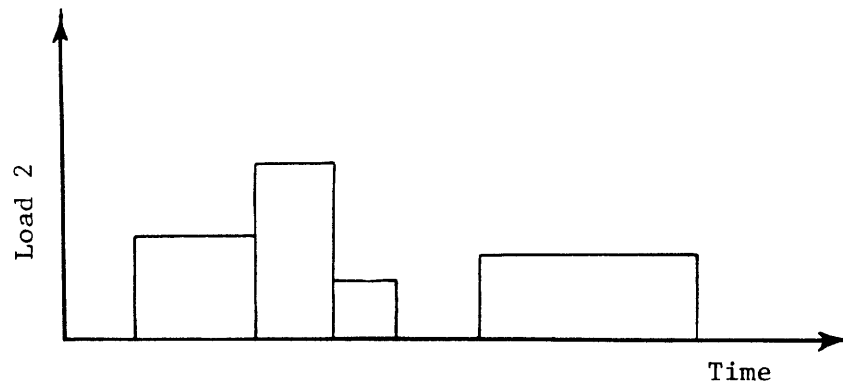
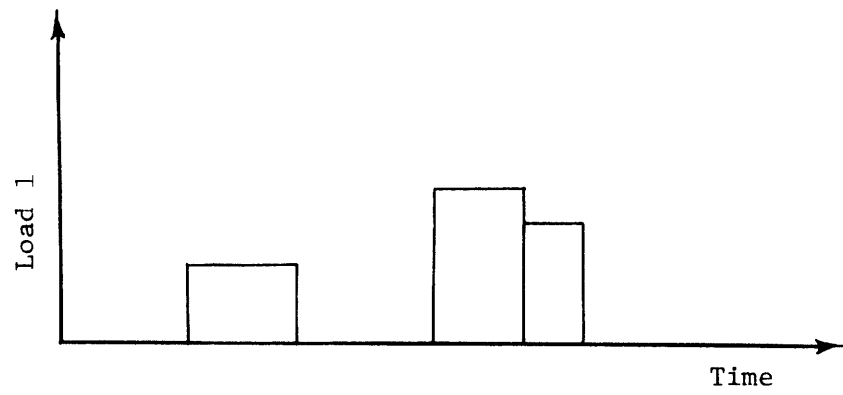
$$\Pi_{1*2} = q_1 q_2$$

These represent the expected or long-run proportion of time spent in each state.

Changes of state in the Markov process constitute possible upcrossing events. Such changes are illustrated in figure 3.1. Note, however, the following convention. When one load is acting and its level changes, transitions from state 1 to state 1, or from state 2 to state 2 are to be counted. This means that upcrossings due to one process or the other acting alone are counted. On the other hand, transitions from state 0 to state 0 are not physically recognizable, and may be ignored. Furthermore, states 1 and 2 are mutually inaccessible, and so are states 0 and 1\*2. This means that the possibility that both underlying processes will be simultaneously changed has again been neglected as second-order.

It is then helpful to examine the mean rates of transition from each state to each other state accessible from it. Denoting these rates by  $\Delta$ , they are found as the rate of transition from a former state to a latter one (from [Q]) multiplied by the total proportion of time spent in the former state (from  $\Pi$ ). There are 11 such rates, but only 7 are of interest:

$$\begin{aligned} \Delta_{0,1} &= v_1 p_1 p_2 q_1 \\ \Delta_{0,2} &= v_2 p_1 p_2 q_2 \\ \Delta_{1,1} &= v_1 q_1^2 p_2 \\ \Delta_{1,1*2} &= v_2 p_2 q_1 q_2 \\ \Delta_{2,2} &= v_2 p_1 q_2^2 \\ \Delta_{2,1*2} &= v_1 p_1 q_1 q_2 \\ \Delta_{1*2,1*2} &= q_1 q_2 (q_1 v_1 + q_2 v_2) \end{aligned}$$



Markov States:

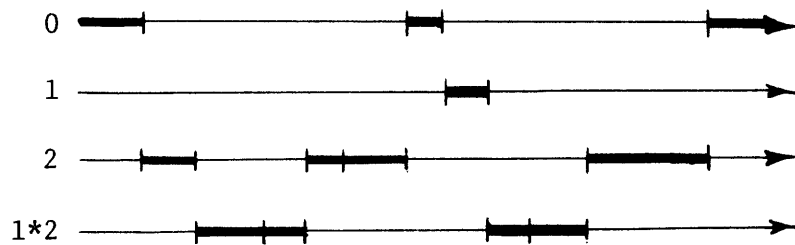


Figure 3.1: Relationship between square wave processes and Markov states 0, 1, 2, and 1\*2.

Further, note that

$$\Delta_{0,1} + \Delta_{1,1} = v_1 q_1 p_2$$

$$\Delta_{0,2} + \Delta_{2,2} = v_2 q_2 p_1$$

Then, the mean rate of upcrossings due to arrivals into state 1, denoted as  $v_{+1}$ , should be:

$$\begin{aligned} v_{+1} &= (\Delta_{0,1} + \Delta_{1,1})P\{\text{Safe}|\text{In states 0 or 1}\}P\{\text{Unsafe}|\text{In state 1}\} \\ &= v_1 q_1 p_2 [p_1 + q_1 F_1(z)] G_1(z) \end{aligned} \quad (3.8)$$

This is precisely the first term of equation 3.6. So, it is clear that this term accounts for upcrossings associated with transitions into state 1, with only the underlying load process 1 active.

Similarly, it can be shown that the other terms of equation 3.6 have Markovian interpretations. The second term accounts for crossings due to transitions into state 2. The third and fourth terms account for transitions into state 1\*2 from states 1 and 2, respectively. Finally, the integral terms account for transitions from state 1\*2 back into state 1\*2. Therefore, the integral terms account for crossings that occur with both load processes active.

### 3.3 Further Simplifications

There are two distinct ways that equation 3.6 may be simplified. The first relates to the level of the failure threshold,  $z$ . The other has to do with the relative renewal rates of the individual load processes. These will be discussed in turn in the following sections.



### 3.3.1 Results for High Failure Thresholds

As the level of  $z$  is increased, the probability that at any given time either load has a value greater than  $z$  tends to unity. That is:

$$F_1(z) \rightarrow 1 \quad \text{and} \quad F_2(z) \rightarrow 1$$

$$\text{as } z \rightarrow \infty$$

However, the function  $F_{1*2}(z)$  increases more slowly than either  $F_1(z)$  or  $F_2(z)$ , which always bound it from above. So, as a more conservative pair of approximations:

$$F_2(z) - F_{1*2}(z) \rightarrow 1 - F_{1*2}(z) = G_{1*2}(z)$$

$$F_1(z) - F_{1*2}(z) \rightarrow 1 - F_{1*2}(z) = G_{1*2}(z)$$

Substitute the above into the first four terms of equation 3.6. The new result, after combining terms, is the desired approximation:

$$\begin{aligned} v_+ \cong & v_1 q_1 p_2 G_1(z) + v_2 p_1 q_2 G_2(z) + (p_1 v_1 + p_2 v_2) q_1 q_2 G_{1*2}(z) \\ & + v_1 q_1^2 q_2 \int_0^z F_1(z-x) G_1(z-x) f_2(x) dx \\ & + v_2 q_1 q_2^2 \int_0^z F_2(z-x) G_2(z-x) f_1(x) dx \end{aligned} \quad (3.9)$$

The accuracy of this approximation depends upon the distributions of 1 and 2, the means and variances, and  $z$  itself. Therefore, the only way to check the accuracy is to actually use equation 3.6. However, since all approximations have been in the nature of increases, the result is conservative. Perhaps the greatest advantage of the result above is the combi-

nation of the third and fourth terms of equation 3.6 into the third term above, placing an even greater emphasis on symmetry.

### 3.3.2 Transience

A transient process is one that models a sequence of events with negligible time duration. Analyses of combinations of transient processes with processes that possess time duration have been carried out. However, they have all used methods quite dissimilar than what will follow here. They implicitly assign a different sort of character to transient processes than to processes of time duration events. Instead, consider that a transient process is simply a limiting case of a modified square wave process, one for which  $p$  is very close to unity. Examine the behavior of equation 3.6 as process 2 becomes transient. Let:

$$p_2 \rightarrow 1 \quad \text{and} \quad v_2 \rightarrow \infty$$

in such a way that

$$p_2 v_2 \rightarrow v_T$$

This yields the upcrossing rate for the sum of a transient process with a modified square wave:

$$v_+ = v_1 q_1 G_1(z) [p_1 + q_1 F_1(z)] + v_T p_1 G_2(z) + v_T q_1 [F_1(z) - F_{1*2}(z)]$$

Numerical studies are still required to explore the range of validity of this result.

### 3.4 Computational Procedures

A Fortran computer program has been written to evaluate  $v_+$  by equation

3.6. It is referred to as the Upcrossing Rate Program, U.R.P. for short.

As input, U.R.P. accepts the following:

1. The parameters  $v_1$ ,  $p_1$ ,  $\mu_1$ ,  $\sigma_1$ ,  $v_2$ ,  $p_2$ ,  $\mu_2$ , and  $\sigma_2$ .
2. The coefficients  $c_1$  and  $c_2$ .
3. The threshold level,  $z$ .

In order to make the results of this program comparable to the earlier program (O.R.P.) normal and gamma distribution functions can again be specified for either load process.

As output, U.R.P. yields the rates due to the individual processes,  $v_{1+}$  and  $v_{2+}$ , as well as the final rate  $v_+$ .

One precaution should be taken when using the program. Simpson's rule is used to numerically perform the integrations of equation 3.6. The error in these routines depends upon the length of the interval,  $dx$ , used for Simpson's rule. The program has been found to give results comparable to those of Hasofer [24] in a particular case involving one transient process. It also appears to give good results over a broad range of stochastic process parameters. However, if it is to be used for very high thresholds (say, more than 4 standard deviations above the mean) of combined loads, its output should be carefully scrutinized. In particular, it would again be helpful to check its results versus any others that may be available so that the number of intervals used can be adjusted accordingly.

Finally, one should note how the simplifications that led to equation 3.6 result in savings of computational effort. In terms of executable statements, O.R.P. had 417, U.R.P. only 194. Time spent in the central processing unit of the I.B.M. 370/67 at M.I.T. is typically reduced more than 50%.

## ENGINEERING PRACTICE FOR LOAD COMBINATIONS

4.1 Past and Present Developments

It is not only interesting, but also educational to study the development of practice with regard to load combinations. Such a study helps to explain the ambiguities and shortcomings in present practice.

Early practice for load combinations reflected the disorderly state of the emerging profession of engineering. The following passage from an 1896 text [20] for structural engineers illustrates this:

All the exterior forces which may possibly act upon a structure should be considered, and due provisions should be made for resisting them. The static load, the live load, pressure from wind and snow, vibration, shock and centrifugal force should be provided for, as should also deterioration from time, neglect, or probable abuse. A truss over a machine shop may at some time be used for supporting a heavy weight by block and tackle, or a line of shafting may be added; a small surplus of material in the original design will then prove of value.... When a live load is joined to a static load, the judgement of the designer, or the one who prepares the specifications for the designer, must be exercised.

The book, although nearly 300 pages long, says essentially nothing more at all about loading. However, most of an entire chapter is devoted to safe working stresses, which amount to a collection of opinions of some eminent engineers as well as a few formulae adopted by various railroads.

As time went on and the profession matured, the present system of structural codes was evolved to promote improved practice in the U.S. Professional organizations (such as the American Concrete Institute and the American Institute for Steel Construction) form special committees which draft recommended codes of standard practice. These are in turn adopted,

sometimes with modifications, by local governments (usually at the municipal level) and so take on the force of law. A similar system is in effect in Europe, where however the committees are nowadays usually on an international level, and the governmental authorities on the level of individual nations. In any case, the judgements of designers have to some degree been replaced by the judgements of the code committees.

Early codes emphasized concerns of structural resistance almost to the exclusion of loading. Laboratory tests on structural members led to better judgements about resistances. Along with the use of higher strength materials, allowable stresses came to be increased. However, load values were selected almost arbitrarily, and so the working stresses were set at artificially low values to provide an extra factor of safety accounting for the uncertainty in the loads.

To rectify this situation, load studies were commissioned. Special emphasis rested upon floor live loads in offices. An early example is the survey made of the Little Building, in Boston [6]. Design levels specified in codes began to be based upon the maximum levels found by this and other surveys.

Anemometer data for wind speeds were collected from meteorological records, and searched for annual maxima. Now, probabilistic concepts began to be applied. Maps were drawn depicting annual extreme wind speeds for 50 and 100 year mean recurrence intervals. Similar maps were drawn for extreme snow loads as well.

This situation is well summarized by the way the checking of a steel member designed by elastic methods might proceed today. Assume that the local building authorities have adopted the recommendations of the American

National Standards Institute for loading, A58.1 - 1972 [ 3 ], and the recommendations of the A.I.S.C. [ 2 ]. First, the 50 year (or 100, for some important structures) return period wind for the site is read from the map, and a corresponding pressure found from a table. Another table, depending upon the type of building, is consulted for the floor live load. Live load reduction factors may apply, depending upon the type and location of the member in the structural system. Nominal unit weights of various construction materials given in the code aid in the estimation of dead load. Using elastic structural analysis, find the stress level,  $f$ , for the superposition of these loads. Now the A.I.S.C. provisions are consulted, and depending upon the type of member, including its specific properties such as size and grade of steel, an allowable stress level,  $f_a$ , is found. According to both A.N.S.I. and A.I.S.C. provisions,  $f_a$  may be increased by 1/3 since lateral loading was considered. The increase is allowed to account for the fact that maximum lateral and maximum gravity loads are not likely to occur at the same time. So, the safety check is simply

$$f \leq 4/3 f_a \quad (4.1)$$

If the above is true, the design is deemed safe, unless a design for the dead and live loads alone, without allowing a 1/3 increase in  $f_a$  results in the selection of a heavier section. In such cases, only the heavier design is deemed safe.

With regard to the issues discussed above, U.S. practice for steel structures has changed little in the past 20 years. The loads specified in the 1972 version of the A.N.S.I. code are essentially the same as in the 1955 version. More significantly though, are the facts that most steel

structures in the U.S. are still designed on the basis of allowable stress, although plastic design is becoming more widely used, and that no distinction is drawn between the effects of dead and live loads.

In Europe, the need for reconstruction following World War II led to the development of new philosophies. While these developments proceeded on an international level, many were first conceived in the U.S.S.R., where many eminent probabilists have emerged. These developments included the concepts of loads specified in terms of characteristic (fractile) values, limit states design, and split safety factor checking formats.

Specification of loads based in terms of characteristic values emphasizes their probabilistic nature in an explicit way, while at the same time helps to provide flexibility. A characteristic value is one for which there is a specified probability of being exceeded in a given length of time. For example, a 5% characteristic value of annual wind speed is one for which there is a probability of 0.05 that it is exceeded in a one year period. U.S. codes have employed characteristic values in a roundabout fashion that can be misleading. Loads described in terms of mean return periods correspond to fractiles of annual maximum distributions. For instance, a mean return period of 100 years corresponds to a probability of exceedence of 0.01 in a given year. Flexibility results from the ability to choose reference periods other than one year and different fractile levels as well.

Some of these concepts have found their way into present U.S. practice. For example, plastic design of steel structures amounts to design for an ultimate limit state defined by the initiation of a collapse mechanism. The ultimate strength design provisions of the A.C.I. [1] are another example of limit states design, and they also use a split safety factor format, like

the Europeans. First, the ultimate design load, U, is found. For cases dealing with dead load, D, and floor live load, L:

$$U = 1.4D + 1.7L \quad (4.2)$$

where D and L are to be based on a loading code, such as A.N.S.I. In case lateral wind load acts:

$$U = 0.75(1.4D + 1.7L + 1.7W) \quad (4.3)$$

This is entirely equivalent to the former 1/3 increase in allowable stress. However, if the effect of dead load is stabilizing, the provisions require the following to be checked:

$$U = 0.9D + 1.3W \quad (4.4)$$

The maximum value of U, computed in the above different ways is then compared to a nominal value of strength (resistance)  $R_n$ :

$$U \leq \phi R_n \quad (4.5)$$

The values of  $\phi$  depend upon the type of member under consideration, and range from 0.70 for compression members to 0.90 for flexural members.

The present ambiguity regarding the use of split factor formats in the U.S. may soon end, however. The most recent proposal for a steel building code also uses a split factor format similar to that of the A.C.I. This code is known as Load and Resistance Factor Design. The basic format of L.R.F.D. is:

$$\phi R_n \geq \gamma_E \sum_{i=1}^n \gamma_i c_i S_i \quad (4.6)$$

where  $c_i$  are the coefficients that transform the loads,  $S_i$ , into effects. Other than the fact that the equation accounts for this transformation ex-



plicitly, it is novel only in its use of  $\gamma_E$ .  $\gamma_E$  is an engineering judgement factor, mainly to account for uncertainty in structural analysis.

The values of the  $\gamma$  factors have been proposed on the basis of a first order, second-moment probabilistic method, as outlined in a report to the American Iron and Steel Institute, which sponsored its drafting [19]. Furthermore, the specific load combination problems considered are the result of the application of the design rule attributed to C. J. Turkstra, discussed in section 1.3. These applications reduce equation 4.6 to special cases, four of which are listed below:

a) Mean Dead plus Mean Maximum Lifetime Live Loads

$$\phi R_n \geq 1.1(1.1c_D D + 1.4c_L L) \quad (4.6a)$$

b) Mean Dead plus Instantaneous Live plus Mean Maximum Lifetime Wind Loads:

$$\phi R_n \geq 1.1(1.1D + 2.0L_I + 1.6W) \quad (4.6b)$$

c) Mean Dead plus Mean Maximum Lifetime Live plus Mean Maximum Daily Wind Loads:

$$\phi R_n \geq 1.1(1.1c_D D + 1.4 c_L L + 2.3c_W W) \quad (4.6c)$$

d) Mean Maximum Lifetime Wind minus Mean Dead Loads:

$$\phi R_n \geq 1.1(1.6W - 0.9D)$$

Since some of the above loads, such as instantaneous live or daily wind loads are not contained in any present U.S. loading code, recommended values will be related to values contained in ANSI-A58.1-1972 in the commentary to the specifications. The commentary will also outline the basis of a reduction factor, applicable to wind forces in certain cases.

## 4.2 Theoretical Objectives in Codified Design

Proceeding hand in hand with changes in specifications, researchers have begun to formulate the theory behind codes. No longer are codes based solely on intuitive grounds; and so, no longer are their aims vaguely defined either. It is the purpose of this section to outline present, and even future aims of codes.

Two papers, by Lind [28] and by Rosenblueth [35], are referenced here. They are especially worth noting since both of these men have been actively involved with code committees.

Lind discusses how the process of selecting consistent partial safety factors can be formulated as a sequence of mathematical operations based on explicit postulates. These postulates reflect the principles upon which current code proposals are based.

Eight postulates are given in all. The first five postulates are generally accepted; the last three are special postulates relating to individual proposals. Four of the first five postulates deal with randomness of loading, randomness in strength, the probability of failure, and the sufficiency of data on loads. All of these have previously discussed in one form or another in this report, however, the fifth one has not. It should be noted carefully, since it is often implicitly assumed, but rarely stated so concisely:

The design values are to be chosen such that the reliability as nearly as possible is constant over the domain of load influence coefficients.

This is, in fact, the main objective of most significant probabilistic code proposals that have been made to date.

Rosenblueth speaks of adopting a strategy for evolution to an "ideal code." First, however, the concept of optimization must be introduced.

The cornerstone in optimization formulations is the concept of utility. Utility is described by an objective function which quantitatively takes into account benefits and costs. Denote the benefits a structure provides by  $B$ ; its initial (including capitalized lifetime maintenance) costs by  $C_i$ ; and finally, costs associated with failure by  $C_f$ . The latter may also include the loss of potential benefits, as well as costs of demolition, etc. All of the individual terms are actually implicit functions of design parameters. Then utility is expressed as:

$$U = B - C_i - p_f C_f \quad (4.7)$$

often in units of monetary value.

The owner of the structure seeks to maximize his own expected utility of the structure,  $E[U]$ . For instance, benefits may consist of rental income, so the owner would desire as much rentable space as possible, until the marginal costs of providing it become greater than the marginal benefits to be received. This is a well established principle of economics. In addition, constraints may exist, such as the amount of capital available to the owner, etc.

For application to codes, this example needs to be broadened and modified. A code committee deals not with a single structure, but with an entire class of structures governed by the code. Roughly speaking, the objective function now sums the contributions of all the structures designed to the code (though the number of structures so designed remains random and unknown). Further, the utility function relates benefits and costs to be

shared by society as a whole; the code committee acts as an agent for society. In this case, benefits may include esthetic considerations, and costs of failure would certainly consider possible loss of life. Finally, the parameter values the committee may control are those contained in the code itself, such as partial safety factors.

The process of maximizing society's objective function with respect to such design criteria is known as code optimization. This is a relatively new field of research, with the first comprehensive treatment being Ravindra, 1970 [33]. Although it is not the purpose here to provide a detailed discussion of the subject, a recent report by Kulkarni [27] serves as an excellent introduction, and provides a referenced summary of others' work.

Now, we may summarize Rosenblueth's three steps:

1. The adoption of partial safety factor formats (similar to L.R.F.D.) dealing with safety on a member by member basis.
2. An explicit treatment of probabilities of failure, recognizing the influence of such matters as static indeterminacy.
3. An optimization format, where the contribution each individual structure makes to society's objective function is openly dealt with.

Rosenblueth concludes that the main obstacles to achieving the ideal code are computational difficulties and a lack of knowledge concerning consequences of failure. He suggests that more work be done in these areas, but foresees steady progress.

The U.S. is still dealing with step 1. However, this does not necessarily reflect the true state of the art, because the Europeans have continued to make major contributions; therefore, these are the subject of the

next section.

### 4.3 Recent European Developments

The most complete applications of new design philosophies are to be found in recent European draft proposals. Three of these are outlined here. The first is a proposal of the European concrete organization, the Comité Européen du Béton (C.E.B.). The volume on structural principles, examined here, is not oriented to concrete construction only. It is more general, and can be applied to a code dealing with any material. Another proposal is due to the Nordic Committee for Building Regulations (N.K.B.). Third, a proposal of the United Nations' Economic Commission for Europe (E.C.E.), which tries to harmonize the C.E.B. and N.K.B. proposals, is outlined. All of these codes are properly viewed as "codes for code writers" more than as practical documents, and as such, place a sharp focus on the state of the art of structural safety in codes.

Before proceeding, it should be noted that all three codes have adopted the general format of partial coefficients. For example, let characteristic load and resistance parameters such as wind velocity, material properties, dimensions, etc. be denoted as  $s_k$  and  $u_k$ . A load parameter is any such that an increase in its value is detrimental to safety, and a resistance parameter is any such that increasing its value is beneficial to safety. Let the partial coefficients be denoted as  $\gamma_s$  and  $\gamma_u$ , respectively, with all  $\gamma$  values greater than 1. Then, use design values  $s_d$  and  $u_d$ :

$$s_d = \gamma_s s_k \quad (4.8a)$$

$$u_d = u_k / \gamma_u \quad (4.8b)$$

Using structural analysis to translate design load values into load effect,  $Q_d$ , and strength of materials to translate the design parameters of resistance into a resistance  $R_d$ , the resistance is required to exceed the loading:

$$Q_d(s_{1d}, s_{2d}, \dots) \leq R_d(u_{1d}, u_{2d}, \dots) \quad (4.9)$$

Such a partial factor format is invariant, unlike the split load and resistance factor formats of U.S. codes. The problem of lack of invariance arises when two different formulations of a safety check of a single structural arrangement that are equivalent in structural mechanics yield different values for a safety index or factor. It is a potential difficulty in conventional as well as probabilistic safety checking. The problem has long been faced when considering soil stability, but has only recently been recognized with building structures, as pointed out by Ditlevsen [15].

#### 4.3.1 C.E.B. Drafts

The draft of the C.E.B. for October 1975 is considered here as representative [12]. Load actions are characterized as "permanent", "variable", or "accidental". Among permanent actions are dead weight, shrinkage, and forces due to expected support settlements. Variable actions include working loads, construction loads, temperature, forces due to wind and snow, and earthquakes "in regions habitually exposed to them." Accidental actions cover other earthquakes, as well as extraordinary settlement, explosions, and other unexpected events. No explicit durations or rates of occurrence are specified to make these definitions more precise. In his review of proposals, Borges indicates that design values for all variable actions are to

Table 4.1 (After the C.E.B.)  
Recommended  $\gamma_s$  values

Action	
1. Associated with	}
Domestic buildings	
Office buildings	
Retail premises	
	0.5
Parking garages	0.6
2. Associated with	
Wind	0.55
Snow	0.55
Wind and Snow	0.55 and 0.4

based on the 5% upper fractile of the annual maximum, however [ 8 ].

For the ultimate limit state, there are two types of classifications for load combinations. First, there are fundamental combinations, with the format:

$$1.25D + 1.45(s_{1k} + \sum_{i=2}^n \gamma_{si}s_{ik}) \quad (4.10)$$

or

$$0.80D + 1.45(s_{1k} + \sum_{i=2}^n \gamma_{si}s_{ik}) \quad (4.10b)$$

where the products  $1.45 \gamma_{si}$  correspond to the  $\gamma_s$  of equation 4.9, in a strictly formal sense. In the above equation,  $s_{1k}$  is considered to be the central variable action in the combination, and  $s_{ik}$  are the accompanying actions. In general, only two such accompanying actions need to be provided for. Furthermore, there is a check for accidental combinations:

$$1.25D + 1.0s_{ik} + \sum_{i=2}^n \gamma'_{si}s_{ik} \quad (4.11)$$

In this combination,  $s_{1k}$  is the characteristic value of a single defined accidental loading, while  $\gamma'_{si}s_{ik}$  represent values of any other variable actions which could act at the same time as the accidental action.

Table 4.1 lists the values suggested for  $\gamma_s$  in this particular draft. However, the code states that values for  $\gamma'_s$  would have to be based on judgement, especially of the nature of the accidental action being dealt with.

It should be emphasized that the individual loads under consideration by this scheme are to be rotated, each in turn taking the place of the central load,  $s_{1k}$ . So, for example, if three variable loads are to be taken



into account in a fundamental combination, three computations should be performed, and the maximum load effect retained. Yet, since the  $\gamma$  values in table 4.1 are often the same, the rule is often simplified.

The provisions of the C.E.B. contrast with those of L.R.F.D. in more than matters of just format. Whereas in L.R.F.D.,  $\gamma$  factors for different loads helped to account for their different variability, the  $\gamma_s$  factors of the C.E.B. do not. Such variability is partly taken into account by the leading 1.45, but mainly accounted for by specifying the loads in terms of characteristic values. Instead, the  $\gamma_s$  factors of the C.E.B. account only for the fact that loads are still specified in terms of annual maxima. Clearly, the C.E.B. implicitly uses Turkstra's suggestion too, but in a different way than L.R.F.D. Instead of defining loads in terms of new distributions (such as maximum daily wind), reductions are made in values relating to annual maxima by  $\gamma_s$ . So, these factors have a role similar to the  $a_i$  and  $b_i$  of equations 1.3 and 1.4, but a more direct one.

#### 4.3.2 N.K.B. Draft

The version of the N.K.B. proposal outlined here was released in October 1974 [11]. It contains two methods; the first is closest to a practical code, the second more theoretical. Since the second method is not substantially different from that based on reference [25], it will not be discussed here.

As in the case of the C.E.B. code, load actions must be classified. The N.K.B. characterized actions as constant, usual short-term, usual non-short-term, unusual, or extreme. The precise method of classification will not be discussed here, since it is expected to be abandoned in any upcoming

draft. However, it is interesting because of the manner in which actions are characterized by means of a parameter  $\alpha$ :

Constant action:  $\alpha = 0$

Non-short-term:  
usual action  $\alpha = 0.5$

Short-term usual:  $\alpha = 1$

Unusual:  $\alpha = 2$

Extreme:  $\alpha = 4$

These values are to be added together. Then, load combinations can be placed in any of three classes. To quote directly from the N.K.B.:

Combination I comprises: Usual actions corrected in view of their duration, in such a number that the sum of  $\alpha$  for all actions does not exceed 4.

Combination II comprises: One unusual action combined with usual actions, corrected in view of their duration, in such a number that the sum of  $\alpha$  for all actions does not exceed 4.

Combination III comprises: One extreme action combined with usual actions, corrected in view of their duration, in such a number that the sum of  $\alpha$  for all actions does not exceed 5.

Correction of a usual action in view of its duration is performed by multiplication of the value relating to usual action by a factor

$$\zeta = 1 - (\alpha + 0.85[1-\xi]) \frac{V}{1 + 0.85 V}$$

where  $V$  is the coefficient of variation for the action and relates to the annual maximum. Normally,  $\xi$  is put = 1, i.e.

$$\zeta = 1 - \frac{\alpha V}{1 + 0.85 V}$$

This scheme appears to be based on a model that assumes the extreme type I (Gumbel) distribution on individual loads. The form of the type I distribution is:

$$F(x) = \exp \left[ -e^{-\alpha(x-u)} \right] \quad (4.12)$$

where  $u$  is the mode of the distribution. In fact, it appears that the  $\alpha$  in the N.K.B. draft has a similar influence as  $\alpha$  in equation 4.12. In the former case, increasing  $\alpha$  values imply a progressively less likely type of load. On the other hand, increasing  $\alpha$  with the Gumbel distribution, with constant  $x$  and  $u$ , results in increasing  $F(x)$ , therefore lower risk. It should be pointed out that the above notation for the Gumbel distribution is standard, contributing to the evidence that the N.K.B. assumed this distribution in their analyses. The commentary to the draft was too incomplete to be conclusive, though.

The partial coefficient  $\gamma_s$  values the N.K.B. recommended are as in table 4.2. These values were used in analyses derived from the theoretical second-moment safety checking method proposed by the N.K.B. A failure function was chosen which linearly combined one resistance and three load variables. For any particular case (corresponding to mean values and coefficients of variation assumed) a value for  $\gamma_u$  was then computed with this method. A range of cases corresponding to those which may be encountered in practice was studied. It was found that the  $\gamma_s$  values chosen tended to make  $\gamma_u$  nearly constant throughout this range, and so the minimum safe value of  $\gamma_u$  was used as the recommended value. Further examples show that the set of  $\gamma_s$  values recommended made  $\gamma_u$  less variable than some other (still apparently reasonable) sets. So, from these studies, the recommended  $\gamma$  values are seen to be based on more than just intuitive grounds. Yet, such studies

Table 4.2 (After the N.K.B.)  
Recommended  $\gamma_s$  values

Load Type	Load Combination		
	I	II	III
Dead loads from the mass of the structure	1.5	1.2	1.0
Earth pressure	1.5	1.2	1.0
Live loads:			
ordinary loads	1.3	1.3	1.0
exceptional loads	---	1.5	---
Accidental loads	---	---	1.0
Loads caused by deformations	1.0	1.0	1.0

do not constitute code optimization. Instead, we choose to call such an approach discretization, meaning a small set of specific  $\gamma$  values are selected to correspond approximately to the continuous range that fully probabilistic or second moment methods would imply. Discretization was also the basis of the L.R.F.D. proposal.

The motivation for presenting this  $\alpha$ -method is that it illustrates just one of the many avenues that have been explored in the hope of making load classification schemes precise and unambiguous. Such an advance, in Rosenblueth's terms, would help promote progress beyond step 1.

4.3.3 E.C.E. Draft

The E.C.E. draft referenced here was dated January 1976 [10]. It is an openly stated attempt to reconcile the C.E.B. and N.K.B. proposals. In most respects, this meant that ideas were taken directly from one proposal or the other; in some cases, sentences or entire paragraphs were taken from the earlier documents. Nevertheless, a substantial change dealing with load combinations was introduced.

Like the C.E.B., loads are classified as permanent, variable, or accidental. The format adopted for cases not involving accidental actions is:

$$D + 1.30(s_{1k} + \sum_{i=2}^n 0.70 s_{ik}) \tag{4.13}$$

and, for cases involving accidental actions:

$$D + 1.0s_{1k} + \sum_{i=2}^n \gamma'_{si} s_{ik} \tag{4.14}$$

where the meanings of the  $s_{ik}$  and  $\gamma'_{si}$  are the same as in equations 4.10 and 4.11. Note the generally lower factors suggested by the E.C.E. report.

This is a consequence of the fact that all variable actions are to be evaluated at the upper 2% characteristic values of the annual maximum distributions. Again, judgement must be exercised in the selection of the  $\gamma'_{Sj}$  values.

A discretization was carried out to get values for  $\gamma_u$ , similar to the N.K.B., and using the same second-moment theoretical method. Again, the values for  $\gamma_s$  were chosen a priori.

After this point, the E.C.E. report departs significantly from the C.E.B. and N.K.B. In an appendix, a method for selecting parameters for distributions other than annual maxima is given. It amounts to a scheme to evaluate equations 1.4 and 1.5, and further, to get the mean and variance of the extreme value distribution for combined effects of loads.

The method (attributed to Ditlevesen) embodies the use of Bosshard's probability  $p$  with the discrete-time (Borges-Castenheta) model. The extreme type I distribution is assumed to hold for load intensities within elementary intervals. For a given load, let the parameters relating to the annual maximum distribution be  $\mu_a$  and  $\sigma_a$ . Again, for this individual load, let the year be divided into  $k$  intervals. Then, we can calculate the mean and standard deviation of the extreme value distribution corresponding to  $K$  intervals,  $K$  being arbitrary:

$$\sigma_K = \mu_a \left[ \frac{A(K) (\sigma_a/\mu_a)^2 - p^K}{A(K) C(K) - B^2(K)} \right]^{1/2} \quad (4.15)$$

and

$$\mu_K = \frac{\mu_a - B(K) \sigma_K}{A(K)} \quad (4.16)$$

where

$$A(K) = 1 - p^K$$

$$B(K) = \sum_{j=1}^K \binom{K}{j} q^j p^{(K-j)} \left[ \frac{\sqrt{6}}{\pi} \ln j \right]$$

$$C(K) = \sum_{j=1}^K \binom{K}{j} q^j p^{(K-j)} \left[ \left[ \frac{\sqrt{6}}{\pi} \ln j \right]^2 + 1 \right]$$

So far, only the implications of the scheme for a single load have been considered. Now, construct a matrix, such as in table 4.3, with its entries corresponding to the number of intervals,  $K$ , to be used for each load. Proceed loadwise from this point. For every load, use the assumption regarding the number of intervals in one year,  $k$ , to calculate the entries corresponding to  $K$ . Using these values for  $K$ , compute  $\mu_K$  and  $\sigma_K$  for each load. The parameters of the distribution of the annual maximum for one combination of  $n$  loads are now given as:

$$\mu_{\text{comb}} = \sum_{\substack{\text{all} \\ \text{loads}}} \mu_K \quad (4.17a)$$

$$\sigma_{\text{comb}} = \left[ \sum_{\substack{\text{all} \\ \text{loads}}} \sigma_K^2 \right]^{1/2} \quad (4.17b)$$

This calculation must be repeated for any other combination number, much the same as Turkstra's result 1.3. Using these with the theoretical second-moment method, non-arbitrary values of  $\gamma_s$  can be chosen. Then, a

Table 4.3 (After the E.C.E.)  
 Numbers of intervals used in the E.C.E. scheme

Combination number	Load Number	1	2	3
		Number of time intervals in one year	$k_1$	$\leq k_2$
1	Number of repetitions	$k_1$	$k_2/k_1$	$k_3/k_2$
2	Number of repetitions	1	$k_2$	$k_3/k_2$
3	Number of repetitions	1	1	$k_3$



discretization process can be carried out without the need to select the  $\gamma_s$  values beforehand.

#### 4.3.4 Reliability Consistency of the European Formats

Clearly, the European draft proposals, taken in concert, portray the evolution of structural codes. However, although based on approximate "second step" methods, they still have not progressed beyond the partial safety factor format the Rosenblueth described as a first step. Accordingly, they cannot guarantee that they satisfy Lind's constant reliability criterion. Therefore a brief study of this subject is offered here, based on the methods discussed in earlier chapters.

Since the codes deal only in scalar terms, the formulation of Chapter 3 is used. As indicated in equation 1.9, the upcrossing rates so obtained can be interpreted as probabilities of exceedence, in reference to a reduced or characteristic capacity level.

This study is directly comparable to study 2, section 2.3.4. All of the stochastic process parameters used there are assumed here as well, with the wind load becoming load 1, the floor load, 2. These values were chosen because they not only represent a realistic situation, but also because in the earlier study they exhibited no pathological behavior, as did case 3E.

The coefficients  $c_1$  and  $c_2$  can now be interpreted as the wind and floor load influence coefficients. They may represent a linearized boundary, or a natural scalar threshold such as moment capacity about a single axis of a beam. In any case, these are the coefficients that define the domain over which the reliability is desired to be a constant. For the purpose of exploring this domain, four combinations of  $c_1$  and  $c_2$  were chosen. Holding

the sum equal to unity,  $c_1$  was taken as 0.2, 0.4, 0.6, and 0.8, giving complimentary values for  $c_2$ .

As a result of this linear and scalar interaction, safety checking is possible in terms of load effects. So, for the C.E.B., equation 4.10:

$$z = 1.25 c_2 D + 1.45(c_1 s_{1k} + 0.5 c_2 s_{2k})$$

or

$$z = 1.25 c_2 D + 1.45(c_2 s_{2k} + 0.5 c_1 s_{1k})$$

whichever is greater. Since  $c_2$  relates in this case to gravity floor load, it is in both cases applied to dead load. Similarly, equation 4.13 yields the checking threshold for the E.C.E.:

$$z = c_2 D + 1.30(c_1 s_{1k} + 0.7 c_2 s_{2k})$$

or

$$z = c_2 D + 1.30(c_2 s_{2k} + 0.7 c_1 s_{1k})$$

where again, the larger result is retained.

For both codes, the characteristic values  $s_k$  (5% for C.E.B., 2% for E.C.E.) relating to the annual maxima were found by application of:

$$\frac{F(x)}{\text{Annual max}} = (p + qF(x)) \exp(-qvG(x)) \quad (4.18)$$

an equation whose basis is explained in Grigoriu's collection [21].

The results are presented in figures 4.1 to 4.6. It should be emphasized that the lines drawn between points are not interpolations, but are only meant to guide the eye of the reader.

A horizontal line would be the result of perfectly consistent reliability. While none are to be found, the results are encouraging. Differences

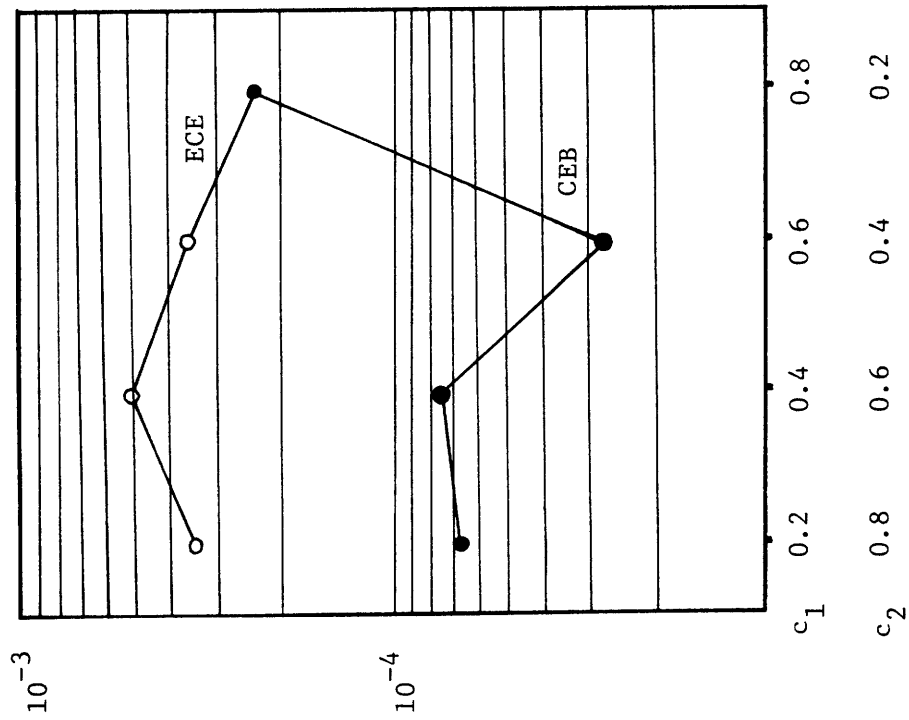


Figure 4.1: Case A, normal distributions.

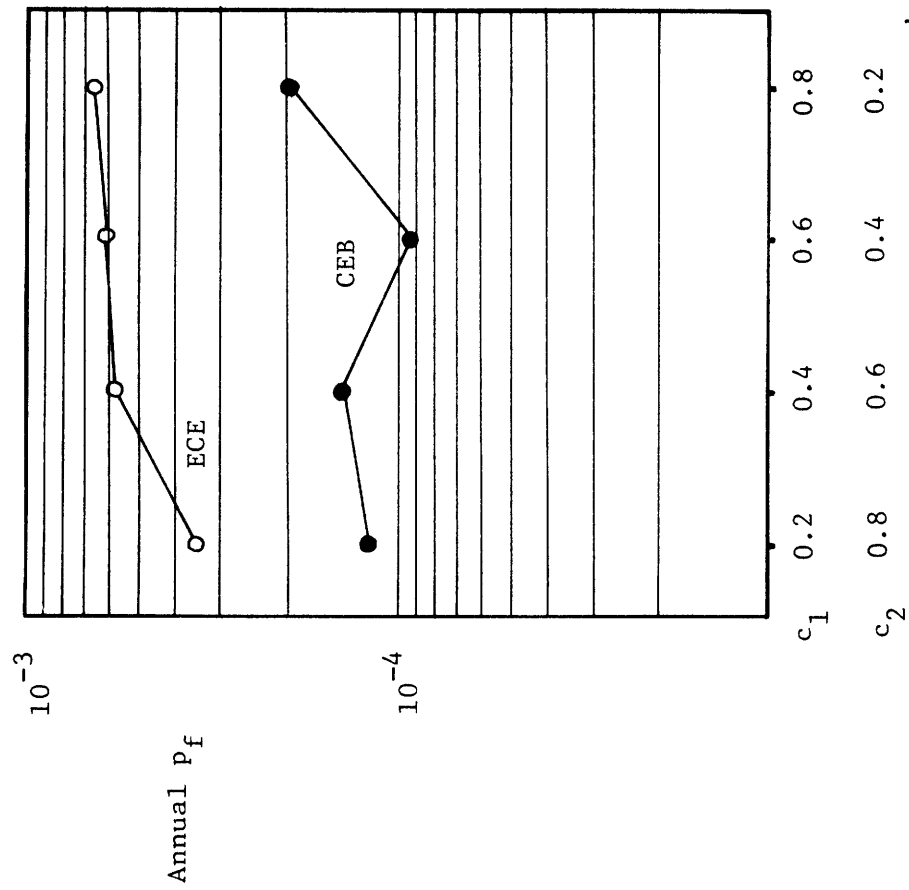


Figure 4.2: Case A, gamma distributions.

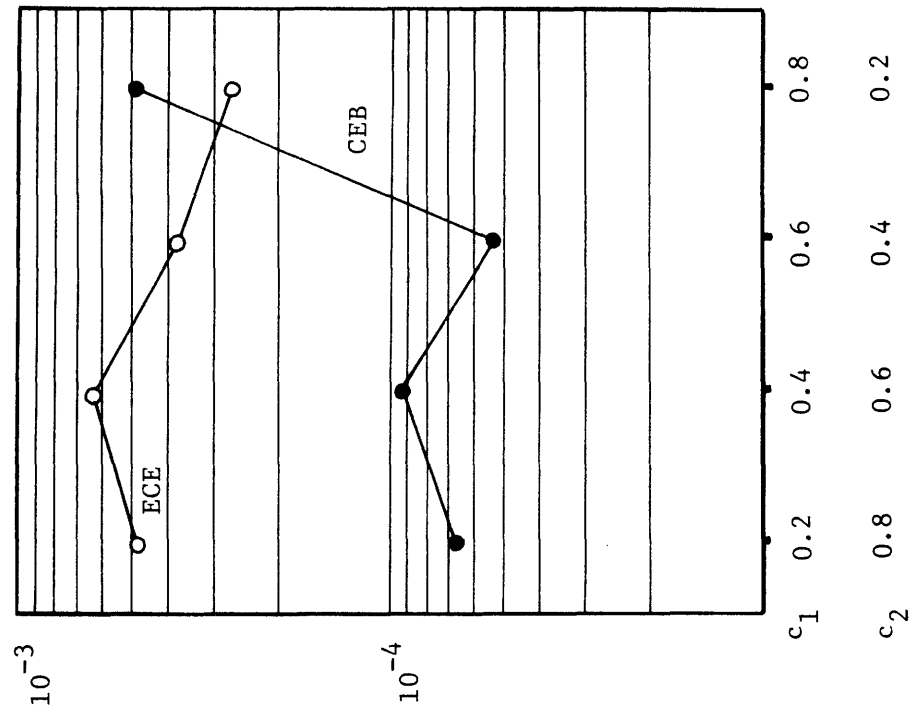
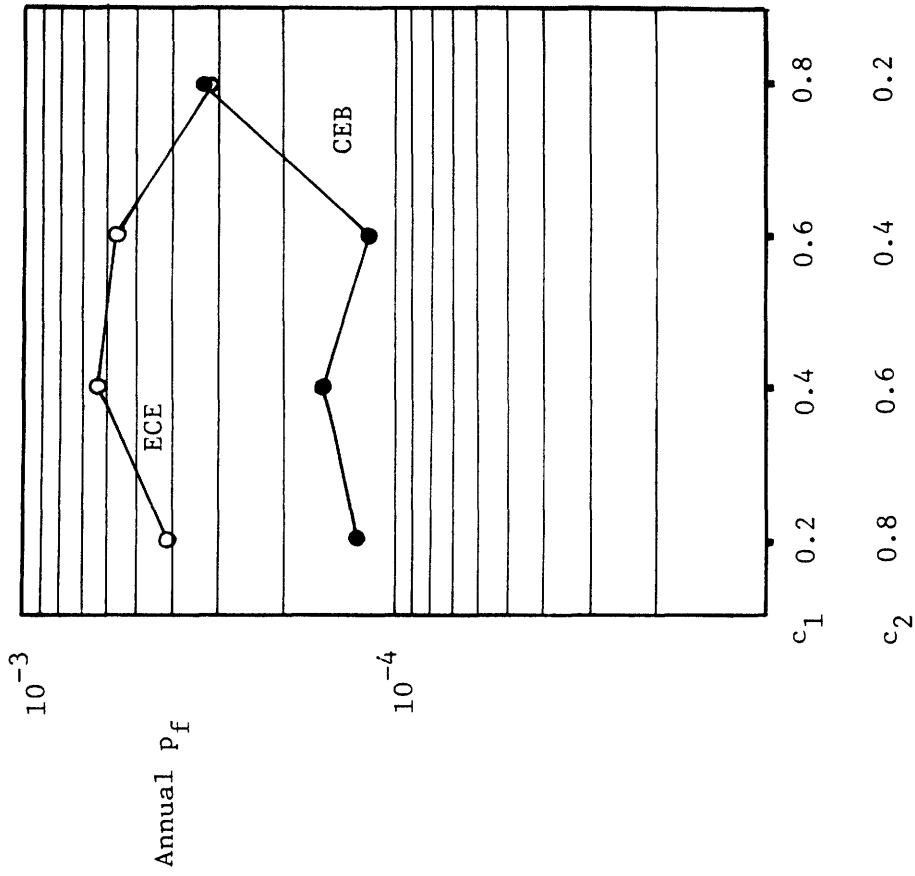


Figure 4.3: Case B, normal distributions.

Figure 4.4: Case B, gamma distributions.

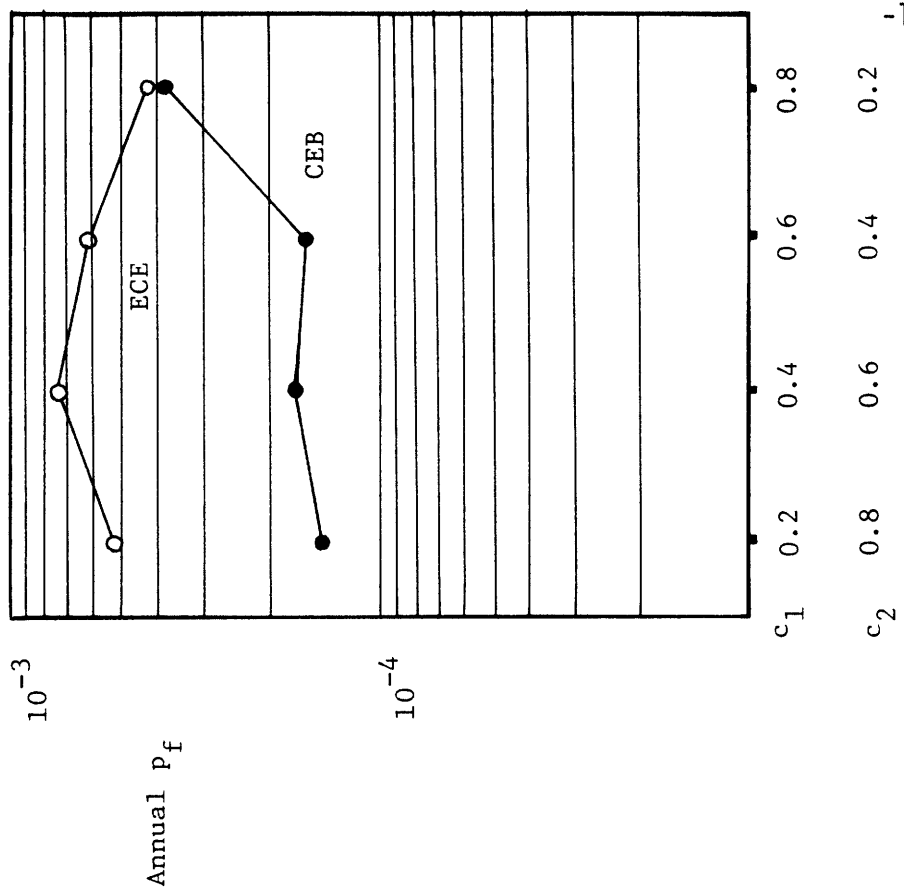


Figure 4.6: Case C, gamma distributions.

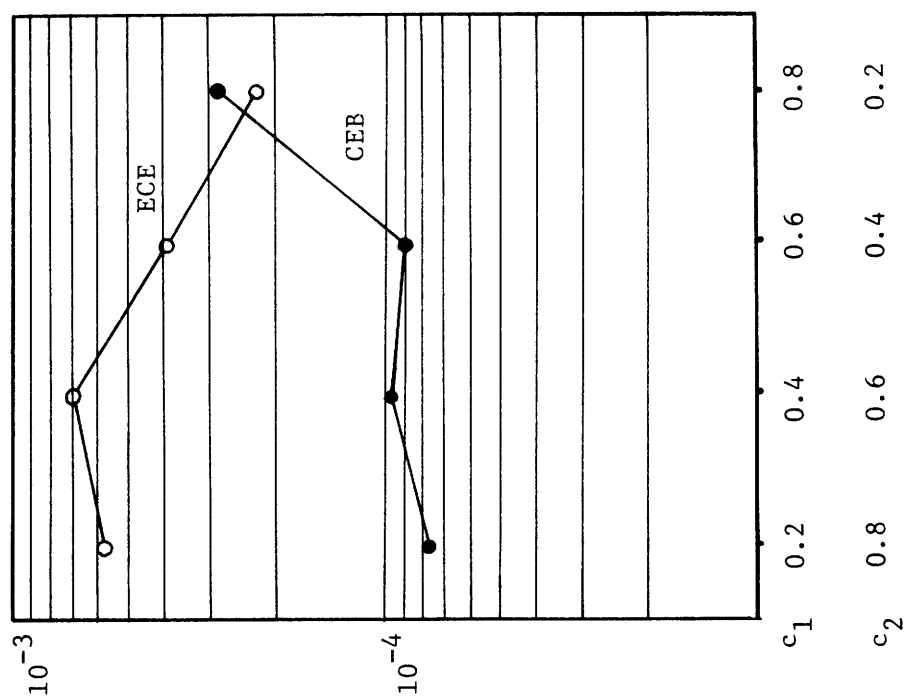


Figure 4.5: Case C, normal distributions.

of greater than an order of magnitude in  $p_f$  are not found, and most are in fact relatively slight.

The most noticeable observation is that in almost every case the E.C.E. implied a higher risk than did the C.E.B. However, this is not of great significance, because the main purpose here is to check consistency within codes, not between them.

More careful inspection reveals other patterns. For instance, the E.C.E. gave generally similar risks regardless of the distributions that were assumed. In fact, the plots were originally made without regard to distribution type (as though figures 4.1 and 4.2 were plotted together) but in this manner the C.E.B. results were overlaid and not readily distinguishable. On the other hand, the C.E.B. gave generally greater risks when the gamma distribution was assumed rather than the normal distribution.

Other similarities exist between cases A, B, and C. Notably, in all cases the C.E.B. gave its peak risk with  $c_1 = 0.8$  and  $c_2 = 0.2$ , and the E.C.E. gave its peak at  $c_1 = 0.4$  and  $c_2 = 0.6$  in all but a single instance. While no similar statement holds true for minimum risks, the plots appear to have the same general shape and risk level from case to case.

Plainly, it would be presumptuous to draw general conclusions from the few examples this study illustrates. However, they demonstrate how the formulation of Chapter 3 can be applied to check design formats. Also, they do show that partial safety factor formats can lead to relative risk consistency, although the limitations of such methods remain unclear.

CHAPTER 5

CONCLUSIONS AND RECOMMENDATIONS

Load combinations were examined in this work from both mathematical and practical points of view. In mathematical terms, two dimensional outcrossing rate problems were analyzed employing both modified Poisson square wave and continuous time Gaussian process formulations. Scalar upcrossing rate problems were also pursued. Relating to engineering practice, design code formats for load combinations were presented and discussed.

Case studies, germane to both mathematical and practical aspects, played an important role in this thesis. Computer programs written to facilitate computations are available, and should be useful in future work.

Based upon this work, including the case studies, the following conclusions are reached:

1. For two dimensional outcrossing problems where loads are assumed to be normally distributed, the modified square wave and continuous time Gaussian process formulations yield similar results. However, the continuous time formulation offers great savings in computational effort, and can be readily extended to three or even higher dimensional situations.
2. A two dimensional failure surface can be replaced by a linear boundary with acceptable accuracy. These linearizations can be made either in terms of loads or effects. In any case, they permit the reduction of the outcrossing problem to a scalar upcrossing problem, which results in significant savings of computational effort.
3. For square wave processes, the mean upcrossing rate reduces to an explicit analytical expression whose terms are readily interpreted. The op-

erations reduce to random variable (rather than stochastic process) operations, i.e., at most convolutions of two probability distributions.

4. Codified approaches to load combinations appear to meet their currently stated objectives. Yet, progress toward eventual goals lags, mainly due to the difficulty in applying mathematical results already in hand.

The following areas are recommended as topics worthy of future research. The first two would repair shortcomings in this work:

1. Outcrossing and upcrossing results should be pursued for sums of processes similar to square waves, but with different pulse shapes. Triangular pulses would especially be useful, say, for studying bending effects due to vehicular traffic on simply supported bridge spans.
2. Non-linear structural interaction should be studied. Perhaps a simulation approach would be required, but at least case studies indicating the amount of error inherent in assuming linear structural behavior could be carried out.

The last recommendation amounts to a remedy of conclusion 4, above.

It is:

3. Study general upcrossing formulae for simplifying cases, in the hope of discovering and developing implied load combination rules at simpler code levels.

Alternatively, the following approach may prove fruitful. A set of charts expressing the influence of the various parameters (i.e.,  $p$ ,  $v$ ,  $\mu$ , and  $\sigma$ ) on the mean annual rate of upcrossings at various thresholds could be constructed. The E.C.E. proposal (e.g., equations 4.15-4.17) indicated that engineers may be willing to accept the modified square wave results of Chapter 3, especially because they lend themselves so well to interpre-



tation. To overcome the involved computations required, even when liberal distribution type assumptions are made, such charts may be necessary. One should note that charted solutions are often favored in situations where calculations are of greater than routine difficulty. Such is the case with column interaction diagrams, for which analytical expressions are available. A given set could relate parameters and distribution types estimated for a given locality with the design levels for individual loads, structural influence coefficients, and  $p_f$  in any manner found to be convenient. At first, these charts would serve mainly as research tools, such as seismic ground motion records do for earthquake engineers. However, they may prove to be precursors of standard design aids of the future.

REFERENCES

- 1 American Concrete Institute, "Building Code Requirements for Reinforced Concrete," ACI 318-71, February, 1971.
- 2 American Institute of Steel Construction, "Specification for the Design, Fabrication, & Erection of Structural Steel for Buildings," February, 1969.
- 3 American National Standards Institute, "Requirements for Minimum Design Loads in Buildings and Other Structures," ANSI A58.1, 1972.
- 4 Asplund, S.O., "Probabilities of Traffic Loads on Bridges," Proceedings of the ASCE, Volume 81, Separate 585, January, 1955.
- 5 Benjamin, J.R., and Cornell, C.A., Probability, Statistics, and Decision for Civil Engineers, McGraw-Hill Book Co., New York, 1970.
- 6 Blackall, C.H., "Live Floor Loads," The American Architect--The Architectural Review, January 3, 1923.
- 7 Borges, J.F., and Castenheta, M., Structural Safety, 2nd Edition, Laboratorio Nacional de Engenharia Civil, Lisbon, 1971.
- 8 Borges, J.F. and Castenheta, M., "Unification and Rationalization of Level I Code Formats," Document VII-2.5, Laboratorio Nacional de Engenharia Civil, Lisbon, February, 1976.
- 9 Bosshard, W., "On Stochastic Load Combination," Department of Civil Engineering, Stanford University, July, 1975.
- 10 Bresdorff, Kukulski, and Skov, "Recommendations on General Principles of Structural Design," ECE Committee on Housing, Building, and Planning, Working Party on Building Industry, Second Draft, January, 1976.
- 11 C.E.B. Bulletin d' Information, Number 108, Paris, March, 1975.
- 12 C.E.B. Bulletin d' Information, Number 111, Paris, October, 1975.
- 13 Cornell, C.A., "A Probability-Based Structural Code," Journal of the American Concrete Institute, Volume 66, Number 12, December 1969.
- 14 Crandall, S.H., and Mark, W.D., Random Vibrations in Mechanical Systems, Academic Press, New York, 1963.
- 15 Ditlevsen, Ove, "Structural Reliability and the Invariance Problem," Report Number 22, Solid Mechanics Division, University of Waterloo, March, 1973.

- 16 Ditlevsen, Ove, Extreme and First Passage Times with Applications to Civil Engineering, Technical University of Denmark, Copenhagen, 1971.
- 17 Ditlevsen, Ove, and Skov, Knud, "The Uncertainty Theoretical Definition of Structural Safety Suggested by the NKB Safety Committee," Unpublished, April, 1975.
- 18 Everard, N.J., and Cohen, E., "Ultimate Strength Design of Reinforced Concrete Columns," Interim Report of ACI Committee 340, ACI Publication SP-7, 1964.
- 19 Galambos, T.V., and Ravindra, M.K., "Tentative Load and Resistance Factor Design Criteria for Steel Buildings," Research Report #18, Structural Division, Department of Civil Engineering, Washington University, St. Louis, 1973.
- 20 Greene, C.E., Structural Mechanics, The Inland Press, Ann Arbor, 1897.
- 21 Grigoriu, M.D., "On the Maximum of the Sum of Random Process Load Models," Internal Project Working Document #1, Structural Loads Analysis and Specifications Project, M.I.T., 1975.
- 22 Grigoriu, M.D., "A Decision Theoretic Approach to Model Selection for Structural Reliability," PhD. Thesis, Department of Civil Engineering, M.I.T., January, 1976.
- 23 Gumbel, E.J., Statistics of Extremes, Columbia University Press, New York, 1958.
- 24 Hasofer, A.M., "The Time-Dependent Maximum of Floor Live Loads," Unpublished, August, 1973.
- 25 Hasofer, A.M., and Lind, N.C., "Exact and Invariant Second-Moment Code Format," Journal of the Engineering Mechanics Division, ASCE, Volume 100, Number EM1, February, 1974.
- 26 Karlin, S., and Taylor, H.M., A First Course in Stochastic Processes, Second Edition, Academic Press, New York, 1975.
- 27 Kulkarni, R.B., "Decisions of Optimum Structural Safety," PhD. Thesis, Department of Civil Engineering, Stanford University, 1974.
- 28 Lind, N.C., "Consistent Partial Safety Factors," Journal of the Structural Division, ASCE, Volume 97, Number ST6, June, 1971.
- 29 McGuire, R.K., and Cornell, C.A., "Live Load Effects in Office Buildings," Research Report R73-28, Department of Civil Engineering, M.I.T., May, 1973.

- 30 Paloheimo, E., and Hannus, M., "Structural Design based on Weighted Fractiles," Journal of the Structural Division, ASCE, Volume 100, Number ST7, July, 1974.
- 31 Parzen, E., Stochastic Processes, Holden-Day, San Francisco, 1962.
- 32 Peir, J.C., "A Stochastic Live Load Model for Buildings," Research Report R71-35, Department of Civil Engineering, M.I.T., October, 1971.
- 33 Ravindra, M.K., "Structural Code Optimization," PhD. Thesis, University of Waterloo, 1970.
- 34 Rice, S.O., "Mathematical Analysis of Random Noise," Bell System Technical Journal, Numbers 23 and 24, 1944.
- 35 Rosenblueth, E., and Esteva, L., "Reliability Basis for Some Mexican Codes," Probabilistic Design of Reinforced Concrete Buildings, Publication SP-31, American Concrete Institute, Detroit, 1972.
- 36 Turkstra, C.J., "Theory of Structural Design Decisions," Solid Mechanics Study Number 2, University of Waterloo, 1972.
- 37 Veneziano, D., "Invariance in Second Moment Reliability," Research Report R74-33, Department of Civil Engineering, M.I.T., April, 1974.
- 38 Veneziano, D., "Safe Regions and Second Moment Reliability Vectors," presented at the ASCE Specialty Conference on Probabilistic Methods in Engineering, Stanford University, June, 1974.
- 39 Veneziano, D., "Basic Principles and Methods of Structural Safety," Research Report R76-2, Department of Civil Engineering, M.I.T., April, 1976.
- 40 Veneziano, D., Grigoriu, M.D., and Cornell, C.A., "Vector Process Models for System Reliability," to be published.
- 41 Winter, G., and Nilson, A.H., Design of Concrete Structures, McGraw-Hill Book Company, New York, 1972.

APPENDIX:  
Computer Programs

```
C *** OUTCROSSING RATE PROGRAM (URP)
C
  DIMENSION TOPX(40,2), LFTY(40,2), BOTX(40,2), RHTY(40,2)
  DIMENSION QX(999), QY(999), ZX(999), ZY(999)
  DIMENSION TRIX(3,999), TRIY(3,999)
  DIMENSION ARRAY(40,5)
  INTEGER PTS
  REAL M, P, E, W, F, PROP, LFTY, MEANL, NUJL
  REAL MEANF, NUF, KF, LAMF, MEANK, NUJ, Kk, LAMW

  NX=999
  NY=999
  NXMI = NX - 1
  NYMI = NY - 1
  K = 5
  L = 6
  KX = 4
  KY = 5

C
  1 READ(K,100,END=999) CWM, CFM, CWP, CFP
  WRITE(L,300)
  WRITE(L,200) CWM, CFM, CWP, CFP
C *** INVERT THE MATRIX
  DET = CWM*CFP - CWP*CFM
  DMW = CFP/DET
  DPW = -CFM/DET
  DMF = -CWP/DET
  DPF = CWM/DET
  WRITE(L,301)
  WRITE(L,201) DMW, DPW, DMF, DPF

C
C *** READ IN INTERACTION DIAGRAM, COMPUTE ECCENTRICITY AND
C *** TRANSFORM TO LOAD SPACE; STORE ALL OF THIS IN ARRAY.
C *** PTS SPECIFIES THE NUMBER OF POINTS THAT WILL BE USED
C *** TO INPUT THE DIGITIZED INTERACTION DIAGRAM.
C
```

```
C
READ(K,101) PTS
WRITE(L,302)
DO 15 I=1, PTS
READ(K,102) M, P
IF(P .EQ. 0.0) GO TO 9
E=M/P
GO TO 10
9 E=900000.0
10 CONTINUE
W = DMW*M + DPW*P
F = DMF*M + DPF*P
ARRAY(I,1) = M
ARRAY(I,2) = P
ARRAY(I,3) = F
ARRAY(I,4) = W
ARRAY(I,5) = F
15 WRITE(L,202) M, P, F, W, F
C
C *** FIND THE EXTREMA
C
XMAX=0.0
XMIN=0.0
YMAX=0.0
YMIN=0.0
DO 20 I=1, PTS
X = ARRAY(I,KX)
Y = ARRAY(I,KY)
IF(X .LT. XMAX) GO TO 17
XMAX = X
IMX = I
17 CONTINUE
IF(X .GT. XMIN) GO TO 18
XMIN = X
ILX = I
18 CONTINUE
```

```
IF(Y .LT. YMAX) GO TO 19
YMAX = Y
IMY=I
```

19 CONTINUE

```
IF(Y .GT. YMIN) GO TO 20
YMIN = Y
ILY = I
```

20 CONTINUE

C

```
WRITE(L,303) XMAX, ARRAY(IMX,3)
WRITE(L,203) YMAX, ARRAY(ILX,3)
WRITE(L,204) YMIN, ARRAY(ILX,3)
WRITE(L,205) YMAX, ARRAY(IMY,3)
WRITE(L,206) YMIN, ARRAY(ILY,3)
```

C

```
DX=(XMAX-XMIN)/(FLOAT(NX) + 1.0)
DY=(YMAX-YMIN)/(FLOAT(NY) + 1.0)
```

C

C \*\*\* THE FOUR PATHS FROM MINIMA TO MAXIMA ARE FOUND  
C \*\*\* AND STORED IN TOPX, LFTY, RHTX, CHTY

C

```
DO 40 I=1,40
DO 40 J=1,2
TOPX(I,J)=900000.0
BOTX(I,J)=900000.0
LFTY(I,J)=900000.0
RHTY(I,J)=900000.0
```

C

```
IF(ILX .GT. IMX) GO TO 55
IT=1
```

```
DO 50 I=ILX, IMX
TOPX(IT,1) = ARRAY(I,KX)
TOPX(IT,2) = ARRAY(I,KY)
50 IT = IT + 1
```

C

```
IS = ILX + 1
```



```
IR = I
DO 52 II=1,ILX
  I = IS - II
  ROTX(IR,1) = ARRAY(I,KX)
  ROTX(IR,2) = ARRAY(I,KY)
52 IB = IR + 1
  IR = ILX
  IS = PTS + IMX
DO 54 II=IMX, PTS
  I = IS - II
  ROTX(IR,1) = ARRAY(I,KX)
  ROTX(IR,2) = ARRAY(I,KY)
54 IB = IB + 1
```

C

```
GO TO 70
55 CONTINUE
IT=1
DO 60 I=ILX, PTS
  TOPX(IT,1) = ARRAY(I,KX)
  TOPX(IT,2) = ARRAY(I,KY)
60 IT = IT + 1
```

C

```
IT = PTS - ILX + 2
DO 65 I=1,IMX
  TOPX(IT,1) = ARRAY(I,KX)
  TOPX(IT,2) = ARRAY(I,KY)
65 IT = IT + 1
  IS = IMX + ILX
  IR = 1
DO 67 II=IMX, ILX
  I = IS - II
  ROTX(IR,1) = ARRAY(I,KX)
  ROTX(IR,2) = ARRAY(I,KY)
67 IB = IB + 1
```

C

```
70 WRITE(L,304)
```

C DO 72 I=1,40  
72 WRITE(L,207) TOPX(I,1), TOPX(I,2), RUTX(I,1), RUTX(I,2)  
IF(ILEY .GT. IMY) GO TO 155  
IT=1

DO 150 I=ILEY, IMY  
LFTY(IT,1) = ARRAY(I,KX)  
LFTY(IT,2) = ARRAY(I,KY)

150 IT = IT + 1  
IS = ILY + 1  
IR = 1

DO 152 II=1, ILY  
I = IS - II  
RHTY(IB,1) = ARRAY(I,KX)  
RHTY(IB,2) = ARRAY(I,KY)

152 IR = IB + 1  
IR = ILY

IS = PTS + IMY  
DO 154 II=IMY, PTS  
I = IS - II  
RHTY(IR,1) = ARRAY(I,KX)  
RHTY(IR,2) = ARRAY(I,KY)

154 IR = IB + 1

C GO TO 170  
155 CONTINUE  
IT=1

DO 160 I=ILEY, PTS  
LFTY(IT,1) = ARRAY(I,KX)  
LFTY(IT,2) = ARRAY(I,KY)

160 IT = IT + 1

C IT = PTS - ILY + 1  
DO 165 I=1,IMY  
LFTY(IT,1) = ARRAY(I,KX)  
LFTY(IT,2) = ARRAY(I,KY)

```
165 IT = IT + 1
    IS = IMY + ILY
    IB = I
    DO 167 II=IMY, ILY
        I = IS - II
        RHTY(IB,1) = ARRAY(I,KX)
        RHTY(IB,2) = ARRAY(I,KY)
167 IB = IB + 1
C
170 WRITE(L,305)
    DO 172 I=1,40
172 WRITE(L,207) LFTY(I,1), LFTY(I,2), RHTY(I,1), RHTY(I,2)
C
C *** CONSTRUCT TRIX (AND TRIY) IN THIS MANNER:
C *** ROW 1: YT (XL)
C *** ROW 2: X (Y)
C *** ROW 3: YB (XR)
C
DE 240 J=1, NX
X = XMIN + FLOAT(J)*DX
DO 235 I=1,40
    IPI = I + 1
    CHK = TOPX(IPI,1) - X
    IF(CHK .GT. 0.0) GO TO 236
235 CONTINUE
236 SX = TOPX(IPI,1) - TOPX(I,1)
    SY = TOPX(IPI,2) - TOPX(I,2)
    PROP = CHK/SX
    TRIX(1,J) = TOPX(IPI,2) - PROP*SY
    TRIX(2,J) = X
    DO 237 I=1,40
        IPI = I + 1
        CHK = ROTX(IPI,1) - X
        IF(CHK .GT. 0.0) GO TO 238
237 CONTINUE
238 SX = ROTX(IPI,1) - ROTX(I,1)
```

```
SY = ROTX(IPI,2) - ROTX(I,2)
PROP = CHK/SX
TRIX(3,J) = ROTX(IPI,2) - PROP*SY
240 CONTINUE
DO 250 J=1, NY
Y = YMIN + FLOAT(J)*DY
DO 245 I=1,40
IPI = I + 1
CHK = LFTY(IPI,2) - Y
IF(CHK .GT. 0.0) GO TO 246
245 CONTINUE
246 SY = LFTY(IPI,2) - LFTY(I,2)
SX = LFTY(IPI,1) - LFTY(I,1)
PROP = CHK/SY
TRYI(1,J) = LFTY(IPI,1) - PROP*SX
TRYI(2,J) = Y
DO 247 I=1,40
IPI = I + 1
CHK = RHTY(IPI,2) - Y
IF(CHK .GT. 0.0) GO TO 248
247 CONTINUE
248 SY = RHTY(IPI,2) - RHTY(I,2)
SX = RHTY(IPI,1) - RHTY(I,1)
PROP = CHK/SY
TRYI(3,J) = RHTY(IPI,1) - PROP*SX
250 CONTINUE
C
C *** X AXIS AND Y AXIS INTERCEPTS
C
DO 259 J=1,NX
X=TRIX(2,J)
IF(X .GT. 0.0) GO TO 260
259 CONTINUE
260 JMI = J - 1
PROP=(-TRIX(2,JMI))/(TRIX(2,J) - TRIX(2,JMI))
YIT = TRIX(1,JMI) + PROP*(TRIX(1,J) - TRIX(1,JMI))
```

```

YIR = TRIX(3,JM1) + PROP*(TRIX(3,J) - TRIX(3,JM1))
DC 269 J=1,NY
Y=TRIX(2,J)
IF(Y.GT. 0.0) GO TO 270
269 CONTINUE
270 JM1 = J - 1
PROP=(-TRIX(2,JM1))/(TRIX(2,J) - TRIX(2,JM1))
XIL = TRIX(1,JM1) + PROP*(TRIX(1,J) - TRIX(1,JM1))
XIR = TRIX(3,JM1) + PROP*(TRIX(3,J) - TRIX(3,JM1))
WRITE(L,209) YIT, XIL, XIR, YIR
C *** LOOP THROUGH FOR DIFFERENT LOADING CASES, WITH NC
C *** TO SPECIFY THE NUMBER OF CASES TO FOLLOW.
C
C
READ(K,103) NC
WRITE(L,210) NC
DO 500 IC=1, NC
READ(K,104) NUW, PW, MEANW, SIGMAW, NUL, MEANL, SIGMAL, D
WRITE(L,211) IC, MEANW, SIGMAW, NUW, MEANL, SIGMAL, NUL, PW, D
QW = 1.0 - PW
C
C
C *** DISTW AND DISTL REFER TO THE DISTRIBUTION TYPES TO BE
C *** ASSUMED FOR WIND AND FLOOR LOADING. ZERO SPECIFIES THE
C *** NORMAL, ANY POSITIVE NUMBER THE GAMMA DISTRIBUTION.
C
READ(K,105) DISTW, DISTL
IF(DISTW.GT. 0.0) GO TO 275
WRITE(L,308)
GO TO 276
275 WRITE(L,309)
276 IF(DISTL.GT. 0.0) GO TO 277
WRITE(L,310)
GO TO 278
277 WRITE(L,311)
NUF=NUI
MEANF=MEANL

```

```
SIGMAF=SIGMAL
C *** GAMMA DISTRIBUTION PARAMETERS
278 KW = (MEANW**2)/(SIGMAW**2)
LAWW = (MEANW)/(SIGMAW**2)
KF = (MEANF**2)/(SIGMAF**2)
LAMF = (MEANF)/(SIGMAF**2)
DO 279 I=1,NX
  TRIX(1,I) = TRIX(1,I) - D
279 TRIX(3,I) = TRIX(3,I) - D
DO 280 I=1,NY
280 TRIY(2,I) = TRIY(2,I) - D
  YIT = YIT - D
  YIR = YIR - D
C
C *** SET UP THE INTEGRATION VECTORS OX, ZX, OY, & ZY, WHERE
C *** OX AND OY STORE CUMULATIVE TERMS, ZX AND ZY DENSITY TERMS.
C
IF(DISTF .GT. 0.0) GO TO 350
DO 335 I=1,NX
C *** OX FOR NORMAL
  U = (TRIX(1,I) - MEANF)/SIGMAF
  H = FN(U)
  HH = GN(U)
  U = (TRIX(3,I) - MEANF)/SIGMAF
  H = H - FN(U)
  HH = FN(U) + HH
OX(I) = H*HH*GW
335 CONTINUE
  U = (YIT - MEANF)/SIGMAF
  H = FN(U)
  U = (YIR - MEANF)/SIGMAF
  H = H - FN(U)
C *** FONLY ACCOUNTS FOR CROSSINGS DUE TO FLOOR LOAD ONLY
  FONLY = PW*F*(1.0 - H)
C
DO 340 I=1,NY
```

```
C *** ZY FOR NORMAL
U = (TR1Y(2,I) - MEANF)/SIGMAF
340 ZY(I) = DN(U)/SIGMAF
GO TO 361
350 CONTINUE
C
DO 355 I=1,NX
C *** OX FOR GAMMA
Y = TR1X(1,I)
H = FG(Y,KF,LAMF)
Y = TR1X(3,I)
H = H - FG(Y,KF,LAMF)
OX(I) = H*(1.0 - H) * QW
355 CONTINUE
H = FG(YIT,KF,LAMF)
H = H - FG(YIR,KF,LAMF)
FONLY = PW*H*(1.0 - H)
DO 360 I=1,NY
C *** ZY FOR GAMMA
Y = TR1Y(2,I)
360 ZY(I) = DG(Y,KF,LAMF)
361 CONTINUE
C
IF(DISTW .GT. 0.0) GO TO 375
DO 365 I=1,NY
C *** OY FOR NORMAL
U = (TR1Y(3,I) - MEANW)/SIGMAW
H = FN(U)
HH = GN(U)
U = (TR1Y(1,I) - MEANW)/SIGMAW
H = H - FN(U)
HH = FN(U) + HH
OY(I) = PW*GW*HH + (QW**2)*H*HH
365 CONTINUE
DO 370 I=1,NX
C *** ZX FOR NORMAL
```

```
U = (TRIX(2,I) - MEANW)/SIGMAW
370 ZX(I) = DN(U)/SIGMAW
SC TC 390
375 CONTINUE
DO 380 I=1,NY
C *** QY FOR GAMMA
X = TRIY(3,I)
H = FG(X,KW,LAMW)
X = TRIY(1,I)
H = H - FG(X,KW,LAMW)
QY(I) = PW*CW*(1.0 - H) + (CW**2)*H*(1.0 - H)
380 CONTINUE
DO 385 I=1,NX
C *** ZX FOR GAMMA
X = TRIX(2,I)
385 ZX(I) = DG(X,KW,LAMW)
390 CONTINUE
DO 438 I=1,NX
TRIX(1,I) = TRIX(1,I) + D
438 TRIX(3,I) = TRIX(3,I) + D
DO 439 I=1,NY
439 TRIY(2,I) = TRIY(2,I) + D
YIT = YIT + D
YIB = YIB + D
C *** X-AXIS INTEGRATION
SDX = 0.0
DO 440 I=1,NX,2
440 SDX = 4.0*CX(I)*ZX(I) + SDX
DO 445 I=2,NXM1,2
445 SDX = 2.0*CX(I)*ZX(I) + SDX
SDX = (DX/3.0)*SDX
C *** Y-AXIS INTEGRATION
```



```

SDY = 0.0
DO 450 I=1,NY,2
450 SDY = 4.0*CY(I)*ZY(I) + SDY
DO 455 I=2,NYM1,2
455 SDY = 2.0*CY(I)*ZY(I) + SDY
SDY = (CY/3.0)*SDY

WRITE(L,212) FONLY, SDX, SDY
WRATE = NUW*SDY
FRATE = NUF*(FONLY + SDX)
RATE = FRATE + WRATE
WRITE(L,213) WRATE, FRATE, RATE
500 CONTINUE

C
100 FORMAT(4E10.4)
101 FORMAT(I3)
102 FORMAT(2E10.4)
103 FORMAT(I3)
104 FORMAT(8E10.4)
105 FORMAT(2F5.2)

200 FORMAT('0',29X,E11.4,2X,E11.4/'0',29X,E11.4,2X,E11.4/'0')
201 FORMAT('0',29X,E11.4,2X,E11.4/'0',29X,E11.4,2X,E11.4/'0')
202 FORMAT('0',10X,5(E11.4,3X))
203 FORMAT('0',24X,'XMAX=',E11.4,2X,'WITH ECCENTRICITY=',E11.4)
204 FORMAT('0',24X,'XMIN=',E11.4,2X,'WITH ECCENTRICITY=',E11.4)
205 FORMAT('0',24X,'YMAX=',E11.4,2X,'WITH ECCENTRICITY=',E11.4)
206 FORMAT('0',24X,'YMIN=',E11.4,2X,'WITH ECCENTRICITY=',E11.4)
207 FORMAT('0',20X,E11.4,2X,E11.4,4X,E11.4,2X,E11.4)
209 FORMAT('0',40X,'INTERCEPTS:/'0',38X,'YIT=',E11.4/'0',
123X,'XIL=',E11.4,14X,'XIR=',E11.4/'0',38X,'YIR=',E11.4/'0')
210 FORMAT('1',20X,'THERE ARE ',I2,' CASES FOR THE INTERACTION SPECIFI
1ED')
211 FORMAT('0'/'0',38X,'FOR CASE NUMBER ',I2,':/'
1'0',32X,'MEAN',7X,'SIGMA',9X,'NU'/'0',
223X,'WIND',3(E11.4,2X)/'0',22X,'FLCOR',3(E11.4,2X)/'0',

```



```
5 L=6  
WRITE(L,123)  
123 FORMAT('0',20X,'K TOO LARGE: CHECK INPUT')  
10 DG = 0.0  
RETURN  
END
```

```
C  
C  
C *** NORMAL DENSITY  
FUNCTION DN(U)  
U2=U**2  
IF(U2 .GT. 100.0) GO TO 5  
DN=(0.398942)*EXP((-0.5)*(U**2))  
RETURN  
5 DN=0.0  
RETURN  
END
```

```
C  
C  
C *** GAMMA CUMULATIVE  
FUNCTION FG(X,RK,RLAM)  
ARG = RLAM*X  
IF(ARG .LT. 0.0) GO TO 5  
CALL MDGAM(ARG,RK,CDF,KKK)  
C *** MDGAM IS AN IMSL LIBRARY ROUTINE  
FG = CDF  
RETURN  
5 FG = 0.0  
RETURN  
END
```

```
C  
C  
C *** NORMAL CUMULATIVE  
FUNCTION FN(U)  
IF(U .LT. -10.0) GO TO 5  
IF(U .GT. 10.0) GO TO 10
```

```
FN = 1.0 - (0.50)*ERFC(0.707107*U)
RETURN
5 FN = 0.0
RETURN
10 FN = 1.0
RETURN
END
```

```
C
C
C *** NORMAL COMPLIMENTARY CUMULATIVE
      FUNCTION GN(U)
      IF(U .LT. -10.0) GO TO 5
      IF(U .GT. 10.0) GO TO 10
      GN = (0.50)*ERFC(0.707107*U)
      RETURN
5 GN = 1.0
RETURN
10 GN = 0.0
RETURN
END
```

```

C *** UPGRADING RATE PROGRAM (UNP) ***
C
REAL M1, M2, NU1, NU2, K1, K2, LAM1, LAM2
DIMENSION ARRY1(4,199), ARRY2(4,199)
NP = 199
NPM1 = NP - 1
NPM2 = NP - 2
K=5
L=6
1 READ(K,100,END=999) NU1, P1, M1, SIGMA1, NU2, P2, M2, SIGMA2
Q1 = 1.0 - P1
Q2 = 1.0 - P2
C
C *** DIST1 AND DIST2 SPECIFY DISTRIBUTION TYPES; ZERO MEANS
C *** THE NORMAL, ANY POSITIVE NUMBER THE GAMMA DISTRIBUTION.
C *** NC SPECIFIES THE NUMBER OF CASES TO FOLLOW, EACH
C *** CORRESPONDING TO A NEW SET OF C1, C2, & Z.
C
READ(K,101) DIST1, DIST2
READ(K,102) NC
DO 99 IC=1,NC
WRITE(L,200) NU1, P1, M1, SIGMA1, NU2, P2, M2, SIGMA2
IF(DIST1 .GT. 0.C) GO TO 5
WRITE(L,301)
GO TO 6
5 WRITE(L,302)
6 IF(DIST2 .GT. 0.C) GO TO 7
WRITE(L,303)
GO TO 8
7 WRITE(L,304)
8 CONTINUE
READ(K,103) C1, C2, Z
WRITE(L,201) C1, C2, Z
C
C *** MESH SIZE
DX=Z/FLOAT(NPM1)

```

```
C *** GAMMA DISTRIBUTION PARAMETERS
      KI = (M1**2)/(SIGMA1**2)
      LAM1 = M1/((SIGMA1**2)*C1)
      K2 = (M2**2)/(SIGMA2**2)
      LAM2 = M2/((SIGMA2**2)*C2)
C
C *** ARRAYS, ROW BY ROW:
C *** ROW 1: X
C *** ROW 2: DENSITY FUNCTION OF X
C *** ROW 3: CDF CF Z - X
C *** ROW 4: 1 - CDF OF Z - X
C
      IF(DIST1 .GT. 0.0) GO TO 20
      A = C1
      B = C2
      X = 0.0
      DO 18 I=1,NP
C *** SET UP ARRAY FOR NORMAL CASE
      U = (X - M1*A)/(SIGMA1*A)
      ARRY1(1,I) = X
      ARRY1(2,I) = DN(U)/(SIGMA1*A)
      Q = Z - X
      U = (Q - M1*A)/(SIGMA1*A)
      ARRY1(3,I) = FN(U)
      ARRY1(4,I) = GN(U)
      X = X + DX
      18 CONTINUE
      U = (Z - M1*A)/(SIGMA1*A)
      F1A = FN(U)
      G1A = GN(U)
      GO TO 24
      20 CONTINUE
      X = 0.0
      DO 22 I=1,NP
C *** SET UP ARRY1 FOR GAMMA CASE
      Q = Z - X
```

```
ARRY1(1,I) = X  
ARRY1(2,I) = DG(X,K1,LAM1)  
ARRY1(3,I) = FG(Q,K1,LAM1)  
ARRY1(4,I) = 1.0 - FG(Q,K1,LAM1)  
X = X + DX
```

22 CONTINUE

```
F1A = FG(Z,K1,LAM1)  
G1A = 1.0 - F1A
```

24 IF(DIST2 .GT. 0.0) GO TO 30  
X = C.0

DO 28 I=1,NP

C \*\*\* SET UP ARRY2 FOR NORMAL CASE  
U = (X - M2\*B)/(SIGMA2\*B)

```
ARRY2(1,I) = X  
ARRY2(2,I) = DN(U)/(SIGMA2*B)
```

Q = Z - X

```
U = (Q - M2*B)/(SIGMA2*B)  
ARRY2(3,I) = FN(U)
```

```
ARRY2(4,I) = GN(U)  
X = X + DX
```

28 CONTINUE

```
U = (Z - M2*B)/(SIGMA2*B)  
F2A = FN(U)
```

```
G2A = GN(U)
```

GO TO 34

30 CONTINUE

X = 0.0

DO 32 I=1,NP

C \*\*\* SET UP ARRY2 FOR GAMMA CASE  
Q = Z - X

```
ARRY2(1,I) = X
```

```
ARRY2(2,I) = DG(X,K2,LAM2)
```

```
ARRY2(3,I) = FG(Q,K2,LAM2)
```

```
ARRY2(4,I) = 1.0 - FG(Q,K2,LAM2)
```

X = X + DX

32 CONTINUE

```

F2A = FG(Z,K2,LAM2)
G2A = 1.0 - F2A
34 CONTINUE
C
C *** HERE IS THE NUMERICAL CONVOLUTION
F12A = 0.0
DO 36 I=2,NPM1,2
F12A = (4.0)*ARRY1(3,I)*ARRY2(2,I) + F12A
36 CONTINUE
DO 38 I=3,NPM2,2
F12A = (2.0)*ARRY1(3,I)*ARRY2(2,I) + F12A
38 CONTINUE
F12A = ARRY1(3,1)*ARRY2(2,1) + ARRY1(3,NP)*ARRY2(2,NP) + F12A
F12A = (F12A*DX)/3.0
C
WRITE(L,202) F1A, G1A, F2A, G2A, F12A
H1 = Q1*P2*G1A*(P1 + Q1*F1A)
HH1= P1*Q1*G2*(F2A - F12A)
H2 = P1*Q2*G2A*(P2 + Q2*F2A)
HH2= P2*Q1*G2*(F1A - F12A)
C
C *** F&G TYPE CONVOLUTIONS NOW FOLLOW
S1 = 0.0
DO 42 I=2,NPM1,2
S1 = (4.0)*ARRY1(4,I)*ARRY1(3,I)*ARRY2(2,I) + S1
42 CONTINUE
DO 44 I=3,NPM2,2
S1 = (2.0)*ARRY1(4,I)*ARRY1(3,I)*ARRY2(2,I) + S1
44 CONTINUE
S1 = ARRY1(4,NP)*ARRY1(3,NP)*ARRY2(2,NP) + S1
S1 = ARRY1(4,1)*ARRY1(3,1)*ARRY2(2,1) + S1
S1 = (S1*DX)/3.0
C
S2 = 0.0
DO 46 I=2,NPM1,2
S2 = (4.0)*ARRY2(4,I)*ARRY2(3,I)*ARRY1(2,I) + S2

```



```

46 CONTINUE
CC 48 I=3,NPM1,2
S2 = (2.0)*ARRY2(4,I)*ARRY2(3,I)*ARRY1(2,I) + S2
48 CONTINUE
S2 = ARRY2(4,1)*ARRY2(3,1)*ARRY1(2,1) + S2
S2 = ARRY2(4,NP)*ARRY2(3,NP)*ARRY1(2,NP) + S2
S2 = (S2*DX)/3.0

C
RATE1 = (H1 + HH1 + (01**2)*Q2*S1)*NUL
RATE2 = (H2 + HH2 + (02**2)*Q1*S2)*NUL
RATE = RATE1 + RATE2
C *** FINAL RESULTS
WRITE(L,203) RATE1, RATE2, RATE
C *** GO BACK FOR MORE CASES
99 CONTINUE
C
C
C *** FORMATS BEGIN HERE
100 FORMAT(8E10.4)
101 FORMAT(2F5.2)
102 FORMAT(I3)
103 FORMAT(3E10.4)
200 FORMAT('1',30X,'INPUT PARAMETERS: /'0',7X,'PROCESS',
12X,' ***P***' ,E11.4,3X,F10.7,2X,E11.4,2X,E11.4/'0',
210X,'1',E11.4,3X,F10.7,2X,E11.4,2X,E11.4/'0',
310X,'2',E11.4,3X,F10.7,2X,E11.4,2X,E11.4)
201 FORMAT('0',34X,'C1=',E11.4/'0',34X,'C2=',E11.4/'0',
135X,'7=',E11.4/'0')
202 FORMAT('0',34X,'F1A=',E11.4/'0',34X,'G1A=',E11.4/'0',
134X,'F2A=',E11.4/'0',34X,'G2A=',E11.4/'0',33X,'F12A=',E11.4/'0')
203 FORMAT('0',34X,'OUTPUT RATES: /'0',32X,'RATE1=',E11.4/'0',
132X,'RATE2=',E11.4/'0',33X,'RATE=',E11.4)
301 FORMAT('0',30X,'DISTRIBUTION 1: NORMAL')
302 FORMAT('0',30X,'DISTRIBUTION 1: GAMMA')
303 FORMAT('0',30X,'DISTRIBUTION 2: NORMAL/'0')
304 FORMAT('0',30X,'DISTRIBUTION 2: GAMMA/'0')

```



```
C *** MDGAM(ARG,RK,CDF,KKK)
C MDGAM IS AN IMSL LIBRARY ROUTINE
C FG = CDF
C RETURN
C END

C
C *** NORMAL CUMULATIVE
C FUNCTION FN(U)
C IF(U .LT. -10.0) GO TO 5
C IF(U .GT. 10.0) GO TO 10
C FN = 1.0 - (0.50)*ERFC(0.707107*U)
C RETURN
C 5 FN = 0.0
C RETURN
C 10 FN = 1.0
C RETURN
C END

C
C *** NORMAL COMPLIMENTARY CUMULATIVE
C FUNCTION GN(U)
C IF(U .LT. -10.0) GO TO 5
C IF(U .GT. 10.0) GO TO 10
C GN = (0.50)*ERFC(0.707107*U)
C RETURN
C 5 GN = 1.0
C RETURN
C 10 GN = 0.0
C RETURN
C END
```



Room 14-0551  
77 Massachusetts Avenue  
Cambridge, MA 02139  
Ph: 617.253.5668 Fax: 617.253.1690  
Email: docs@mit.edu  
<http://libraries.mit.edu/docs>

## **DISCLAIMER OF QUALITY**

Due to the condition of the original material, there are unavoidable flaws in this reproduction. We have made every effort possible to provide you with the best copy available. If you are dissatisfied with this product and find it unusable, please contact Document Services as soon as possible.

Thank you.

**Some pages in the original document contain pictures, graphics, or text that is illegible.**